Reactivity of Dioxygen−Copper Systems

Elizabeth A. Lewis and William B. Tolman*

Department of Chemistry and Center for Metals in Biocatalysis, University of Minnesota, 207 Pleasant Street SE, Minneapolis, Minnesota 55455

Received July 9, 2003

Contents

Elizabeth A. Lewis grew up in Pembrokeshire, Wales, and obtained her Bachelor's degree in Chemistry from the University of York, UK in 1996. She then received a Master's degree from Dalhousie University, Nova Scotia (with Robert L. White) in 1998 and a Ph.D. from the University of York, UK (with John R. Lindsay Smith and Paul H. Walton) in 2002. After this time, she moved to the University of Minnesota and joined the group of William B. Tolman as a postdoctoral researcher focusing on the synthesis of novel Cu/O_2 species. She is currently a Welcome Trust postdoctoral research fellow at the University of Hull, UK, with Stephen J. Archibald, investigating Cu complexes for medical applications.

William B. Tolman is a Distinguished McKnight University Professor of Chemistry at the University of Minnesota, Twin Cities. He obtained his B.A. from Wesleyan University in 1983 and subsequently worked in the laboratory of Prof. K. Peter C. Vollhardt at the University of California, Berkeley, for his Ph.D. (1987). After a postdoctoral stint in the laboratory of Prof. Stephen J. Lippard at the Massachusetts Institute of Technology, he joined the faculty at the University of Minnesota in 1990. Current research activities range from synthetic modeling of metalloprotein active sites to the development and mechanistic study of catalysts for the synthesis of biodegradable polymers from renewable resources.

1. Introduction

1.1. Background

Copper proteins that bind and/or activate dioxygen perform a variety of critical biological functions.[1−3] These include O_2 transport (hemocyanin, Hc),[4] aromatic ring oxidations (tyrosinase, Tyr,[5] catechol oxidase, CO,[6] and quercetin 2,3-dioxygenase, QDO[7−9]),[3] the biogenesis of neurotransmitters and peptide hormones (dopamine β-monooxygenase, DβM,[10] and peptidylglycine α-amidating monooxygenase, PHM[11,12]),[2] hydrogen peroxide generation (galactose and glyoxal oxidases, GAO and GLO),[13−18] iron homeostasis (ceruloplasmin[3] and Fet3p[19−21]), and methane oxidation (particulate methane monoxygenase, pMMO),[22−25] among others (Table 1).[16,26−42] Post-translational synthesis of organic cofactors also may involve the reaction of dioxygen with copper protein active sites.[43] Usually, the chemical pathway traversed by these various proteins involves the reaction of reduced Cu(I) centers with dioxygen to yield an adduct or intermediate species, which subsequently reacts with substrate. Despite such fundamental commonality, diverse mechanisms of action are pos-

* To whom correspondence should be addressed. Phone: 612-625-4061. E-mail: tolman@chem.umn.edu. FAX: 612-624-7029.

10.1021/cr020633r CCC: $48.50
Published on Web 01/13/2004

Table 1. Copper Proteins that Bind and/or Activate Dioxygen

protein (abbreviation)	no. Cu ions involved in O_2 activation	reaction performed	selected lead refs
amine oxidase (AO)	1	aldehydes and H_2O_2 from primary amines	2, 16, 26−28
galactose oxidase (GAO)	1	aldehydes and H_2O_2 from alcohols	2, 13−16
glyoxal oxidase (GLO)	1	carboxylic acids and H_2O_2 from aldehydes	2, 17, 18
dopamine β-monooxygenase (DβM)	2 (uncoupled)[a]	hydroxylation of dopamine to yield epinephrine	2, 10
peptidylglycine α-amidating monooxygenase (PHM)	2 (uncoupled)[a]	hydroxylation at α-position of glycine	2, 11, 12
quercetin 2,3-dioxygenase (QDO)	1	oxidative ring opening of quercetin	7−9
hemocyanin (Hc)	2	reversible binding of O_2	1, 3, 4
tyrosinase (Tyr)	2	hydroxylation of aromatic ring	3, 5
catechol oxidase (CO)	2	oxidation of catechol to *o*-quinone	3, 6
methane monoxygenase (MMO)	*b*	hydroxylation of methane to methanol	22−25
ammonia monoxygenase (AMO)	*b*	oxidation of ammonia to hydroxylamine	3, 29, 30
multicopper oxidases[c]	3		1, 3, 31
laccase (Lc)	3	oxidative coupling of catechols	32−34
ascorbate oxidase (AO)	3	oxidation of ascorbate	35
ceruloplasmin (Cp)	3	oxidation of Fe(II) to Fe(III)	36
Fet3	3	oxidation of Fe(II) to Fe(III)	37, 38
phenoxazinone synthase (POS)	3	oxidative coupling of aminophenols	39, 40
cytochrome *c* oxidase	1 (+ Fe))	establishment of membrane proton gradient	41, 42

[a] These proteins contain two copper ions separated by ~11 Å, but it is unclear if one or both activates dioxygen. [b] Nuclearity of the O_2 activating copper sites is unclear. [c] Only selected examples of multicopper oxidases are listed; for more complete discussion, see refs 1 and 3.

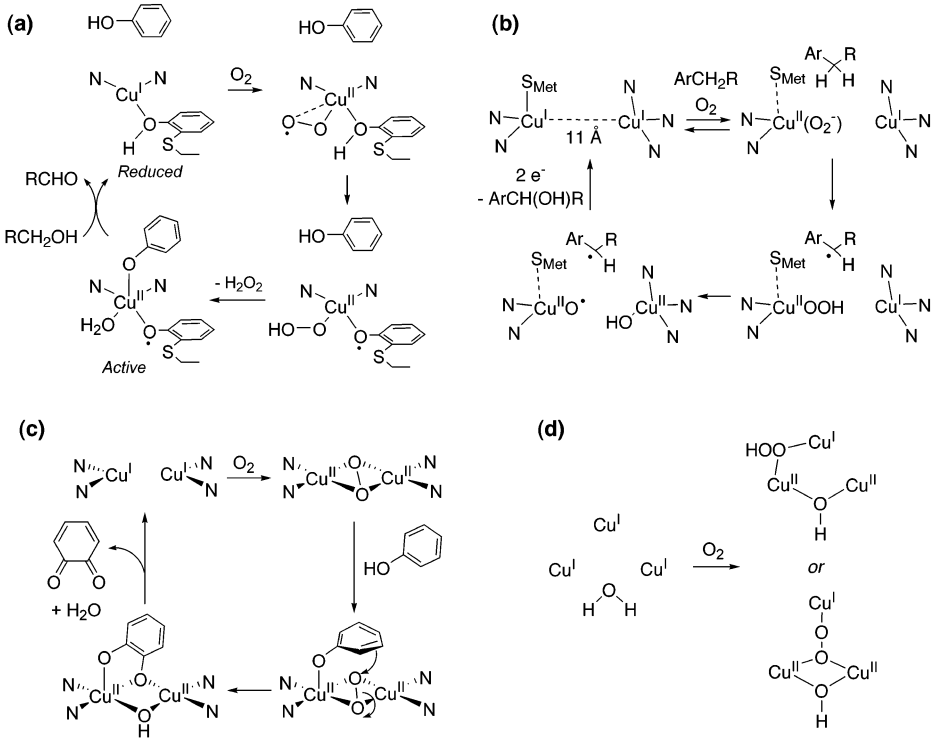

Figure 1. Aspects of the mechanisms proposed for (a) GAO and GLO,[44] (b) DβM,[47] (c) Tyr,[1,3] and (d) the multicopper oxidases.[53] The symbol "N" refers to a histidine imidazolyl group. Axial ligands in (c) and all protein ligands in (d) are omitted for clarity. Reversible O_2 binding in Hc occurs according to the top O_2 coordination step in (c); CO activity is postulated be similar to the last step in (c).[1,3,49]

sible because of the varied protein active site structures (nuclearities, ligands, geometries) and types of transformations promoted.

To illustrate this point, selected aspects of proposed catalytic mechanisms are drawn in Figure 1 for representative examples of proteins that contain active sites with nuclearities ranging from 1 to 3 copper ions. In Figure 1a is shown a proposed pathway by which the active Cu(II)-tyrosyl radical form of GAO (and GLO) is formed.[44] In the first step, binding of O_2 to the reduced Cu(I) form yields a Cu(II)-superoxide, which has yet to be observed through spectroscopic means. Subsequent internal hydrogen atom (or proton coupled electron) transfer is suggested to yield a (tyrosyl radical)Cu(II)-hydroperoxide, from which H_2O_2 evolves to yield the active form identified by spectroscopy that oxidizes substrate. Intermediates formulated as Cu(II)-OOH, Cu(II)-O_2^-, and Cu(II)-O•/Cu(III)═O have been proposed for PHM and DβM on the basis of kinetic

evidence (Figure 1b).[2,45−47] Despite much study of these enzymes, however, many mechanistic questions remain, including ones concerning how these putative oxidants are formed[48] and which is (are) responsible for attacking the substrate C−H bond.[45−47] A (μ-η^2:η^2-peroxo)dicopper(II,II) unit has been identified conclusively in Hc,[3,4] Tyr,[3] and CO[6,49] (Figure 1c). Substrate accessibility appears to determine the fate of this unit, such that in Hc (no substrate access) only reversible O_2 binding occurs, but in Tyr and CO wherein substrate can approach and/or bind to the Cu_2O_2 moiety, an aromatic ring is hydroxylated and/or a catechol(ate) is converted to an *ortho*-quinone. The Tyr hydroxylation mechanism shown (Figure 1c) involving direct electrophilic attack of the peroxo unit onto the aromatic ring is supported by recent experimental[50] and theoretical results.[51] Finally, an unusual mixed-valent tricopper-hydroperoxo structure has been suggested as a reactive intermediate in reduction of O_2 to H_2O by the multicopper oxidases (Figure 1d).[52−54] Taken together, and despite being described only briefly, these examples demonstrate the diversity of structures and pathways proposed for Cu/O_2 species in proteins; more comprehensive mechanistic analyses of many of the biological systems listed in Table 1 are presented in various reviews.[1−6,11,13,16,43]

Among the central chemical issues to be addressed to understand the function of the copper proteins listed in Table 1, those that center on the geometry, electronic structure, interconversions, and substrate reactivity of the Cu/O_2 adducts or intermediates have attracted the most attention, particularly by scientists who examine small molecule models with which detailed physicochemical and mechanistic insights may be obtained.[55] Thus, stimulated by the fascinating biological systems, as well as by relevance to many copper-promoted transformations in homogeneous[56,57] and heterogeneous catalysis,[58,59] extensive studies of the reaction of Cu(I) complexes with O_2 have been performed. In large part, these studies have attempted to address questions such as: How does O_2 coordinate to the copper ion, and what are the kinetics and thermodynamics for O_2 binding? How do supporting ligands (topology, electronic properties) influence the structure and stability of the species derived from the $Cu(I)/O_2$ reaction? How do these species react (what are the mechanisms?)? What are the most important geometric and/or electronic structural features for controlling their reactivity? As discussed below, through detailed kinetics and other mechanistic studies of synthetic copper compounds, studies aimed at answering these questions have provided fundamental chemical insights of value for understanding copper protein function.

1.2. Scope

There are many reviews describing different aspects of Cu/O_2 adduct formation, characterization, and subsequent reactivity toward substrates.[60−89] In this article, we provide an overview of the kinetic, thermodynamic, and mechanistic features of Cu/O_2 adduct formation and subsequent reactivity. The literature covered extends to summer 2003. The spectroscopy and structures (including theoretical descriptions) of the various types of adducts that have been characterized to date are discussed in the preceding article in this issue.[90] We divide our discussion as follows. First, we consider the kinetics and thermodynamics of the reactions of O_2 with Cu(I) complexes that lead to discrete adducts and related complexes. Second, interconversions among specific isomeric complexes that result from $Cu(I)/O_2$ reactions are discussed. Alternate synthetic routes to Cu/O_2 species are then presented. Finally, we evaluate the mechanisms of the reactions of Cu/O_2 species with endogenous and exogenous substrates. Although there are many examples of oxidation reactions catalyzed by Cu complexes in the literature, in this review we focus on the formation and reactivity of Cu/O_2 complexes that are well-defined through spectroscopic studies and/or X-ray crystal structure analyses.

2. Reactivity of Cu(I) Complexes with O_2

2.1. Overview

Early kinetic studies on reactions of Cu(I) complexes with O_2 implicated formation of Cu/O_2 adducts, but evidence was lacking for the unambiguous identification of these often thermally unstable species. For example, the kinetics of autoxidation of Cu(I) complexes of substituted imidazoles in aqueous acetonitrile showed competing one- and two-electron O_2 reduction pathways.[91,92] It was argued that the existence of the former route provided indirect evidence for formation of an unstable 1:1 Cu/O_2 adduct in solution. Because clear spectroscopic or structural support for such hypotheses was unavailable, early experimental approaches generally focused on preparing more readily isolated and characterized complexes with endogeneous bridging ligands that might model O_2 interactions (e.g., N_3^-, RO^-).[62]

Since these initial studies, the understanding of Cu/O_2 systems has improved dramatically as a result of a combination of technological advances (e.g., CCD detectors for X-ray crystallography and Raman spectroscopy, instrumentation for low-temperature stopped flow kinetics measurements), the use of low-temperature sample handling methods, and the judicious application of ligand design principles.[93,94] A number of discrete copper-dioxygen and related species have been stabilized sufficiently for characterization using a wide variety of ligands (Chart 1, listed in order of discussion in the text; structural motifs are summarized in Chart 2). A key research objective has been to unravel the mechanism(s) by which these species form; toward this end, the kinetics of the oxygenations of Cu(I) complexes have been examined extensively. Due to the typically quite rapid rates of $Cu(I)/O_2$ reactions and the thermal instability of the resulting complexes, the development of low temperature stopped-flow kinetic techniques and the application of numerical methods and factor analysis to interpret the data collected from these experiments have been particularly useful for unraveling oxygenation pathways.[95−98] As a result, the individual steps

Chart 1

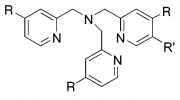

TMPA, **1**: R = R' = H
4R-TMPA,
2a: R' = H, R = Me
2b: R' = H, R = tBu
2c: R' = H, R = OMe
2d: R' = H, R = NMe_2
TMPAE, **3**: R' = $C(O)CH_3$, R = H

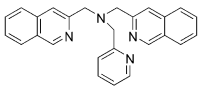

BQPA, **4**

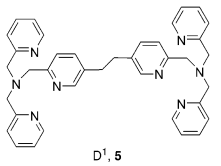

D^1, **5**

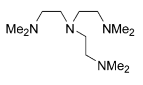

Me_6tren, **6**

L^{Me3}, **7a**: R = R' = Me
L^{iPr3}, **7b**: R = R' = *i*Pr
L^{Bn3}, **7c**: R = R' = $CH_2C_6H_5$
$L^{(OMeBn)3}$, **7d**: R = R' = $CH_2C_6H_4OMe$
$L^{(tBuBn)3}$, **7e**: R = R' = $CH_2C_6H_4tBu$
$L^{(CF3Bn)3}$, **7f**: R = R' = $CH_2C_6H_4CF_3$
L^{iPr2Bn}, **7g**: R = *i*Pr, R' = $CH_2C_6H_5$

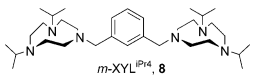

m-XYL^{iPr4}, **8**

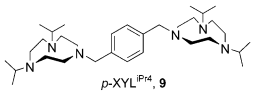

p-XYL^{iPr4}, **9**

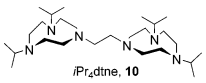

iPr_4dtne, **10**

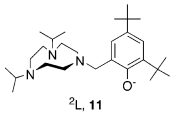

^{2}L, **11**

AN, **12a**: R = H
MeAN, **12b**: R = Me

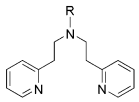

^{H}Py2, **13a**: R = H
^{H}$Py2^{Me}$, **13b**: R = Me
^{H}$Py2^{Phe}$, **13c**: R = $CH_2CH_2C_6H_5$
^{H}$Py2^{Phe(Me)}$, **13d**: R = CH_2CH_2-*p*-$CH_3C_6H_4$
^{H}$Py2^{Phe(Cl)}$, **13e**: R = CH_2CH_2-*p*-ClC_6H_4
^{H}$Py2^{Phe(NO2)}$, **13f**: R = CH_2CH_2-*p*-$NO_2C_6H_4$
^{H}$Py2^{Phe(2OH)}$, **13g**: R = CH_2CH_2-*m*-HOC_6H_4
^{H}$Py2^{Phe(3OH)}$, **13h**: R = CH_2CH_2-*p*-HOC_6H_4
^{H}$Py2^{Phe(4OHMe)}$, **13i**: R = CH_2CH_2-*o*-OH-*p*-CH_3-C_6H_3
^{H}$Py2^{Bz}$, **13j**: R = $CH_2C_6H_5$
^{H}$Py2^{BzO}$, **13k**: R = CH_2-*o*-C_6H_4-O^-
^{H}$Py2^{Ind}$, **13l**: R = indane
^{H}$Py2^{PhePh}$, **13m**: R = $CH_2CH(C_6H_5)_2$
^{H}$Py2^{tBu}$, **13n**: R = tBu
^{H}$Py2^{NEt2}$, **13o**: R = $CH_2CH_2NEt_2$
^{H}$Py2^{NEtAm}$, **13p**: R = $CH_2CH_2N(Et)CH_2Ch_2N(H)COtBu$

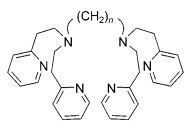

N_5Py2, **14a**: *n* = 3
N_4Py2, **14b**: *n* = 4
N_5Py2, **14c**: *n* = 5

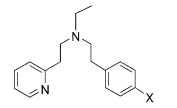

^{H}$Py1^{Et,Phe}$, **22a**: X = H
^{H}$Py1^{Et,Phe(OMe)}$, **22b**: X = OMe
^{H}$Py1^{Et,Phe(Me)}$, **22c**: X = Me
^{H}$Py1^{Et,Phe(Cl)}$, **22d**: X = Cl
^{H}$Py1^{Et,Phe(NO2)}$, **22e**: X = NO_2

Me_4pda, **23a**: R_1 = R_2 = Me
iPr_2Me_2pda, **23b**: R_1 = *i*Pr, R_2 = Me
Et_4pda, **23c**: R_1 = R_2 = Et

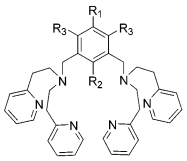

XYL-H, **24a**: R_1 = H, R_2 = H, R_3 = H
OMe-XYL-H, **24b**: R_1 = OCH_3, R_2 = H, R_3 = H
*t*Bu-XYL-H, **24c**: R_1 = *t*Bu, R_2 = H, R_3 = H
F-XYL-H, **24d**: R_1 = F, R_2 = H, R_3 = H
CN-XYL-H, **24e**: R_1 = CN, R_2 = H, R_3 = H
NO_2-XYL-H, **24f**: R_1 = NO_2, R_2 = H, R_3 = H
XYL-O^-, **24g**: R_1 = H, R_2 = O^-, R_3 = H
XYL-Me, **24h**: R_1 = H, R_2 = CH_3, R_3 = H
Me_2-XYL-Me, **24i**: R_1 = H, R_2 = CH_3, R_3 = CH_3

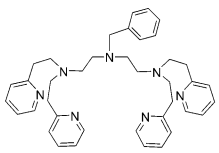

D, **25**

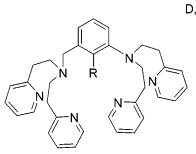

UN, **26a**: R = H
UN-O^-, **26b**: R = O^-

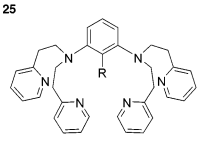

PD, **27a**: R = H
PD-O^-, **27b**: R = O^-

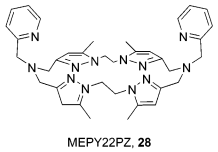

MEPY22PZ, **28**

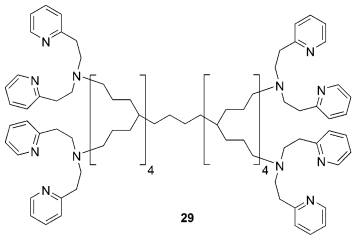

29

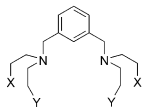

X	Y
30a: 2-benzimidazolyl	2-benzimidazolyl
30b: 1-pyrazolyl	1-pyrazolyl
30c: 1-(3,5-Me_2-pyrazole)	1-(3,5-Me_2-pyrazole)
30d: 2-pyridyl	2-pyridyl
30e: 2-(*N*-Me-imidazoyl)	2-(*N*-Me-imidazoyl)
30f: 2-pyridyl	1-pyrazolyl
30g: 2-pyridyl	1-(3,5-Me_2-pyrazole)
30h: 2-pyridyl	2-(*N*-Me-imidazoyl)

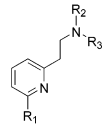

^{H}$Py1^{Et,Bz}$, **15a**: R_1 = H, R_2 = CH_2CH_3, R_3 = $CH_2C_6H_5$
^{H}$Py1^{Me,Me}$, **15b**: R_1 = H, R_2 = CH_3, R_3 = CH_3
^{Me}$Py1^{Et,Bz}$, **15c**: R_1 = CH_3, R_2 = CH_2CH_3, R_3 = $CH_2C_6H_5$

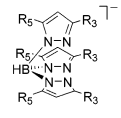

$Tp^{tBu,iPr}$, **16a**: R_3 = *t*Bu, R_5 = *i*Pr
Tp^{iPr2}, **16b**: R_3 = R_5 = *i*Pr
Tp^{Me2}, **16c**: R_3 = R_5 = Me
$Tp^{tBu,Me}$, **16d**: R_3 = *t*Bu, R_5 = Me

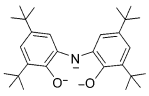

^{1}L, **17**

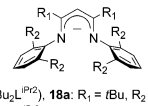

H(Bu_2L^{iPr2}), **18a**: R_1 = *t*Bu, R_2 = *i*Pr
H(Me_2L^{iPr2}), **18b**: R_1 = Me, R_2 = *i*Pr
H(Me_2L^{Me2}), **18c**: R_1 = Me, R_2 = Me

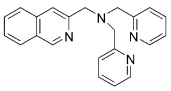

BPQA, **19**

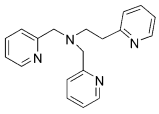

PMEA, **20**

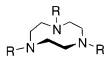

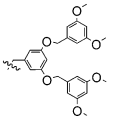

(L2)$_3$tacn, **21a**: R =

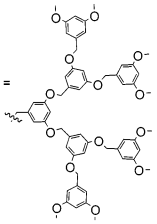

(L3)$_3$tacn, **21b**: R =

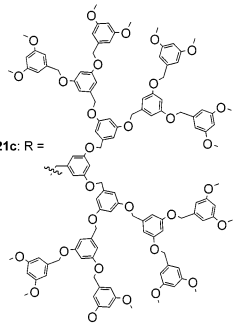

(L4)$_3$tacn, **21c**: R =

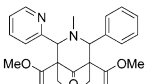

BPL, **31**

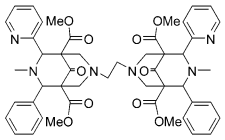

BPL2, **32**

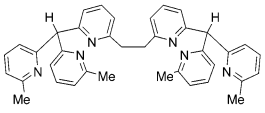

N_2tripy, **33**

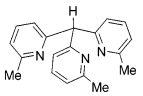

tripy, **34**

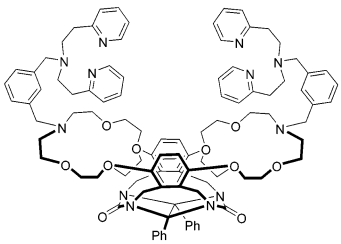

$L_3(Py2)_2$, **35**

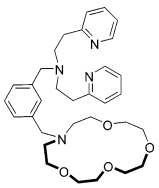

L_1Py2, **36**

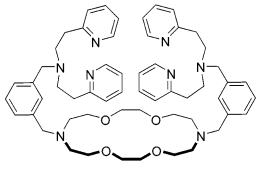

$L_2(Py2)_2$, **37**

Me_4Cyda, **38a**: R_1 = R_2 = Me
Me_2Et_2Cyda, **38b**: R_1 = Et, R_2 = Me
Et_4Cyda, **38c**: R_1 = R_2 = Et

Chart 1 (continued)

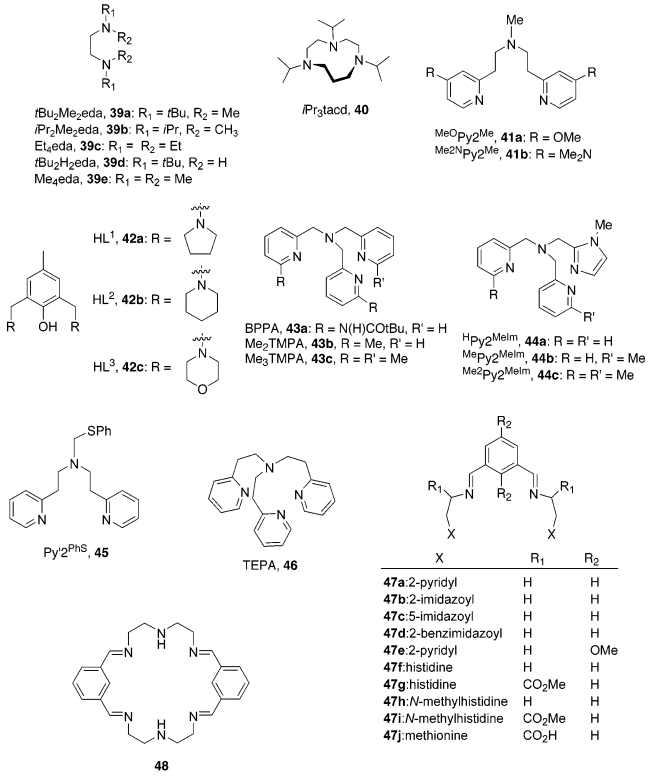

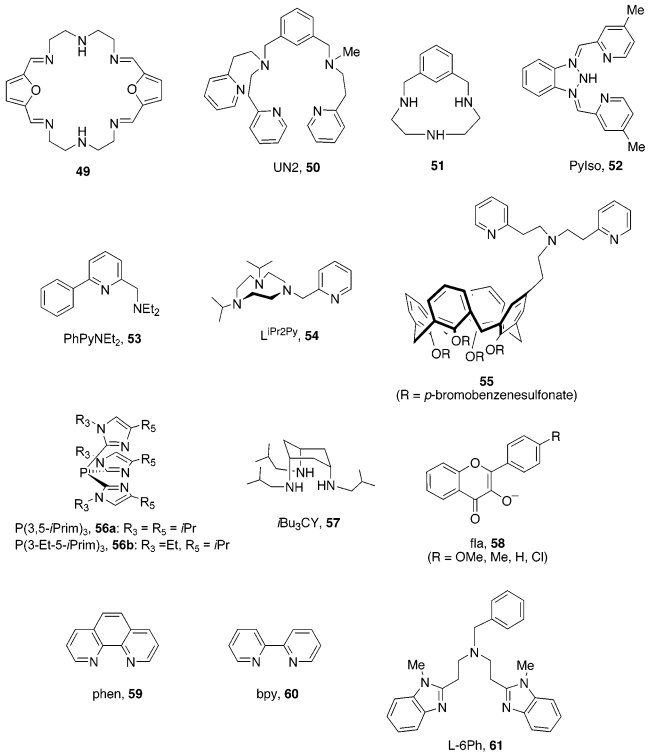

Chart 2

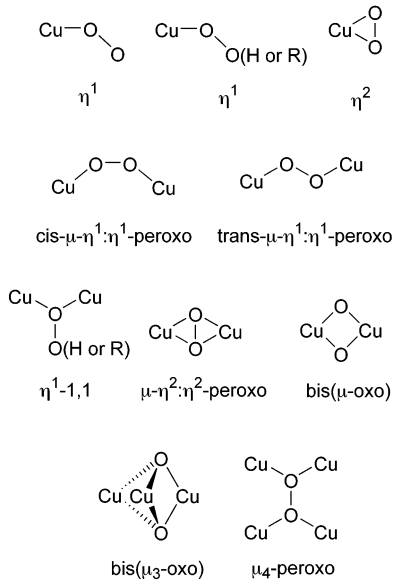

Scheme 1

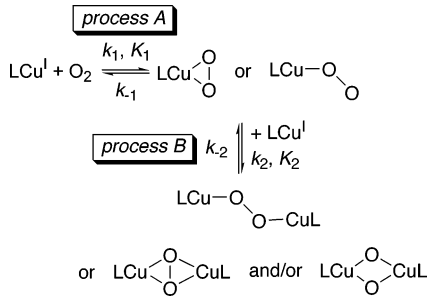

leading to the formation of well-defined Cu/O_2 species have now been elucidated for a range of different systems and their kinetic and thermodynamic parameters determined.[99−101]

We discuss these results within the context of a general mechanistic framework shown in Scheme 1. According to this scheme, dioxygen initially binds to a Cu(I) center to form a 1:1 Cu/O_2 adduct (process A). This adduct usually, but not always, reacts with a second Cu(I) complex to form one or more binuclear Cu_2O_2 species (process B). Further reaction with LCu(I) can occur to give trinuclear or tetranuclear adducts (not shown). While this general picture adequately encompasses the oxygenation pathways observed to date, differences in details are often significant, and reflect important influences of supporting ligand structure on the dioxygen activation mechanism.

It is important to appreciate that while kinetic and thermodynamic parameters are of critical importance in understanding the reactivity of model Cu(I) complexes with O_2 they do not provide information about the nature of O_2 binding to the metal center(s) (although sometimes specific intermediates may be more logical mechanistically). Spectroscopic and, if possible, structural data are required to complement kinetic information and provide a complete mechanistic representation. Finally, it is worth noting a warning[99] against establishing mechanistic arguments on the sole basis of a comparison of kinetic and equilibrium constants at a given temperature because these can sometimes be very misleading; use of activation and thermodynamic parameters is preferred.

2.2. Formation of 1:1 Cu/O_2 Adducts

Most commonly, 1:1 Cu/O_2 adducts have been implicated in stopped-flow kinetic studies as short-

lived intermediates on the pathway to well-defined 2:1 Cu/O_2 complexes.[95,97,100,102−117] Broadly speaking, three kinetic situations have been identified. In some cases (e.g., complexes supported by TMPA (**1**),[102−106] 4R-TMPA (**2a**−**d**),[105] TMPAE (**3**),[107] BQPA (**4**),[104] D^1 (**5**),[111] or Me_6tren (**6**)[96,97,108,109]), the rates of formation and decay of the intermediate 1:1 adduct are such that both processes may be monitored and the intermediate may be observed spectroscopically. In other instances, formation of the initial 1:1 adduct is slow and rate-determining, with fast subsequent trapping of this adduct by an additional Cu(I) center that prevents observation of the 1:1 complex (e.g., with $L^{RR'}$ (**7**),[115,116] *m*-XYL^{iPr4} (**8**),[115] *p*-XYL^{iPr4} (**9**),[115] or *i*-Pr_4dtne (**10**)[115,117]). For both scenarios, kinetic and thermodynamic parameters for 1:1 adduct formation (k_1, k_{-1}, K_1) may be determined. Finally, there are instances in which the equilibrium for binding of O_2 to a single Cu site is reached very rapidly, which prevents determination of k_1 and k_{-1} values (e.g., for TMPA (**1**) or 4-OMe-TMPA (**2c**) in THF,[105] ^{2}L (**11**),[118] AN or MeAN (**12a**,**b**),[114] ^{H}Py2^{Me} (**13b**),[119] or N_4Py2 (**14b**)[112]) and/or leads to kinetics that are second order in the starting Cu(I) complex due to slow, rate-controlling trapping of a putative 1:1 adduct (e.g., ^{H}Py2^{Phe} (**13c**)[113] or ^{H}Py1^{Et,Bz} (**15a**)[120]). In fact, through the use of particularly sterically bulky supporting ligands, reaction of a 1:1 adduct with a second Cu(I) complex may be prevented completely. This strategy has facilitated spectroscopic characterization of 1:1 Cu/O_2 complexes[104,105] and, in a few instances, has enabled them to be isolated as solids ($Tp^{tBu,Me}$ (**16d**),[121,122] ^{1}L (**17**),[123] $H(R_2L^{iPr2})$ (**18a**, R = tBu; **18b**, R = Me[124,125])). Note that in one case, an X-ray crystal structure of a 1:1 Cu/O_2 adduct[126] was later reassigned[127] as a Cu(II)−hydroxide complex, presumably derived from a decomposition process.[128,129]

Selected kinetic and thermodynamic parameters for 1:1 Cu/O_2 adduct formation are compared in Table 2. Some general similarities are evident among systems supported by different N-donor ligands. Thus, activation enthalpies for oxygenation ($\Delta H_1^{\ddagger}$) of Cu(I) complexes of tris(pyridyl)methylamines (TMPA (**1**), TMPAE (**3**), BQPA (**4**)) and of triazacyclononanes (L^{iPr3} (**7b**), *m*-XYL^{iPr4} (**8**), *i*-Pr_4dtne (**10**)) fall within a relatively narrow range (30−40 kJ mol^{-1}), with an exception being the TMPA (**1**) system studied by flash photolysis (discussed below).[106] Unfavorable activation entropies generally are observed (−62 to ca. 0 J K^{-1} mol^{-1}), consistent with loss of degrees of freedom upon binding of O_2. The thermodynamics for 1:1 adduct formation are similar for most of the tris(pyridyl)methylamine systems (at 183 K, $K_1 = 10^2$−10^3 M^{-1}), and feature comparably favorable reaction enthalpies ($\Delta H° \sim -30$ kJ mol^{-1}) and unfavorable reaction entropies ($\Delta S° \sim -125$ J K^{-1} mol^{-1}) that preclude observation of the adducts at room temperature.

Notwithstanding the aforementioned general similarities, interesting differences in kinetic and thermodynamic parameters for 1:1 adduct formation have been identified among systems that vary with respect to supporting ligand structure or solvent medium. For example, slower O_2 association (k_1) and dissociation (k_{-1}) were observed for the more sterically hindered BQPA (**4**) system relative to its TMPA (**1**) and TMPAE (**3**) congeners. Less favorable $\Delta S^{\ddagger}$ values for both processes for the BQPA (**4**) case (by ∼50 J K^{-1} mol^{-1}) underly its slower reactions. On the other hand, increased rate constants for O_2 association and greater stabilization of 1:1 Cu/O_2 complexes (larger K_1 at low temperature and more negative $\Delta H°$ values) than seen for (TMPA)Cu(I) were noted in cryogenic stopped-flow kinetics studies of systems supported by Me_6tren (**6**), ^{2}L (**11**) and 4-R-TMPA (**2c**, R = OMe or **2d**, R = NMe_2). For Me_6tren (**6**), a more than 4-fold increase in oxygenation rate at low temperature (183 K) compared to the TMPA (**1**) complex may be traced to a more favorable $\Delta H_1^{\ddagger}$ (by ∼15 kJ mol^{-1}) that is only partially offset by a more negative $\Delta S_1^{\ddagger}$ (by ∼60 J mol^{-1} K^{-1}). A redox influence was cited[109] as a possible rationale for this difference in oxygenation kinetics, whereby the polypyridyl ligation of TMPA (**1**) better stabilizes Cu(I) than the more electron donating alkylamines of Me_6tren (**6**), resulting in faster formation of the Cu(II)−superoxide complex for the latter.

An analogous electronic effect was identified and more rigorously separated from possible steric influences in a detailed kinetic study comparing the TMPA (**1**) system with derivatives substituted at the remote 4-position on the pyridyl rings, 4-R-TMPA (**2a**−**d**).[105] For the cases in which R is strongly electron donating (**2c**, R = OMe or **2d**, R = NMe_2), faster rates of oxygenation and increased stabilization of the 1:1 Cu/O_2 adduct were observed. These differences were attenuated when the kinetics were studied in EtCN solvent, which binds strongly to Cu(I) and competes with O_2 coordination. When more weakly coordinating THF was used as solvent, much faster 1:1 Cu/O_2 adduct formation was observed for TMPA (**1**). Indeed, in a recent study using a "flash-and trap" technique to examine the oxygenation rate of $[(TMPA)Cu(I)THF]^+$ derived from photolysis of $[(TMPA)Cu(I)CO]^+$, extraordinarily high k_1 values (greater than for reduced iron heme complexes),[130] a correspondingly small $\Delta H_1^{\ddagger}$ value and a negative $\Delta S_1^{\ddagger}$ were measured (Table 2) that were consistent with direct attack of O_2 onto the Cu site with essentially no interference from solvent.[106] The electronic effects of the remote 4-substituents in the systems supported by 4-R-TMPA (**2a**−**d**) also were enhanced in THF solvent. These effects correlate nicely with the basicity of the 4-substituted pyridines and the (4-R-TMPA)Cu(I)/(II) complex redox potentials measured by cyclic voltammetry in CH_3CN; the electron donating substituents increase pyridyl ring basicity, decrease the Cu(II)/(I) reduction potentials, and increase the rate of oxygenation and thermodynamic stability of the 1:1 Cu/O_2 adducts. Similar correlations, in particular between redox potentials and O_2 binding thermodynamics, are known for iron and cobalt complexes.[101,131] Interestingly, when acetone was used as solvent, a significant shift in the oxygenation mechanism was identified (Scheme 2). In acetone, the Cu(I) precursor was shown to be dimeric from independent conductivity and NMR evidence; related dimeric structures had also been

Table 2. Selected Kinetic and Thermodynamic Parameters for the Formation of 1:1 Cu/O_2 Adducts upon Low Temperature Oxygenation of Cu(I) Complexes[a]

ligand	solvent	k_1[b]	activation parameters (k_1)[c]	k_{-1}[b]	activation parameters (k_{-1})[c]	K_1[d]	thermodynamic parameters (K_1)[c]	ref
TMPA (**1**)	EtCN	$(1.18 \pm 0.01) \times 10^4$	$\Delta H^{\ddagger} = 31.6 \pm 0.5$ $\Delta S^{\ddagger} = 10 \pm 3$	15.9 ± 0.1	$\Delta H^{\ddagger} = 61.5 \pm 0.5$ $\Delta S^{\ddagger} = 118 \pm 3$	$(7.42 \pm 0.04) \times 10^2$	$\Delta H° = -29.8 \pm 0.2$ $\Delta S° = -108 \pm 1$	105
	THF	$\geq 2 \times 10^6$				$(7 \pm 3) \times 10^5$	$\Delta H° = -41 \pm 2$ $\Delta S° = -112 \pm 9$	105
	THF[e]	1.5×10^8 (293 K)	$\Delta H^{\ddagger} = 7.62$ $\Delta S^{\ddagger} = -45.1$	240 (193 K)	$\Delta H^{\ddagger} = 58$ $\Delta S^{\ddagger} = 105$	6.5×10^5 (193 K)	$\Delta H° = -48.5$ $\Delta S° = -140$	106
4OMe-TMPA (**2c**)	EtCN	$(1.93 \pm 0.04) \times 10^4$	$\Delta H^{\ddagger} = 30.5 \pm 0.6$ $\Delta S^{\ddagger} = 8 \pm 3$	1.11 ± 0.06	$\Delta H^{\ddagger} = 62.2 \pm 0.7$ $\Delta S^{\ddagger} = 100 \pm 3$	$(1.73 \pm 0.08) \times 10^4$	$\Delta H° = -31.8 \pm 0.4$ $\Delta S° = -93 \pm 2$	105
TMPAE (**3**)	EtCN	$(8.2 \pm 0.\ 4) \times 10^3$	$\Delta H^{\ddagger} = 31 \pm 5$ $\Delta S^{\ddagger} = 5 \pm 29$	29 ± 2	$\Delta H^{\ddagger} = 63 \pm 5$ $\Delta S^{\ddagger} = 132 \pm 29$	$(2.84 \pm 0.09) \times 10^2$	$\Delta H° = -32 \pm 1$ $\Delta S° = -127 \pm 3$	106
BQPA (**4**)	EtCN	18 ± 1	$\Delta H^{\ddagger} = 30 \pm 2$ $\Delta S^{\ddagger} = -53 \pm 8$	$(6.1 \pm 0.7) \times 10^{-3}$	$\Delta H^{\ddagger} = 65 \pm 4$ $\Delta S^{\ddagger} = 72 \pm 19$	$(2.9 \pm 0.3) \times 10^3$	$\Delta H° = -35 \pm 6$ $\Delta S° = -125 \pm 27$	104
D^1 (**5**)	EtCN	$(1.63 \pm 0.01) \times 10^4$	$\Delta H^{\ddagger} = 20 \pm 1$ $\Delta S^{\ddagger} = -53 \pm 6$	8.0 ± 0.2	$\Delta H^{\ddagger} = 55 \pm 1$ $\Delta S^{\ddagger} = 76 \pm 6$	$(2.03 \pm 0.04) \times 10^3$	$\Delta H° = -35.3 \pm 0.4$ $\Delta S° = -129 \pm 2$	106
Me_6tren (**6**)	EtCN	$(9.5 \pm 0.4) \times 10^4$	$\Delta H^{\ddagger} = 17.1 \pm 0.6$ $\Delta S^{\ddagger} = -52 \pm 3$	$(7.0 \pm 0.3) \times 10^{-2}$	$\Delta H^{\ddagger} = 62.0 \pm 0.6$ $\Delta S^{\ddagger} = 76 \pm 3$	$(1.35 \pm 0.04) \times 10^6$	$\Delta H° = -44.9 \pm 0.2$ $\Delta S° = -128 \pm 1$	109
L^{iPr3} (**7b**)	acetone	0.191 (193 K)	$\Delta H^{\ddagger} = 37.2 \pm 0.5$ $\Delta S^{\ddagger} = -62 \pm 2$					115,116
m-XYL^{iPr4} (**8**)	acetone	2.46 (193 K)	$\Delta H^{\ddagger} = 39.4 \pm 0.5$ $\Delta S^{\ddagger} = -30 \pm 2$					115
i-Pr_4dtne (**10**)	acetone	1.87 (193 K)	$\Delta H^{\ddagger} = 39.4 \pm 0.1$ $\Delta S^{\ddagger} = -32.0 \pm 0.4$					115,117
^{2}L (**11**)	THF					$(3 \pm 1) \times 10^{10}$	$\Delta H° = -69 \pm 1$ $\Delta S° = -177 \pm 4$	118

[a] All data from cryogenic stopped-flow kinetics measurements except where indicated; the rate and equilibrium constants are for process A in Scheme 1. Except for $[(BQPA)Cu]^+$ and $[^2LCu]$, the 1:1 Cu/O_2 adducts are short-lived intermediates only. Solvent coordination is likely in many of the complexes, but is not shown for clarity. [b] Units are $M^{-1}\ s^{-1}$, with values at 183 K unless noted otherwise. [c] Units are kJ mol^{-1} ($\Delta H^{\ddagger}$, $\Delta H°$) or J K^{-1} mol^{-1} ($\Delta S^{\ddagger}$, $\Delta S°$). [d] Equal to k_1/k_{-1}; units are M^{-1}, with values at 183 K unless noted otherwise. [e] Data obtained using "flash-and-trap" method, whereby the carbon monoxide complex was flash-photolyzed and the trapping of the intermediate THF complex by O_2 was measured.

Scheme 2

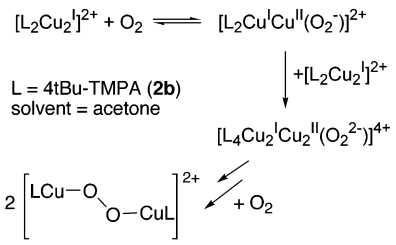

noted for other multidentate ligand systems.[132,133] Kinetic data for the system supported by 4-tBu-TMPA (**2b**) were interpreted to indicate binding of O_2 to one Cu(I) ion in the dimer to yield a mixed-valent Cu(I)Cu(II) superoxo species. Subsequent reaction with another dicopper(I) complex to afford a tetracopper peroxo intermediate (a precedented motif; section 4)[134,135] was suggested to precede cleavage and reaction with a second O_2 molecule to yield the final 2:1 Cu/O_2 product.

Even greater enhancement of the stability of a 1:1 adduct was observed for ^{2}L (**11**); $^2LCuO_2$ is remarkably more stable than the adducts supported by other tetradentate tripodal ligands by virtue of a significantly more negative reaction enthalpy ($K_1 = 3 \times 10^{10}$ M^{-1} at 183 K corresponding to a $\sim 10^8$-fold enhancement relative to TMPA (**1**), $\Delta H° = -69 \pm 1$ kJ mol^{-1}).[117] The negative charge provided by ^{2}L (**11**) may be construed as a basis for this result, through stabilization of the Cu(II) state of the adduct. An alternative rationale may be considered in which differences in O_2 coordination modes are invoked, but while there is resonance Raman spectroscopic evidence in favor of η^2-O_2 coordination in $^2LCuO_2$, the mode of binding in the other tetradentate ligand systems is not known.

2.3. Reactions of 1:1 Cu/O_2 Adducts to Yield Higher Nuclearity Complexes

With only a few exceptions, initially formed 1:1 Cu/O_2 complexes generally react rapidly to yield 2:1 (and sometimes higher nuclearity) species that in many cases exhibit thermodynamic stability sufficient for detailed characterization. The most commonly observed products contain μ-η^1:η^1-peroxo-, μ-η^2:η^2-peroxo-, or bis(μ-oxo)dicopper cores (Chart 2), the structural and spectroscopic features of which have been well defined.[61−90] In the following discussion, we first consider the reactions of monocopper(I) complexes with O_2 that follow the pathway in Scheme 1 to yield 2:1 Cu/O_2 species. We then discuss the formation of such species from dicopper(I) precursors comprising dinucleating supporting ligands, for which less clear evidence for prior 1:1 adduct generation is typically available. Finally, mechanistic aspects of the formation of 3:1 Cu/O_2 species are presented.

Stopped-flow kinetic studies of the reactions of mononuclear Cu(I) complexes of the tetradentate tripodal ligands TMPA (**1**),[102−104] 4R-TMPA (**2a**−**d**),[105] TMPAE (**3**),[105] BPQA (**19**),[104] BQPA (**4**),[104] Me_6tren (**6**),[96,97,108,109] and ^{2}L (**11**)[118] generally support similar pathways for the formation of 2:1 Cu/O_2 products via trapping of 1:1 adducts by unreacted Cu(I) species, but with significant differences in thermodynamic parameters for the individual steps that result from ligand structural disparities and/or solvent effects (Table 3). A μ-η^1:η^1-peroxodicopper product is the thermodynamically most stable species (vs the 1:1 precursor) for TMPA (**1**), TMPAE (**3**), BPQA (**19**), and Me_6tren (**6**). As for the 1:1 Cu/O_2 adducts described above for TMPA (**1**) and 4-substituted derivatives (**2a**−**d**), the peroxo species are more stable when THF is used as solvent (e.g., for TMPA (**1**), $\Delta H°$ ($\beta = K_1K_2$) $= -77$ kJ mol^{-1} in EtCN vs. -94 kJ mol^{-1} in THF) and when the ligand is more electron donating (4-OMe-TMPA, **2c**). On the other hand, the replacement of a pyridyl arm in TMPA (**1**) to yield the more hindered BPQA (**19**) results in decreased stability. Substituting a second pyridyl group in TMPA with a quinolyl group introduces sufficient steric bulk (BQPA, **4**) to make the initial 1:1 Cu/O_2 adduct the thermodynamic product, rather than the μ-η^1:η^1-peroxodicopper complex. Analogous, yet less drastic destabilization of the 2:1 Cu/O_2 complex supported by Me_6tren (**6**) relative to its 1:1 precursor also has been attributed to steric effects. Other ligand effects on Cu/O_2 reaction kinetics are more subtle, such as the finding that the Cu(I) complex of PMEA (**20**), which differs from TMPA only by virtue of one additional methylene spacer in one pyridylmethyl arm, yields a μ-η^1:η^1-peroxo species directly (without an observable intermediate) that is unstable toward irreversible decomposition.[136]

Similar to the aforementioned case of BQPA (**4**), initial binding of O_2 to the Cu(I) of ^{2}L (**11**) in THF gives rise to a thermodynamically stable 1:1 Cu/O_2 adduct that subsequently evolves to a relatively unstable μ-η^1:η^1-peroxo species that is only observed by spectroscopy under conditions when sub-stoichiometric O_2 is used. In the presence of excess O_2, the peroxo species is only detected in steady-state concentrations with a small equilibrium constant, indicating that the overall equilibrium eq 1 lies to the left. The enormous difference in relative stabilities (also alluded to above, section 2.2) of the 1:1 and 2:1 complexes supported by TMPA (**1**) and ^{2}L (**11**) is reflected by the reaction enthalpies associated with K_1 and K_2. For TMPA (**1**), $\Delta H_2°$ is more negative (favorable) than $\Delta H_1°$, but the situation is reversed for ^{2}L (**11**), where $\Delta H_2°$ is rather small (-25 kJ mol^{-1}). In an alternative comparison, at 223 K for TMPA (**1**) $K_1/K_2 = 4.0 \times 10^{-5}$, whereas for ^{2}L (**11**) this ratio is 3.8×10^3, a $\sim 10^8$ fold difference.

$$2\ ^2LCuO_2 \rightleftarrows [(^2LCu)_2(O_2)] + O_2 \qquad (1)$$

Oxygenation rate data are available for mononuclear Cu(I) complexes of the tridentate ligands $L^{RR'}$ (**7a**−**g**),[115,116] (L*n*)$_3$tacn (**21a**−**c**),[137] AN (**12a**),[114] MeAN (**12b**),[114] ^{H}Py2^{Me} (**13b**),[119] ^{H}Py2^{Phe} (**13c**),[113] and ^{H}Py1^{Et,Phe} (**22a**),[120] which yield μ-η^2:η^2-peroxo and/or bis(μ-oxo)dicopper complexes. For the Cu(I) complex of L^{iPr3} (**7b**) in acetone, both types of isomeric dicopper complexes form in parallel according to the simple rate law eq 2.[115,116]

$$\text{rate} = k[(L^{iPr3}Cu)^+][O_2] \qquad (2)$$

Table 3. Selected Kinetic and Thermodynamic Parameters for the Formation of 2:1 Cu/O_2 Adducts upon Low Temperature Oxygenation of Cu(I) Complexes[a]

ligand	solvent	k_2[b]	activation parameters (k_2)[c]	k_{-2}[b]	activation parameters (k_{-2})[c]	K_2[d]	thermodynamic parameters (K_2)[c]	ref
TMPA (**1**)	EtCN	$(1.34 \pm 0.02) \times 10^4$	$\Delta H^{\ddagger} = 22.6 \pm 0.1$ $\Delta S^{\ddagger} = -38.6 \pm 0.6$	$(2.0 \pm 0.2) \times 10^{-5}$	$\Delta H^{\ddagger} = 69.8 \pm 0.6$ $\Delta S^{\ddagger} = 51 \pm 3$	$(6.7 \pm 0.7) \times 10^8$	$\Delta H° = -47.2 \pm 0.6$ $\Delta S° = -89 \pm 2$	105
	THF	$(1.0 \pm 0.2) \times 10^5$	$\Delta H^{\ddagger} = 17.5 \pm 0.1$ $\Delta S^{\ddagger} = -50 \pm 1$	2×10^{-6}	$\Delta H^{\ddagger} = 70 \pm 4$ $\Delta S^{\ddagger} = 32 \pm 14$	5×10^{10}	$\Delta H° = -53 \pm 4$ $\Delta S° = -82 \pm 14$	105
4OMe-TMPA (**2c**)	EtCN	$(1.85 \pm 0.01) \times 10^4$	$\Delta H^{\ddagger} = 20.59 \pm 0.06$ $\Delta S^{\ddagger} = -46.7 \pm 0.3$	$(8 \pm 2) \times 10^{-6}$	$\Delta H^{\ddagger} = 69 \pm 1$ $\Delta S^{\ddagger} = 40 \pm 5$	$(2.4 \pm 0.7) \times 10^9$	$\Delta H° = -49 \pm 1$ $\Delta S° = -87 \pm 5$	105
TMPAE (**3**)	EtCN	15.2 ± 0.5	$\Delta H^{\ddagger} = 21 \pm 1$ $\Delta S^{\ddagger} = -43 \pm 3$	$(2.1 \pm 0.4) \times 10^{-5}$	$\Delta H^{\ddagger} = 66 \pm 1$ $\Delta S^{\ddagger} = 33 \pm 5$	$(7 \pm 2) \times 10^5$	$\Delta H° = -45 \pm 1$ $\Delta S° = -76 \pm 6$	106
BQPA (**4**)	EtCN					$(2.0 \pm 0.2) \times 10^3$	$\Delta H° = -15$ $\Delta S° = -20$	104
Me_6tren (**6**)	EtCN	$(1.53 \pm 0.04) \times 10^4$	$\Delta H^{\ddagger} = 17.0 \pm 0.2$ $\Delta S^{\ddagger} = -67.9 \pm 0.9$	$(5.8 \pm 0.9) \times 10^{-5}$	$\Delta H^{\ddagger} = 63.7 \pm 0.8$ $\Delta S^{\ddagger} = 26 \pm 3$	$(1.4 \pm 0.7) \times 10^8$	$\Delta H° = -46.7 \pm 0.9$ $\Delta S° = -94 \pm 3$	109
D^1 (**5**)	EtCN	35.1 ± 0.5	$\Delta H^{\ddagger} = 37 \pm 1$ $\Delta S^{\ddagger} = -9 \pm 2$	$(3.9 \pm 0.3) \times 10^{-1}$	$\Delta H^{\ddagger} = 37 \pm 1$ $\Delta S^{\ddagger} = -49 \pm 3$	90 ± 7	$\Delta H° = 0.5 \pm 0.6$ $\Delta S° = 40 \pm 3$	106
^{2}LCu (**11**)	THF	$(8.7 \pm 0.2) \times 10^3$ (213 K)	$\Delta H^{\ddagger} = 22.9 \pm 0.4$ $\Delta S^{\ddagger} = -40 \pm 0.2$	19 ± 9 (213 K)	$\Delta H^{\ddagger} = 48 \pm 12$ $\Delta S^{\ddagger} = 6 \pm 53$	$(5 \pm 2) \times 10^3$ (213 K)	$\Delta H° = -25 \pm 12$ $\Delta S° = -46 \pm 53$	118
AN (**12a**)	CH_2Cl_2	$(2.7 \pm 0.1) \times 10^4$ [e]	$\Delta H^{\ddagger} = -9.9 \pm 0.6$ $\Delta S^{\ddagger} = -210 \pm 3$			$(1.02 \pm 0.07) \times 10^6$ [f]	$\Delta H° = -24 \pm 1$ $\Delta S° = -14 \pm 6$	114
MeAN (**12b**)	CH_2Cl_2	$(6.9 \pm 0.7) \times 10^2$ [e]	$\Delta H^{\ddagger} = -27 \pm 3$ $\Delta S^{\ddagger} = -335 \pm 16$			$(7.6 \pm 0.6) \times 10^{-2}$ [f]	$\Delta H° = -28 \pm 2$ $\Delta S° = -61 \pm 12$	114
$^{H}Py2^{Me}$ (**13b**)	CH_2Cl_2	$(1.91 \pm 0.03) \times 10^4$ (253 K)[e]	$\Delta H^{\ddagger} = -0.7 \pm 1$ $\Delta S^{\ddagger} = -164 \pm 4$			$(5.9 \pm 0.3) \times 10^5$ [f]	$\Delta H° = -89 \pm 3$ $\Delta S° = -240 \pm 9$	119
$^{H}Py2^{Phe}$ (**13c**)	THF	11 ± 1 (193 K)	$\Delta H^{\ddagger} = 19.3 \pm 0.4$ $\Delta S^{\ddagger} = -91.6 \pm 2.0$					113
BPQA (**19**)	EtCN			$(1.5 \pm 0.8) \times 10^{-4}$	$\Delta H^{\ddagger} = 61 \pm 3$ $\Delta S^{\ddagger} = 19 \pm 10$	$(1.7 \pm 0.2) \times 10^{10}$ [f]	$\Delta H° = -69 \pm 2$ $\Delta S° = -181 \pm 5$	104
$^{H}Py1^{Et,Phe}$ (**22a**)	acetone	*g*	$\Delta H^{\ddagger} = 25.3 \pm 1.1$ $\Delta S^{\ddagger} = -22.8 \pm 6.0$					120

[a] All data from cryogenic stopped-flow kinetics measurements. Except where noted, the rate and equilibrium constants are for process B in Scheme 1. Solvent coordination is likely in many of the complexes, but is not shown for clarity. [b] Units are M^{-1} s^{-1}, with values at 183 K unless noted otherwise. [c] Units are kJ mol^{-1} ($\Delta H^{\ddagger}$, $\Delta H°$) or J K^{-1} mol^{-1} ($\Delta S^{\ddagger}$, $\Delta S°$). [d] Equal to k_2/k_{-2}; units are M^{-1}, with values at 183 K unless noted otherwise. [e] No discernible 1:1 Cu/O_2 intermediate; reported rate constant is interpreted as composite ($k_{on} = k_2K_1$), with units M^{-2} s^{-1}. [f] A composite, overall equilibrium constant, with units M^{-2}. [g] Not reported.

This rate law and the similarity of the activation parameters to those of the system supported by BQPA (**4**, Table 2) support 1:1 adduct formation as rate-limiting, with all subsequent steps leading to the final product mixture being fast. As described below (section 3), the data are also consistent with rapid equilibration between the isomeric 2:1 Cu/O_2 products. Dendrimer size influences the oxygenation rates of the Cu(I) complexes of $(Ln)_3$tacn (**21a**−**c**), the rate constant for $(L2)_3$tacn (**21a**, $k = 1.39\ M^{-1}\ s^{-1}$) being 2 orders of magnitude larger than for $(L3)_3$tacn (**21b**, $k = 1.3 \times 10^{-2}\ M^{-1}\ s^{-1}$).[137] Complete shielding of the Cu(I) sites by $(L4)_3$tacn (**21c**) prevents oxygenation entirely. The Cu(I) complexes of AN (**12a**) and MeAN (**12b**) in CH_2Cl_2 yield either a bis(μ-oxo)- or a μ-η^2:η^2-peroxodicopper complex, respectively.[114] Both reactions are reversible, lack observable intermediates, and are characterized by negative activation enthalpies and large negative activation entropies (Table 3). These data have been interpreted to indicate a rapid, left-lying preequilibria involving a 1:1 Cu/O_2 intermediate, eq 3. Similar results were communicated for the system comprising $^{H}Py2^{Me}$ (**13b**), although in this case kinetic and spectroscopic data indicate that the product is a mixture of equilibrating μ-η^2:η^2-peroxo and bis(μ-oxo) species.[119] Irreversible formation of a μ-η^2:η^2-peroxo complex was observed with $^{H}Py2^{Phe}$ (**13c**) as supporting ligand, and a second-order dependence on the Cu(I) precursor concentration on the rate of product formation was determined.[113] Similar kinetics were observed for bis(μ-oxo)dicopper complex formation upon oxygenation of the Cu(I) complex of the bidentate ligand $^{H}Py1^{Phe}$ (**22a**).[120] The results for both systems were interpreted to indicate rate-controlling reaction between a Cu(I) complex and O_2 to yield a 1:1 adduct formed in a rapid preequilibrium.

$$LCu + O_2 \rightleftarrows LCuO_2$$

(L = AN (**12a**), MeAn (**12b**), $^{H}Py2^{Me}$ (**13b**)) (3)

Because of equilibria such as that shown in eq 3 and the usually rapid trapping of 1:1 adducts (process B, Scheme 1), the stepwise synthesis of 2:1 Cu/O_2 species by the sequential reaction of a 1:1 adduct with a second Cu(I) complex, which by itself could react with O_2, is generally not possible. However, this route was made feasible by the discovery that the 1:1 Cu/O_2 adduct supported by Me_2L^{iPr2} (**18a**) is stable in solution at low temperature in the absence of O_2.[124,125] Thus, after removal of excess O_2, $(Me_2L^{iPr2})CuO_2$ was treated with the Cu(I) complexes of Me_2L^{Me2} (**18c**),[125] Me_4pda (**23a**),[125] L^{Me3} (**7a**),[125] or L^{iPr3} (**7b**)[138] to yield the "asymmetric" bis(μ-oxo) complexes with different supporting ligands on each copper center (Scheme 3). These products were identified by UV−vis and resonance Raman spectroscopy, as well as by X-ray crystallography in one instance. The success of this stepwise approach for the synthesis of such 2:1 Cu/O_2 complexes provides precedence for broader potential applications, such as the preparation of mixed metal species (e.g., $[(Me_2L^{iPr2})Cu(O)_2ML]^{n+}$).

The overall pathway in Scheme 1 also generally applies to oxygenation reactions of dicopper complexes comprising dinucleating ligands, although the kinetics are sometimes more complicated and 1:1 species are less readily observable for these systems. For example, consider the complexes of the series *m*-XYL^{iPr4} (**8**),[115] *p*-XYL^{iPr4} (**9**),[115] and *i*-Pr_4dtne (**10**),[115,117] where the structural attributes of the linker bridging the triazacyclononane moieties signficantly influences the oxygenation mechanism (Scheme 4). For *i*-Pr_4dtne (**10**) in which a short ethylene linker tethers the macrocycles, bis(μ-oxo)-dicopper complex formation proceeds with kinetics similar to that observed for L^{iPr3} (**7b**), such that initial 1:1 adduct formation is rate-determining and subsequent 2:1 adduct formation is fast. Similar rate-determining 1:1 Cu/O_2 complex formation ensues with *m*-XYL^{iPr4} (**8**) and *p*-XYL^{iPr4} (**9**), but for the former the nature of the final product depends on the initial concentration of the dicopper(I,I) precursor, such that the μ-η^2:η^2-peroxo core predominates under dilute conditions and the bis(μ-oxo) unit is favored at high concentration. Only bis(μ-oxo) core formation is seen with *p*-XYL^{iPr4} (**9**). These results were interpreted to indicate a competition between intramolecular and intermolecular dioxygen activation pathways (Scheme 4). An intramolecular path is geometrically possible with *m*-XYL^{iPr4} (**8**), and because of the steric constraints of the *m*-xylyl bridge that enforce relatively large intermetal separations, the μ-η^2:η^2-peroxo motif is favored relative to the isomeric bis(μ-oxo) core. At higher concentrations for *m*-XYL^{iPr4} (**8**), and under all conditions for *p*-XYL^{iPr4} (**9**), intermolecular species predominate, and bis(μ-oxo) core formation becomes favored because closer approach of the metal ions is enabled (e.g., because of loss of the bridge geometric constraint operative in the intramolecular adduct of *m*-XYL^{iPr4} (**8**)).

Related competition between intra- and intermolecular paths occurs with the dicopper system supported by D^1 (**5**).[111] Through a detailed analysis of the stopped flow kinetic data, the effects of the ethylene linker in D^1 (**5**) on the activation and thermodynamics of dioxygen binding were assessed. Not surprisingly, the linker has no discernible effect on the initial O_2 binding reaction, as indicated by similar ΔH_1° and ΔS_1° values for the TMPA (**1**) and D^1 (**5**) systems. However, the μ-η^1:η^1-peroxo complex formation process (k_2) for D^1 (**5**) is characterized by a significantly (~70 $J\ K^{-1}\ mol^{-1}$) more favorable entropy of activation and a less favorable $\Delta S^\ddagger$ for the back reaction (k_{-2}) than for TMPA (**1**). As a result, the reaction entropy for μ-η^1:η^1-peroxo formation is more favorable for D^1 (**5**) by ~140 $J\ K^{-1}\ mol^{-1}$. On the other hand, this entropic stabilization of the 2:1

Scheme 3

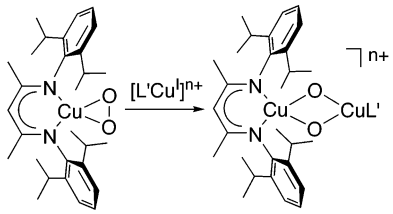

L' = Me_2L^{Me2-} (**18c**, n = 0), Me_4pda (**23a**, n = 1), L^{Me3} (**7a**, n = 1), L^{iPr3} (**7b**, n = 1)

Scheme 4

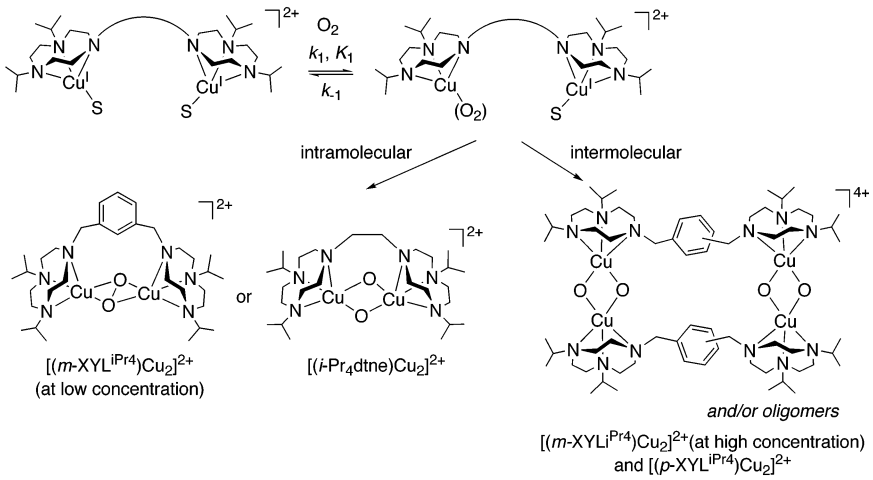

Scheme 5

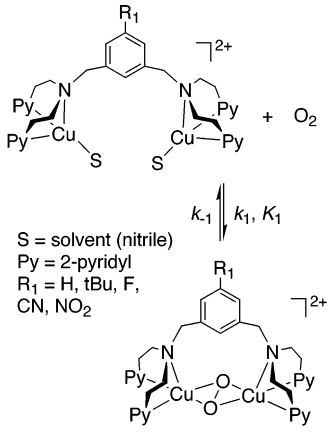

Cu/O_2 species by the tether linking the N donors in D^1 (**5**) is offset by enthalpic destabilization (i.e., strain) that is reflected in a higher $\Delta H^{\ddagger}_2$, a lower $\Delta H^{\ddagger}_{-2}$, and a correspondingly decreased enthalpic driving force ($\Delta H°$ more positive by almost 50 kJ mol^{-1}) compared to the TMPA (**1**) case. Relief of enthalpic strain is accomplished through intermolecular adduct formation (oligomerization), as seen for the *m*-XYL^{iPr4} (**8**) system.

Potentially tridentate bis(pyridyethyl)amine or similar donor groups are linked in R-XYL-H (**24a**−**f**),[139,140] R-XYL-O^- (**24g**),[139,141] D (**25**),[142] UN−O^- (**26b**),[143,144] PD (**27a**),[145] N_4Py2 (**14b**),[112] MEPY22PZ (**28**),[146] and dendrimer **29**,[147] and the variable tethers also influence the Cu/O_2 reactivity, albeit apparently without the complication of competition between intra- and intermolecular paths.[148] With one exception (**24b**, R = OMe), the series of related complexes $[(R\text{-}XYL\text{-}H)Cu_2]^{2+}$ (ligands **24a,c**−**f**, R = H, *t*Bu, F, CN, NO_2) yield μ-η^2:η^2-peroxo species upon low-temperature oxygenation (Scheme 5).[139,140] By varying the remote substituent (R_1 in the drawing of the ligand in Chart 1 and Scheme 5) the influence of changes in the electronic properties of the spacer could be investigated systematically (Table 4). In general, the activation enthalpies for initial O_2 binding are low (<10 kJ mol^{-1}) but are offset by significantly negative activation entropies. Studies at high pressure revealed a correspondingly negative volume of activation ($\Delta V^{\ddagger}$) of -15 ± 2.5 cm^3 mol^{-1} for the oxygenation (k_1) of the system with R = H (**24a**) in acetone.[149] For R = MeO (**24b**), NMR studies indicate that at low temperature the substituent interacts with the Cu(I) centers resulting in formation of a complex that is unsuitable for O_2 binding to yield the μ-η^2:η^2-peroxo unit. A similar effect in the fluoro-substituted system (**24d**) is thought to explain anomalies in thermodynamic and kinetic data for adduct formation compared to the other systems. The cyano- substituted system (**24e**) does form the 2:1 Cu/O_2 adduct at low temperature, but an interfering photochemical reaction prevents the process from being followed spectrophotometrically so no kinetic or thermodynamic data can be obtained. Comparing the cases in which R = NO_2 (**24f**) versus R = *t*Bu (**24c**), activation enthalpies for O_2 dissociation are lower and overall reaction enthalpies for peroxo complex formation are less favorable for the nitro-subsituted system. Two possible explanations have been offered for the apparently stronger binding of O_2 to the dicopper complex when the remote R group is more electron-donating.[140] According to one hypothesis, direct interaction of the electrophilic Cu_2O_2 core with the arene ring (as proposed for the mechanism of ring hydroxylation, section 5.1) is suggested to result in differential stabilization of the peroxo complex when R is varied. A second suggestion is that there are differences in the stabilities of the conformations of the dicopper(I) complex and/or the intermediate 1:1 Cu/O_2 adduct for the differently substituted ligands (cf. the flexibility of the benzylic linkages) that somehow influence the kinetic parameters.

A related argument invoking differences in conformational flexibility was invoked to explain the $\sim 10^3$-fold weaker binding of O_2 at 195 K to the dicopper(I) complex of **30** relative to $[(XYL\text{-}H)Cu_2]^{2+}$, in which identical xylyl groups link different N-donors (benzimidazolyl vs pyridyl).[150] Entropic stabilization conferred by the MEPY22PZ ligand (**28**) also was cited to rationalize the room-temperature stability of its μ-η^1:η^1-peroxo complex.[146] Similar arguments were presented to explain the enhanced stability (relative to irreversible decay) of the peroxo complexes supported by BPL2 (**31**, $t_{1/2} \sim 50$ min at 298 K) relative to BPL (**32**, $t_{1/2} \sim 15$ s at 250 K),[151] and by N_2tripy

Table 4. Selected Kinetic and Thermodynamic Parameters for the Formation of 2:1 Cu/O_2 Adducts upon Low Temperature Oxygenation of Dicopper(I) Complexes[a]

complex	k_1[b]	activation parameters (k_1)[c]	k_{-1}[b]	activation parameters (k_{-1})[c]	K_1[d]	thermodynamic parameters (K_1)[c]	ref
XYL-H (**24a**)	385 ± 5	$\Delta H^{\ddagger} = 8.2 \pm 1$ $\Delta S^{\ddagger} = -146 \pm 1$	$(1.5 \pm 0.4) \times 10^{-5}$	$\Delta H^{\ddagger} = 70 \pm 1$ $\Delta S^{\ddagger} = 50 \pm 6$	2.6×10^7	$\Delta H° = -62 \pm 1$ $\Delta S° = -196 \pm 6$	139,140
tBu-XYL-H (**24c**)	$(4.9 \pm 0.2) \times 10^2$	$\Delta H^{\ddagger} = 9.1 \pm 0.3$ $\Delta S^{\ddagger} = -140 \pm 1$	$(5 \pm 2) \times 10^{-6}$	$\Delta H^{\ddagger} = 83 \pm 4$ $\Delta S^{\ddagger} = 110 \pm 20$	9.6×10^7	$\Delta H° = -74 \pm 4$ $\Delta S° = -250 \pm 20$	140
F-XYL-H (**24d**)	9.3 ± 0.3	$\Delta H^{\ddagger} = 29 \pm 1$ $\Delta S^{\ddagger} = -66 \pm 1$	$(3 \pm 1) \times 10^{-6}$	$\Delta H^{\ddagger} = 81 \pm 3$ $\Delta S^{\ddagger} = 90 \pm 10$	3.3×10^6	$\Delta H° = -52 \pm 3$ $\Delta S° = -156 \pm 10$	140
NO_2-XYL-H (**24f**)	109 ± 2	$\Delta H^{\ddagger} = 6.4 \pm 0.1$ $\Delta S^{\ddagger} = -167 \pm 1$	$(1.8 \pm 0.2) \times 10^{-5}$	$\Delta H^{\ddagger} = 59 \pm 1$ $\Delta S^{\ddagger} = -8 \pm 4$	5.9×10^6	$\Delta H° = -53 \pm 1$ $\Delta S° = -159 \pm 4$	140
30a[e]	1.1		7.8×10^{-5}		1.4×10^4		150
XYL-O^- (**24g**)	$>10^6$ [f]				6.5×10^8	$\Delta H° = -66 \pm 1$ $\Delta S° = -192 \pm 2$	139
N_4Py2 (**14b**)[g]	**A**: $(1.1 \pm 0.1) \times 10^4$ **B**: $(8.5 \pm 0.2) \times 10^3$	$\Delta H^{\ddagger} = 0 \pm 3$ $\Delta S^{\ddagger} = -162 \pm 18$ $\Delta H^{\ddagger} = 18 \pm 2$ $\Delta S^{\ddagger} = -70 \pm 9$	*h* *h*		$(4.5 \pm 0.4) \times 10^2$ $(7 \pm 3) \times 10^7$	$\Delta H° = -28 \pm 3$ $\Delta S° = -101 \pm 19$ $\Delta H° = -58 \pm 2$ $\Delta S° = -165 \pm 8$	112

[a] All data from cryogenic stopped-flow kinetics measurements, CH_2Cl_2 solvent. The rate and equilibrium constants are for the processes denoted in the respective Schemes 5–7. Solvent coordination is likely in many of the complexes, but is not shown for clarity. [b] Units are M^{-1} s^{-1}, with values at 183 K unless noted otherwise. [c] Units are kJ mol^{-1} ($\Delta H^{\ddagger}$, $\Delta H°$) or J K^{-1} mol^{-1} ($\Delta S^{\ddagger}$, $\Delta S°$). [d] Equal to k_1/k_{-1}; units are M^{-1}, with values at 183 K unless noted otherwise. [e] Values measured at 195 K. [f] Equilibration with O_2 in <5 ms. [g] **A** and **B** refer to data corresponding to k_1^A or K_1^A and k_1^B or K_1^B, respectively (Scheme 7). [h] Not reported, but may be calculated from k_1 and K_1.

Scheme 6

(**33**, $t_{1/2}$ = 25.5 h at 298 K) compared to tripy (**34**, observable only at low temperature).[152]

In the oxygenation of the dicopper(I) complex of XYL-O^- (**24g**), where a phenolate links the two Cu(I) ions, an asymmetrically disposed peroxide bridge is proposed to form (Scheme 6).[139,141] A similar adduct forms upon oxygenation of the complex supported by UN−O^- (**26b**), but it is more stable, such that it may be isolated as a solid.[143] One-electron oxidation of this adduct yields a species formulated as a unique dicopper-superoxide, which also may be accessed by direct low-temperature oxygenation of the mixed-valence precursor [(UN−O^-)Cu(I)Cu(II)]$^{2+}$.[144] For XYL-O^- (**24g**), dioxygen is bound reversibly and too rapidly for kinetic data to be obtained, even at 173 K, but overall thermodynamic data for O_2 binding are in line with other systems, including R-XYL-H (**24a**−**f**). The increase in the rate of binding of O_2 relative to the complexes of R-XYL-H is proposed to arise from preorganization of the system in a conformation suitable for 2:1 complex formation (k_1 in Table 4). Greater electron donation by the phenolate moiety also could be a basis for the increased oxygenation rate.

The linker in N_4Py2 (**14b**) is significantly more flexible than the xylyl bridges in R-XYL-H (**24a**−**f**) and XYL-O^- (**24g**), and as a result a more complicated reaction scheme for oxygenation of [(N_4Py2)Cu_2]$^{2+}$ is observed (Scheme 7).[112] Two peroxodicopper species form in parallel, the μ-η^1:η^1 (end-on) complex **A**, which is characterized by UV−vis spectroscopic features similar to those of [(TMPA)$_2Cu_2(O_2)$]$^{2+}$, and the μ-η^2:η^2 (side-on) compound **B**. Species **B** is thermodynamically favored relative to **A**, as indicated by the overall reaction enthalpies of −58 versus −28 kJ mol^{-1}, respectively (Table 4). However, the kinetic data rule out sequential formation of **B** directly from **A**, and require the intermediacy of either the starting dicopper(I) complex or a transient 1:1 adduct ("**Tr**"). The complex **Tr** is not observed, but is thought to be a steady-state intermediate formed in a rapid preequilibrium because (a) the formation of the initial peroxo species **A** occurs with an activation enthalpy of zero and (b) it is unlikely that 2:1 Cu/O_2 adduct formation proceeds in synchronous fashion. It is noteworthy that both **A** and **B** form more quickly than the peroxo complex supported by R-XYL-H (**24a**; compare k_1 values in Table 4). This result has been

Scheme 7

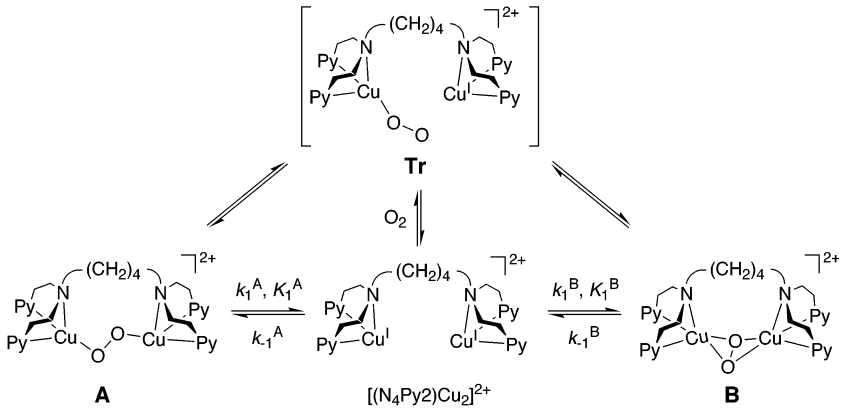

interpreted to indicate that increased rates of O_2 adduct formation may result from greater flexibility in a dinucleating ligand.[100]

The effect of the linker in a dinucleating ligand system was explored in studies of the O_2 reactivity of a dicopper(I) complex of $L_3(Py2)_2$ (**35**), which contains a substrate receptor between bis(pyridylethyl)amine chelates.[153] Complexes of L_1Py2 (**36**) and $L_2(Py2)_2$ (**37**) were studied for comparison. Although detailed kinetics data for the oxygenations are not available, pseudo-first-order rate constants for the formation of 2:1 Cu/O_2 species obtained at 188 K revealed faster oxygenations of $[(L_3(Py2)_2)_2Cu_2]^{2+}$ ($k_{obs} = 3.41 \times 10^3$ s^{-1}) and $[(L_2(Py2)_2)_2Cu_2]^{2+}$ ($k_{obs} = 23 \times 10^3$ s^{-1}) than $[(L_1Py2)Cu]^+$ ($k_{obs} = 2.56 \times 10^2$ s^{-1}). These results were interpreted to support intramolecular adduct formation for the dinucleating ligand systems.

Finally, species of higher nuclearity than two have been targeted to model O_2 activation at the tricopper active sites of the multicopper oxidases. One strategy involves building multinucleating ligand scaffolds designed to preorganize N-donor groups so that three or more metal centers are collected in close proximity. While several such scaffolds have been constructed,[154−157] to date none have led to well-characterized Cu/O_2 adducts.[158] However, a few 3:1 Cu/O_2 adducts have been prepared by using simple bidentate ligands with substituents featuring minimized steric bulk (see a recent review[89] for discussion of this steric issue). Thus, a bis(μ_3-oxo)tricopper(II,II,III) complex was reported upon low-temperature oxygenation of the Cu(I) complex of Me_4Cyda (**38a**) at concentrations > 10 mM.[159,160] Reaction of an initially formed bis(μ-oxo)dicopper compound with a third Cu(I) precursor is a reasonable pathway for tricopper complex formation, but supporting mechanistic evidence is lacking for this system. An analogous product was recently reported for the oxygenation of the Cu(I) complex of $^{H}Py1^{Me,Me}$ (**15c**), and in this case mechanistic data for the process were obtained.[161] When a 5.0 mM solution of $[(^{H}Py1^{Me,Me})Cu(O_3SCF_3)]$ in acetone was oxygenated, the rate of formation of the tricopper species showed a first-order dependence on the copper(I) complex concentration, indicating that 1:1 Cu/O_2 formation is rate-determining and that subsequent additions of Cu centers are fast. Direct support for the trapping of a bis(μ-oxo)dicopper species by a Cu(I) complex was obtained in experiments performed at lower concentrations of starting Cu(I) compound (e.g., 0.2 mM), where UV−vis spectroscopy indicated that a mixture of bis(μ-oxo)-dicopper and bis(μ_3-oxo)tricopper products formed. Addition of more starting Cu(I) complex to these mixtures resulted in conversion of the dicopper to the tricopper species, and a second-order rate constant for this reaction was determined ($3.4 \pm 0.2 \times 10^2$ M^{-1} s^{-1} at 179 K).

3. Isomerism between μ-η^2:η^2-Peroxo- and Bis(μ-oxo)dicopper Complexes

Interconversion of the isomeric μ-η^2:η^2-peroxo- and bis(μ-oxo)dicopper cores represents a possible pathway for the reversible making and breaking of the dioxygen O−O bond in a dimetal system. As such, it is relevant to a variety of biological and other processes, such as aerobic oxidations, catalytic decomposition of NO to N_2 and O_2,[162] and photosynthetic O_2 evolution.[163] Initially discovered for the system supported by L^{iPr3} (**7b**, Scheme 8),[116] the process has been identified for a number of other complexes of N-donor ligands and has been the subject of numerous theoretical studies.[164−171] A key finding from theory is that the reaction involves a continuous diabatic correlation of occupied orbitals, analogous to symmetry-allowed pericyclic reactions.[164]

Scheme 8

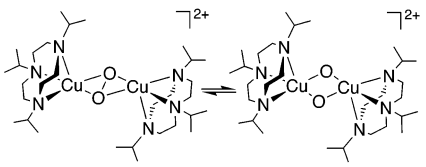

The existence of a rapid equilibrium between $[(L^{iPr3}Cu)_2(\mu\text{-}\eta^2\text{:}\eta^2\text{-}O_2)]^{2+}$ and $[(L^{iPr3}Cu)_2(\mu\text{-}O)_2]^{2+}$ in solution was postulated on the basis of several lines of evidence.[116,172] As noted above, stopped-flow kinetics data showed that the oxygenation of $[L^{iPr3}Cu(MeCN)]^+$ in acetone obeys a rate law that is first order with respect to the concentrations of O_2 and Cu(I) complex (eq 2). These data indicate that formation of a 1:1 adduct is rate determining, even though such an adduct is not observed. The observed products in

acetone are a ~4:1 mixture of the μ-η^2:η^2-peroxo and bis(μ-oxo) complexes, and each forms at the same rate over a range of temperatures (190−223 K). A mechanism consistent with these data involves fast reaction of the initially formed 1:1 adduct with a Cu(I) starting complex to yield a rapidly equilibrating mixture of the peroxo and bis(μ-oxo) isomers. In further support of this equilibrium, reversible temperature-dependent shifts of their ratio in dilute THF solution were identified, and thermodynamic parameters were determined: $\Delta H° = 4$ kJ mol^{-1} and $\Delta S° = 25$ J mol^{-1} K^{-1}. Also consistent with the existence of the equilibrium, solvent influences the ratio of the isomers, with the peroxo favored in CH_2Cl_2 and the bis(μ-oxo) favored in THF. Importantly, the isomer ratios were shifted immediately in solvent mixing experiments.

Other systems for which direct evidence supporting facile equilibration of the peroxo and bis(oxo) isomers has been obtained are those supported by the bidentate diamines $R_2R'_2$eda (**39**) and $R_2R'_2$pda (**23**)[89,173,174] and the tridentate ligand ^{H}Py2^{Me} (**13b**).[119,171] For the diamines, ratios of peroxo and bis(μ-oxo) isomers that are dependent on supporting ligand structure, solvent, counteranion, and temperature were observed. With one exception (see below), a rapid equilibrium for each diamine-supported system was indicated by the finding that the relative amounts of the isomers in THF, acetone, or CH_2Cl_2 varied reversibly with changes in temperature. Changing the counterion in select cases also shifted the product ratio.[89] For the system ligated by tBu_2Me_2eda (**39a**), thermodynamic parameters associated with K_{eq} (= [peroxo]/[bis(μ-oxo)]) in CH_2Cl_2 were estimated to be $\Delta H° \sim 3$ kJ mol^{-1} and $\Delta S° \sim 8$ J mol^{-1} K^{-1}, similar to the L^{iPr3} case discussed above. Oxygenation kinetics data for the tridentate ^{H}Py2^{Me} (**13b**) system also were interpreted to support rapid equilibration between peroxo and bis(μ-oxo) isomers, both of which were observed by various spectroscopic means in solution and in the solid state (including as a compositionally disordered X-ray crystal structure).[119,171]

The combined data for all of the above systems support a very low barrier for the interconversion of the peroxo and bis(μ-oxo) isomers that have rather similar thermodynamic stabilities. A higher barrier has been observed in one case, the tBu_2Me_2eda (**39a**) system in MeTHF solvent,[174] where decomposition of the peroxo isomer is significantly faster than the bis(μ-oxo) complex. The indicated slow equilibration between the two isomers in this instance has enabled the differential reactivity of the two isomers to be examined (section 6). Sluggish conversion of a peroxo to a bis(μ-oxo) species with ^{Me}Py1^{Et,Bz} (**15c**) also has been invoked on the basis of kinetic data for an intramolecular C−H bond activation reaction (section 5).[113,161]

Insights into the basis for the relative thermodynamic stabilities of the two isomers have come both from studies of the above systems in which an equilibrium between them has been identified, from theoretical calculations,[164−171] and from analysis of the nature of the products observed in other oxygenations for which no direct evidence for equilibration is available. The most important factor controlling which of the two isomers is favored appears to be interligand substituent steric interactions in the dicopper complexes, which differ significantly in their intermetal separations, ~3.6 Å for the peroxo vs ~2.8 Å for the bis(μ-oxo).[70,85] A consensus view is that the more compact bis(μ-oxo) core is inherently more stable in most instances, but can be disfavored when supporting ligand substituents are of sufficient size to result in prohibitive interligand steric clashes. For example, copper(I) complexes of triazacyclononane ligands with substituents that are less sterically demanding than *i*Pr (e.g., L^{Bn3} (**7c**)[175] or L^{Me3} (**7a**)[173]) yield bis(μ-oxo) cores only. Similar steric effects were found for the Cu/O_2 chemistry with ^{H}Py1^{Et,Bz} (**15a**) and ^{Me}Py1^{Et,Bz} (**15c**), which exclusively yielded bis(μ-oxo) and peroxo cores, respectively.[120,176] In addition, comparison of K_{eq} (= [peroxo]/[bis(μ-oxo)]) values across the series of bidentate diamine supporting ligands revealed the size of the substituents to be the most important determining factor [cf. K_{eq}($^{i}Pr_2Me_2$-pda, **23b**) > K_{eq}(Me$_4$pda, **23a**)].[174] The size of the ligand chelate ring also was found to be important, as indicated by the trend K_{eq}($^{i}Pr_2Me_2$pda, **23b**) > K_{eq}-($^{i}Pr_2Me_2$eda, **39b**) and the finding that the $^{i}Pr_3$tacd system (**40**, with one more methylene spacer than L^{iPr3}, **7b**) yields the peroxo isomer only.[168] Through structural analysis of Cu(I) precursors and theoretical calculations, the basis for the chelate ring effect for the latter example was argued to be greater interligand steric conflict resulting from the conformational preferences of the larger macrocyclic ligand.

Other ligand geometric effects on the relative stabilities of the isomers have been identified. One is proposed to be the N_{eq}−Cu−N_{eq} bite angle for bidentate ligands, with smaller values favoring the bis(μ-oxo) structure because of angular dependencies of Cu and O orbital interactions (evaluated by theoretical calculations).[170] A related effect concerns the internal bite angles in tridentate ligands, such that a propensity to support a square pyramidal copper ion geometry correlates with greater stability of the dicopper(III) core of the bis(μ-oxo) form.[165,168] The nature of the linkers in binucleating ligands also influences peroxo/bis(μ-oxo) stability. For example, peroxo formation is inhibited for the system supported by $^{i}Pr_4$dtne (**10**), in which the short ethylene tether prohibits attainment of the requisite long (~3.6 Å) intermetal separation.[117] Conversely, the intramolecular adducts formed for the *m*-XYL^{iPr4} (**8**) and N_2tripy (**33**) systems are peroxos in large part because the geometric constraints of the linkers prohibit the short (~2.8 Å) intercopper distance of the bis(μ-oxo) isomers (cf. Scheme 4).[115,152] More recently, hydrogen bonding was found to preferentially stabilize the peroxo isomer when the secondary diamine supporting ligand tBu_2H_2eda (**39d**) was used.[177] This result is particularly noteworthy in view of the fact that the more hindered tBu_2Me_2eda (**39a**) yields mixtures of both isomers.

Finally, electronic effects on the relative stabilities of the isomers have been identified from a comparison of Raman spectral data for the oxygenated species ligated by the series of ligands ^{R}Py2^{Me} (R = H (**13b**),

MeO (**41a**), Me_2N (**41b**)), which present identical steric influences but variable electron donating ability due to the different *para*-substituents on the pyridyl rings.[178] Greater electron donation was shown to result in the relative stabilization of the bis(μ-oxo) core, in line with what one would expect from the higher oxidation state of its copper centers.

4. Alternate Syntheses of Copper–Dioxygen and Related Complexes

Treatment of Cu(II) starting materials with H_2O_2 in some instances has been shown to yield the same Cu/O_2 species that form upon oxygenation of Cu(I) precursors (analogous to the "shunt" pathway in heme-iron chemistry).[179] For example, a μ-η^2:η^2-peroxo complex supported by Tp^{iPr2} (**16b**) may be accessed from low-temperature oxygenation of a Cu(I) precursor or from the reaction of its bis(μ-hydroxo)dicopper(II) complex with H_2O_2.[180] In another illustration, a novel and quite thermally stable 4:1 Cu/O_2 complex featuring a μ_4-peroxo unit may be prepared either by exposure of a basic MeOH solution of HL^1 (**42a**) and Cu(I) salt to O_2, or by addition of H_2O_2 (or catechol + O_2) to a mixture of HL^1 (**42a**), a Cu(II) salt, and NEt_3 in MeOH.[134,135] Similar μ_4-peroxo complexes may be prepared using HL^2 (**42b**) or HL^3 (**42c**). Evidence has also been cited to suggest that the μ_4-peroxo compounds may be accessed by addition of H_2O_2 (or catechol + O_2) to (μ_4-oxo)tetracopper species.[135]

Reactions of Cu(II) compounds with H_2O_2 or ROOH (R = alkyl or acyl group), sometimes in the presence of base, also have led to isolable hydro-, alkyl-, or acylperoxo complexes that are of great interest due to their relevance to postulated reactive intermediates (e.g., Cu_nOOH moieties) in copper oxidase and oxygenase catalytic cycles.[1–3] Mononuclear (1:1) CuOOR (R = H, alkyl, or acyl) complexes have been prepared via this route using the supporting ligands Tp^{iPr2} (**16b**),[181–183] $^{H}Py2^{tBu}$ (**13n**),[184] $^{H}Py2^{Net2}$ (**13o**),[185] $^{H}Py2^{NEtAm}$ (**13p**),[185] BPPA (**43a**),[186] TMPA (**1**),[187] $^{R}Py2^{MeIm}$ (**44a**–**c**, R = H, Me, Me_2),[188] 2-dimethylimidazole,[187] and $^{H}Py2^{BzO}$ (**13k**),[187] and $Py'2^{PhS}$ (**45**).[189] The last example in which thioether coordination to copper is implicated is particularly noteworthy because of specific relevance to the $MetHis_2Cu$ site in peptidylglycine- and dopamine β-monooxygenases.[2,11,12] Mechanistic information on the formation and reactivity of 1:1 CuOOH species was provided by stopped-flow studies of the reaction of H_2O_2 in the presence of NEt_3 with Cu(II) complexes of $^{H}Py2^{PhePh}$ (**13m**), $^{H}Py2^{Phe}$ (**13c**), and TEPA (**46**, 0.2 mM) at 183 K in MeOH.[190] Saturation kinetics for both substrates (H_2O_2 and NEt_3) were recorded, consistent with the path for formation of a 1:1 CuOOH compound **C** shown in Scheme 9. For the system supported by $^{H}Py2^{PhePh}$ (**13m**), the 1:1 complex underwent a slower first-order reaction (rate independent of $[H_2O_2]$ or $[NEt_3]$; $k_2 = 1.6 \pm 0.1\ s^{-1}$) to a species tentatively assigned as a novel monocopper(II) η^2-peroxide (**D** in Scheme 9). This species then decayed to the μ-η^2:η^2-peroxo complex $[(^{H}Py2^{PhePh})_2Cu_2(O_2)]^{2+}$ at higher concentrations (2.0 mM) of Cu(II) starting material via a second-order process ($k_3 = 2.6 \pm 0.1 \times 10^2\ M^{-1}\ s^{-1}$).

Scheme 9

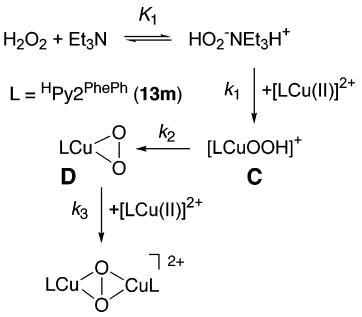

Several 2:1 Cu_2OOR (R = H, alkyl, or acyl) complexes have been prepared, by reaction of 1 equiv of H^+ or an acylating agent (m-$ClC_6H_4C(O)Cl$) to a peroxodicopper species supported by XYL-O^- (**24g**) or UN–O^- (**26b**),[143,191,192] by oxygenation of the dicopper(I) complex of the protonated ligand UN–OH,[143] or by addition of H_2O_2 to $[(XYL\text{-}O\text{-})Cu_2(OH)]^{2+}$.[191,192] In each case, a μ-1,1-hydroperoxo or acylperoxo derivative was produced.

5. Intramolecular Reactions of Copper–Dioxygen Complexes

With few exceptions,[146,152,193–195] copper–dioxygen complexes are stable in solution for reasonable periods (hours) only at low temperature (< −40 °C). Warming usually causes decomposition, typically to Cu(II) complexes via processes involving intramolecular oxidation of a supporting ligand. Although such processes are inherently destructive and thus may be undesired from the point of view of catalyst development, detailed mechanistic studies are nonetheless worthwhile for providing fundamental mechanistic information relevant to the reactivity of Cu/O_2 species in enzymatic and other catalytic systems. Indeed, significant insights into the pathways by which Cu/O_2 species attack organic moieties have been obtained from experimental and theoretical assessments of intramolecular ligand oxidations.

5.1. Arene Hydroxylations and Related Reactions

A commonly observed reaction of 2:1 Cu/O_2 adducts is the hydroxylation of a *m*-xylyl linker in a dinucleating ligand (Scheme 10). Interest in this reaction

Scheme 10

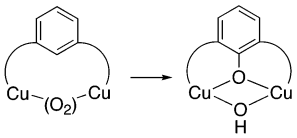

has been stimulated by its relevance to the activity of tyrosinase, in which a coupled dicopper active site converts phenols to catechols and/or orthoquinones.[3,5,196,197] The most detailed mechanistic understanding of the xylyl hydroxylation process has come from studies of the set of compounds $[(R\text{-}XYL\text{-}H)Cu_2]^{2+}$ (ligands **24a**–**c**,**e**,**f**, R = H, OMe, *t*Bu, CN, or NO_2).[139,140,149,198,199] Reaction of these complexes with O_2 at room-temperature results in the formation of $[(R\text{-}XYL\text{-}O)Cu_2(OH)]^{2+}$ (Scheme 11), with both of the

Scheme 11

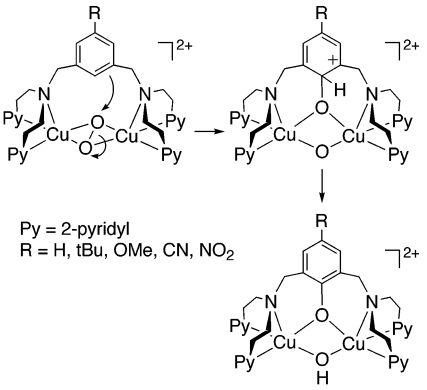

newly introduced O atoms derived from O_2 (and not H_2O) as determined from experiments using $^{18}O_2$. On the basis of kinetic and spectroscopic studies performed at low temperature (section 2.3), the reactive intermediate has been identified as the 2:1 Cu/O_2 adduct $[(R\text{-}XYL)Cu_2(O_2)]^{2+}$. The lifetime of this adduct is increased when R is electron withdrawing, enabling characterization by resonance Raman spectroscopy for the case R = NO_2 (**24f**).[199] Only peaks corresponding to μ-η^2:η^2-peroxo species were observed and an upper limit for the amount of bis(μ-oxo) isomer present in 4 mM solutions was calculated to be ~0.13%. Thus, while it is conceivable that the hydroxylating species is either the observed μ-η^2:η^2-peroxo compound or a small amount of bis(μ-oxo) formed in a rapid preequilibrium, the latter would have to be a ~1000 times more reactive hydroxylating agent than the former. The results of theoretical calculations have been interpreted to indicate that this reactivity order is unlikely to be correct,[199] and stereochemical considerations further support the μ-η^2:η^2-peroxo as the hydroxylating agent in this system (see below).

The mechanism proposed for xylyl ring hydroxylation by the μ-η^2:η^2-peroxo intermediate involves electrophilic attack onto the arene π system to yield a carbocation intermediate (Scheme 11). Subsequent proton transfer and rearomatization yields the final product. Several pieces of evidence support this path. The lack of a kinetic isotope effect when the hydrogen at the hydroxylated position is replaced by deuterium is consistent with rate-controlling attack onto the π system.[139] The possible involvement of radicals is not supported by the kinetic analysis or the fact that radical traps have no effect on the Cu/O_2 adduct decay rate. Consistent with the peroxo acting as an electrophile, a decrease in hydroxylation rate constants (k_3) and an increase in $\Delta H^{\ddagger}$ values with the electron withdrawing power of the R substituents was observed, reflected by a negative Hammet $\rho = -2.1$ at 193 K.[140] On the other hand, the magnitude of ρ is small compared to those typical for electrophilic aromatic substitutions.[200] Possible explanations offered for this modest ρ value are that (a) k_3 is a composite rate constant, incorporating several of the steps involved in the overall transformation, or (b) the μ-η^2:η^2-peroxo group is so reactive an electrophile that it is relatively insensitive to electronic changes in the aromatic ring. Although it appears unlikely that the peroxo unit is intrinsically so reactive, its ideal orientation and close proximity to the aromatic ring may explain its high reactivity and lack of sensitivity toward changes in the ring substituents. This notion is supported by the results of high pressure kinetic studies that yielded a relatively small and negative volume of activation $\Delta V^{\ddagger}$ (k_2) of -4.1 ± 0.7 cm^3 mol^{-1}, interpreted to indicate minimal geometrical rearrangement during attack of the peroxo at the xylyl ring.[149] Theoretical calculations that provide an orbital picture for this process have been described.[199,201]

Scheme 12

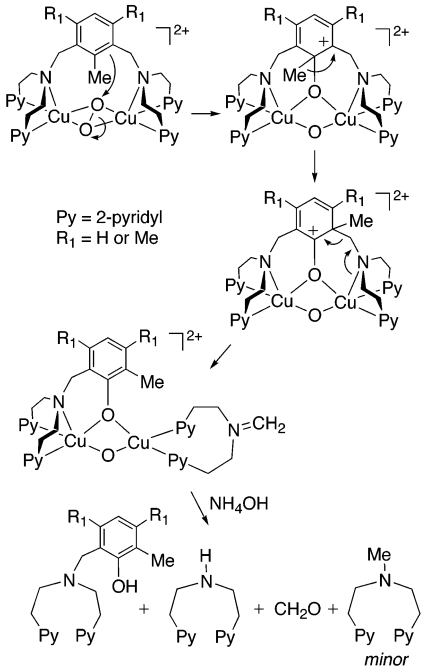

Further experimental support for an electrophilic pathway involving a carbocationic intermediate was provided by the results of oxygenations of systems with methyl-substituted rings, $[(XYL\text{-}Me)Cu_2]^{2+}$ and $[(Me_2XYL\text{-}Me)Cu_2]^{2+}$ (ligands **24h** and **24i**; Scheme 12).[202,203] Hydrolytic workup of the reactions of these complexes with O_2 yielded the indicated phenols, secondary amines, and formaldehyde. A key proposed step in the mechanism of these reactions involves a 1,2-methyl migration ("NIH shift") in a cationic cyclohexadienyl intermediate analogous to that postulated for the hydroxylations discussed above.

The reaction of the dicopper(II) complex of XYL-H (**24a**) with H_2O_2 also resulted in ring hydroxylation.[204] Notably, the kinetics were pH dependent and indicated a second-order dependence on the dicopper(II) complex, suggesting a tetracopper intermediate or transition state. It was proposed that a (μ-1,1-hydroperoxide)dicopper species forms and that a second dicopper(II) complex acts as a Lewis acid to activate the hydroperoxide for electrophilic aromatic substitution. In a related ligand system with benzimidazolyl instead of pyridyl donors (**30a**), double hydroxylation occurs upon reaction of its dicopper(II) complex with H_2O_2 (Scheme 13).[205] On the basis of the results of a mechanistic study, attack of a (μ-1,1-hydroperoxide)dicopper intermediate at the 5-position was proposed, with functionalization of the 2-position occurring subsequently.

Scheme 13

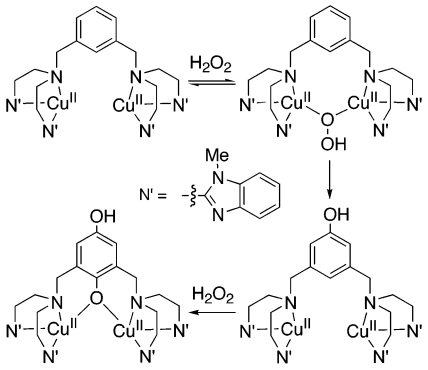

Scheme 14

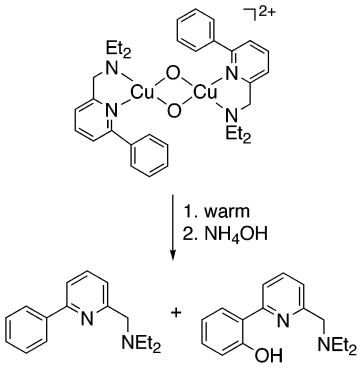

In addition to the aforementioned XYL series (**24**), the reactivity of dicopper(I) complexes of numerous other xylyl-linked dinucleating ligands (**30** and **47**−**51**, as well as a trinucleating analogue[158]) has been examined, and some undergo arene hydroxylation upon treatment of their dicopper(I) complexes with O_2. In most instances, however, little is known about the factors that affect the observed reactivity or the nature of the Cu/O_2 species involved.[206−219] The nature of the N-donors is important, as indicated by the fact that hydroxylation occurs for XYL (**24**) systems comprising solely pyridyl donors, but not for the analogous ligands with various other N-heterocyles (**30**), which instead yield products resulting from four-electron reduction of O_2 (e.g., bis(hydroxo)-dicopper(II) complexes).[206,220] On the other hand, for the series of Schiff base ligands **47a**−**j**, xylyl hydroxylation is observed for X = 2-pyridyl (**47a**), 2-imidazolyl (**47b**), 5-imidazolyl (**47c**), or 2-benzimidazolyl (**47d**).[207] Interestingly, when methoxy substituents are incorported into the 2- (site of hydroxylation) and 5-position of the xylyl linker (**47e**, X = 2-pyridyl), oxidative demethylation of the 2-methoxy group occurs.[208,209] For the histidine donor series **47f**−**j**, when they are *N*-methylated (**47h** and **47i**) hydroxylation occurs, but not when the histidines have H or CO_2Me substituents (**47f** and **47g**), unless protic solvents are used.[210] In the latter cases, the ratio of arene hydroxylation to four-electron O_2 reduction may be increased by addition of small amounts of acid, implying the intermediacy of a hydroperoxo adduct. Oxygenation of the dicopper(I) complex of the tetra-Schiff base ligand **48** results in hydroxylation of one of the xylyl rings,[212−215] but four-electron O_2 reduction occurs instead in an analogous system **47** with furan instead of xylyl linkers.[216] The unsymmetrical relatives of the XYL series, UN (**26a**)[217] and UN2 (**50**),[218] also undergo hydroxylation (albeit more sluggishly), and a μ-η^2:η^2-peroxo intermediate was identified at low temperature for the former. Similarly, hydroxylation of *m*-XYL^{iPr4} (**8**) occurs upon decomposition of its intramolecular (μ-η^2:η^2-peroxo)-dicopper complex,[115] but the intermolecular bis(μ-oxo) species of this ligand that is formed in parallel (Scheme 4) reacts differently (N-dealkylation, section 5.2). Hydroxylation of the aromatic ring in the tridentate ligand **51** occurs upon treatment of its Cu(I) complex with O_2, despite the entirely different disposition of the xylyl unit compared to the aforementioned binucleating ligands.[219] Consideration of all of these systems indicates that ligand structure influences the course of the oxygenation processes, and that proper disposition of a bridging peroxo unit is one prerequisite for xylyl hydroxylation. Still, the bases for many of the ligand structural effects (cf. variation of N-donors) remain obscure.

Intramolecular hydroxylations of ligand pyridyl rings have been reported, in one case upon treatment of a Cu(I) complex of $^{H}Py2^{Phe}$ (**13c**) with iodosylbenzene[221] and in another via reaction of the Cu(I) complex of PyIso (**52**) with O_2.[222] Mechanistic data for these reactions are not available.

Decomposition of bis(μ-oxo)dicopper complexes supported by $PhPyNEt_2$ (**53**) resulted in phenyl ring hydroxylation (Scheme 14), providing precedence for the notion that a bis(μ-oxo) core is a possible oxidant in tyrosinase even though it has not been observed.[74,223] On the other hand, even though no indication of the presence of a μ-η^2:η^2-peroxo isomer was found in Raman spectra for the synthetic system, hydroxylation by a small, undetectable amount of such an isomer in rapid equilibration with the bis-(μ-oxo) form could not be ruled out. In any case, an electrophilic aromatic substitution pathway like that delineated for the XYL (**24**) system was supported by the lack of a H/D kinetic isotope effect and the finding that the rate and overall yield of hydroxylation were inversely correlated with the electron withdrawing capability of phenyl ring substituents.

5.2. N-Dealkylations and Benzylic Oxidations

A commonly observed result of decomposition of Cu/O_2 complexes and of room-temperature oxygenation of Cu(I) compounds is intramolecular oxidation of C−H bonds that are "activated" due their position α to an amine donor and/or to a phenyl ring. For the former, the result is oxidative N-dealkylation to yield a secondary amine and an aldehyde or ketone, a process well-studied (yet still mechanistically controversial) for heme-iron oxidants, such as cytochrome P450.[224,225] Such N-dealkylations have been observed for copper systems supported by L^{R3} (**7a**−**c**, R = Me, ^{i}Pr, Bn),[173,175,226] $^{i}Pr_4$dtne (**10**),[117] *m*- and *p*-XYL^{iPr4} (**8** and **9**),[115] (L*n*)$_3$tacn (**21a**−**c**),[137] $R_2R'_2$Cyda (**38a**−**c**),[173] $^{H}Py1^{Et,Bz}$ (**15a**),[176] $^{Me}Py1^{Et,Bz}$ (**15c**),[176] D (**25**),[142] $L_2(Py2)_2$ (**37**),[153] $L_3(Py2)_2$ (**35**),[153] Me_2TMPA (**43b**),[227] and Me_3TMPA (**43c**).[228] Available activation parameters for these processes are listed in Table 5. A mechanistic study of the decomposition

Table 5. Activation Parameters and Kinetic Isotope Effects for Intramolecular Ligand Degradation Reactions of Cu/O_2 Species

ligand	type of O_2 complex/solvent	reaction	activation parameters[a]	KIE (298 K)[b]	ref
L^{Me3} (**7a**)	bis(μ-oxo)/CH_2Cl_2	N-dealkylation	$\Delta H^{\ddagger}_H = 53 \pm 2$ $\Delta S^{\ddagger}_H = -75 \pm 4$		173
L^{iPr3} (**7b**)	bis(μ-oxo)[c]/THF	N-dealkylation	$\Delta H^{\ddagger}_H = 55 \pm 2$ $\Delta S^{\ddagger}_H = -57 \pm 5$ $\Delta H^{\ddagger}_D = 62 \pm 2$ $\Delta S^{\ddagger}_D = -54 \pm 5$	11	226
L^{Bn3} (**7c**)[d]	bis(μ-oxo)/CH_2Cl_2	N-dealkylation	$\Delta H^{\ddagger}_H = 58 \pm 2$ $\Delta S^{\ddagger}_H = -41 \pm 5$ $\Delta H^{\ddagger}_D = 63 \pm 2$ $\Delta S^{\ddagger}_D = -50 \pm 5$	25	226
$^{i}Pr_4$dtne (**10**)	bis(μ-oxo)/CH_2Cl_2	N-dealkylation	$\Delta H^{\ddagger}_H = 56 \pm 2$ $\Delta S^{\ddagger}_H = -59 \pm 5$ $\Delta H^{\ddagger}_D = 68 \pm 2$ $\Delta S^{\ddagger}_D = -42 \pm 5$	16	117
(L*2*)tacn (**21b**)	bis(μ-oxo)/CH_2Cl_2	N-dealkylation	$\Delta H^{\ddagger}_H = 60$ $\Delta S^{\ddagger}_H = -23$		137
(L*3*)tacn (**21c**)	bis(μ-oxo)/CH_2Cl_2	N-dealkylation	$\Delta H^{\ddagger}_H = 62$ $\Delta S^{\ddagger}_H = -39$		137
Me_4Cyda (**38a**)	bis(μ-oxo)/CH_2Cl_2	N-dealkylation	$\Delta H^{\ddagger}_H = 56 \pm 2$ $\Delta S^{\ddagger}_H = -100 \pm 4$		173
Me_2Et_2Cyda (**38b**)[e]	bis(μ-oxo)/CH_2Cl_2	N-dealkylation	$\Delta H^{\ddagger}_H = 52 \pm 2$ $\Delta S^{\ddagger}_H = -95 \pm 4$ $\Delta H^{\ddagger}_D = 55 \pm 2$ $\Delta S^{\ddagger}_D = -92 \pm 5$	2.3	173
$^{H}Py1^{Et,Bz}$ (**15a**)	bis(μ-oxo)/CH_2Cl_2	N-dealkylation	$\Delta H^{\ddagger}_H = 55 \pm 1$ $\Delta S^{\ddagger}_H = -31 \pm 4$ $\Delta H^{\ddagger}_D = 67 \pm 2$ $\Delta S^{\ddagger}_D = -5 \pm 8$	5.6	176
$^{Me}Py1^{Et,Bz}$ (**15c**)	bis(μ-oxo)/CH_2Cl_2	N-dealkylation	$\Delta H^{\ddagger}_H = 31 \pm 1$ $\Delta S^{\ddagger}_H = -121 \pm 4$ $\Delta H^{\ddagger}_D = 41 \pm 2$ $\Delta S^{\ddagger}_D = -84 \pm 12$	1 (270 K)	176
L^{iPr2Py} (**54**)	1,2-peroxo/CH_3CN	amidation	$\Delta H^{\ddagger}_H = 53 \pm 2$ $\Delta S^{\ddagger}_H = -96 \pm 8$	2.5 ± 0.5[f]	232
$^{H}Py2^{Et,Phe}$ (**22a**)	μ-η^2:η^2-peroxo/THF	benzylic hydroxylation	$\Delta H^{\ddagger}_H = 28.1 \pm 1.0$ $\Delta S^{\ddagger}_H = -155 \pm 5$ $\Delta H^{\ddagger}_D = 40.3 \pm 1.3$ $\Delta S^{\ddagger}_D = -107 \pm 6$	1 (254 K)	113
$^{H}Py1^{Et,Phe}$ (**22a**)	bis(μ-oxo)/acetone	benzylic hydroxylation	$\Delta H^{\ddagger}_H = 39.1 \pm 0.4$ $\Delta S^{\ddagger}_H = -72.6 \pm 1.9$ $\Delta H^{\ddagger}_D = 52.8 \pm 0.5$ $\Delta S^{\ddagger}_D = -31.1 \pm 2.3$	1.7	120
i-Bu_3CY (**57**)	bis(μ-oxo)/CH_2Cl_2	aliphatic hydroxylation	$\Delta H^{\ddagger}_H = 42.2 \pm 1.8$ $\Delta S^{\ddagger}_H = -62 \pm 10$		242

[a] Values of $\Delta H^{\ddagger}$ and $\Delta S^{\ddagger}$ reported in units of kJ mol^{-1} and J mol^{-1} K^{-1}, respectively. Subscripts "H" and "D" refer to values obtained from rate measurements with ligands perprotiated or perdeuterated, respectively, at the position adjacent to the N atom (the carbon that is oxidized). [b] KIE = k_H/k_D, calculated from the activation parameters (except where noted). [c] Major species present, but minor amount of μ-η^2:η^2-peroxo complex probably present as well. [d] Values corrected from those provided in ref 173, which were inadvertently calculated from the Arrhenius (ln k vs T^{-1}) instead of the Eyring (ln(k/T) vs T^{-1}) plots. [e] Values calculated from Eyring plot provided as Supporting Information in ref 173. Note that only the α positions on the ethyl substituents (and not the methyl substituents) were perdeuterated, so the H/D KIE may not be fully expressed in the data provided. [f] Directly measured value at 243 K (activation parameters for deuterated ligand not available).

of the bis(μ-oxo)dicopper complex supported by L^{Bn3} serves as an illustrative example (Scheme 15).[226] Labeling studies with $^{18}O_2$ show that the O atom in the aldehyde or ketone originates from the bis(μ-oxo) core. Decay of the bis(μ-oxo)dicopper complex obeys first-order kinetics and exhibits a large KIE when deuterium is introduced α to the nitrogen, consistent with C−H bond breaking in the rate-determining step. In addition, crossover and double labeling experiments have been performed to show that the bis(μ-oxo) core is responsible for O transfer during the N-dealkylation process and not 1:1 Cu/O fragments in equilibrium with the dimeric species. A Hammett study of the decomposition reaction of a

Scheme 15

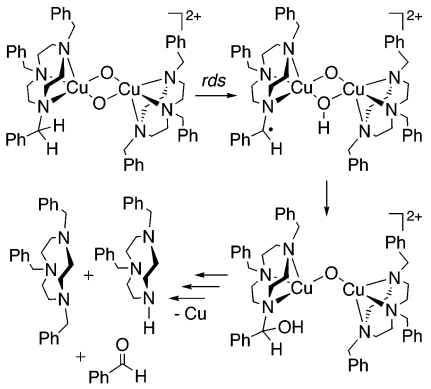

series of *para*-substituted L^{Bn3} systems **7c**−**f** gave a ρ value of −0.4,[229] which is similar to those measured for benzylic hydrogen atom abstractions by free radicals[230] and indicative of electrophilic character for the bis(μ-oxo)dicopper core. The electrophilicity is postulated to arise from a low-lying LUMO+1 orbital having dominant lobes extending from the bridging oxygen atoms.[164] On the basis of the experimental evidence, a mechanism for the N-dealkylation process was proposed (Scheme 15). According to this hypothesis, hydrogen abstraction from the α-CH bond generates a carbon centered radical that is then quickly trapped by a hydroxyl group in a mechanism akin to the paradigmatic cytochrome P450 "rebound" path.[179] Alternatively, C−H bond scission and O atom transfer may occur simultaneously in a concerted mechanism (not shown). Both pathways result in the formation of a carbinolamine species that decomposes to give the secondary amine and aldehyde or ketone as the final products. Strong preferential support for the hydrogen atom abstraction pathway has been provided by the results of integrated molecular orbital molecular mechanics electronic structure calculations, which revealed a relatively late transition state structure featuring C- - -H and H- - -O distances of 1.310 and 1.217 Å, respectively (Figure 2).[231]

Analogous mechanisms appear to be followed in N-dealkylations of other systems. Thus, for example, decomposition of bis(μ-oxo) complexes of $R_2R'_2$Cyda (**38a**−**c**) occurs via hydrogen atom abstraction from the α-CH bonds of the R/R′ substituents, with relative rates that correlate with the relevant C−H bond strengths (e.g., $-CH_3 < -CH_2CH_3$).[173] As noted previously (section 2.3) products of oxygenation of $[(m\text{-}XYL^{iPr4})Cu_2]^{2+}$ and $[(p\text{-}XYL^{iPr4})Cu_2]^{2+}$ differ, the former yielding both intramolecular μ-η^2:η^2-peroxo and intermolecular bis(μ-oxo) species but the latter only intermolecular bis(μ-oxo) species (Scheme 4). These species decay via different paths as well; the μ-η^2:η^2-peroxo hydroxylates the bridging xylyl group (section 5.1), but the intermolecular bis(μ-oxo) species decompose through *N*-dealkylation of the ligand isopropyl groups.[115] The regioselectivity of the bis(μ-oxo) core attack at the isopropyl rather than the benzylic C−H groups in these complexes is proposed to be controlled by geometric constraints, where the former lie in the equatorial coordination position near the reactive oxo moiety. In keeping with a structural explanation and the significant H/D KIE values

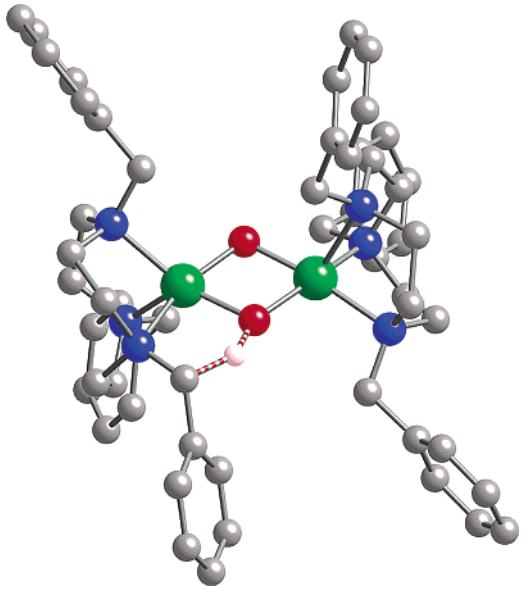

Figure 2. Calculated stucture of the transition state for the hydrogen atom abstraction step in the intramolecular N-dealkylation depicted in Scheme 15.[231] Figure reprinted with permission from ref 85. Copyright 2002 Wiley Interscience.

measured for the L^{iPr3} system (Table 5), selective deuteration of the isopropyl groups in m-XYL^{iPr4}-d_{28} (**8**-d_{28}) shifts the reactivity of the system toward benzylic C−H rather than isopropyl C−D bond scission. Moreover, *N*-dealkylation of the bis(μ-oxo) complex supported by iPr$_4$dtne (**10**) is quantitative and completely regioselective, giving rise only to products derived from cleavage of an isopropyl group and not from scission of the ethyl linker, again consistent with the differing proximity of their respective C−H bonds to the reactive oxo unit.[117]

Both the bis(μ-oxo) and μ-η^2:η^2-peroxo complexes supported by ^{H}Py1^{Et,Bz} (**15a**) and ^{Me}Py1^{Et,Bz} (**15c**), respectively, decompose to give products resulting from N-dealkylation, but with different kinetic parameters.[176] While the bis(μ-oxo) complex decomposition exhibits a large KIE (33 at 218 K; 5.6 at 298 K) and activation parameters similar to those observed for the L^{Bn3} system (**7c**, Table 5), a much smaller KIE (~1 at 270 K) and quite different activation parameters (Table 5) were measured for decay of the peroxo complex of ^{Me}Py1^{Et,Bz} (**15c**). The latter results were interpreted to indicate that slow isomerization to a bis(μ-oxo) isomer occurred prior to C−H bond attack, similar to the path suggested for benzylic hydroxylation by the μ-η^2:η^2-peroxo complex of ^{H}Py2^{Phe} (**13c**, see below).[86,113]

While reaction of the dicopper(I) complex of the binucleating ligand D (**25b**) with O_2 at 273 K results in oxidation of the central N atom to an *N*-oxide, the same reaction run at ambient temperature for longer times (> 12 h) resulted in N-dealkylation via hydroxylation of one of the methylene carbons adjacent to the central nitrogen.[142] The reactive species responsible for these transformations is not known, however, because both the N-oxidation and N-dealkylation reactions require reaction times significantly longer than the lifetime of the μ-η^2:η^2-peroxo complex spectroscopically observed at 193 K (section 2.3).

Scheme 16

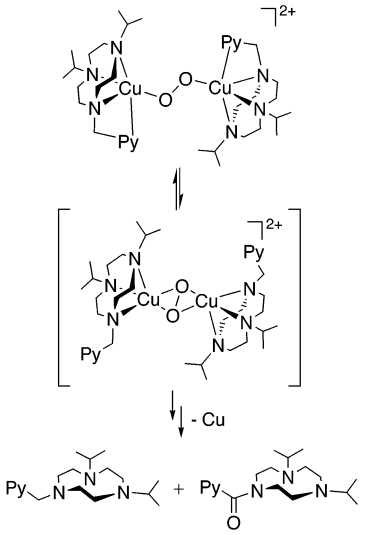

Activation of a C−H bond α to an N donor also occurs upon decomposition of the μ-1,2-peroxo complex supported by the tetradentate tripodal ligand L^{iPr2Py} (**54**), but oxidation to an amide occurs instead of N-dealkylation (Scheme 16).[232] A mechanism was proposed in which the C−H activation step is preceded by a rate-controlling unimolecular isomerization, speculated to yield a μ-η^2:η^2-peroxo species in which a pyridyl group is not bound. The requirement for such an isomerization was based on the combined observations of (a) first-order kinetics for peroxo complex decay, with a negative activation entropy (Table 5) that argues against cleavage into monomers, and (b) a relatively low H/D KIE (2.5 at 243 K) for experiments involving isotope substitution at the methylene group that is oxidized.

Intramolecular hydroxylation of benzylic positions not adjacent to N-donor atoms to yield alcohol functional groups has been observed upon decay of Cu/O_2 species supported by $^{H}Py2^{Phe(X)}$ (**13c**−**f**),[86,113] $^{H}Py1^{Et,Ph}$ (**22a**−**e**),[120] $^{H}Py2^{Ind}$ (**13l**),[233] CalixNPy2 (**55**),[234] and P(3-R-5-^{i}PrIm)$_3$ (**56a** and **56b**, R = ^{i}Pr or Et).[235] These reactions are of particular interest due to their resemblence to the benzylic hydroxylation catalyzed by dopamine β-monooxygenase.[2,11,12] For the case of $^{H}Py2^{Et,Phe(X)}$ (**22a**−**e**), the hydroxylated product forms upon decay of a μ-η^2:η^2-peroxo species identified by spectroscopy, but, similar to the situation noted above for L^{iPr2Py} (**54**) and $^{Me}Py1^{Et,Bz}$ (**15c**), kinetic data (Table 5) were interpreted to indicate that isomerizaton to a bis(μ-oxo) species occurred prior to attack at the benzylic C−H bond (Scheme 17). For example, a low KIE was measured (1.7 at 233 K, extrapolated to 1 at 254 K), and the rate of decay of the peroxo compound was found to be relatively insensitive to *para* substitution of the aromatic ring.[113] Direct attack at the benzylic position by an observable bis(μ-oxo) species was shown for the system supported by $^{H}Py1^{Et,Phe}$ (**22a**),[120] as supported by a large KIE for bis(μ-oxo) decay (35 at 193 K) and a ρ value of −1.48 from a Hammett study, both of which are similar to values obtained for N-dealkylation of L^{Bn3} (**7c**) upon decay of its bis(μ-oxo) complex.[226] In another example, the reversibly formed μ-η^2:η^2-peroxo complex of P(3,5-iPrIm)$_3$ (**56a**) decomposed to yield

Scheme 17

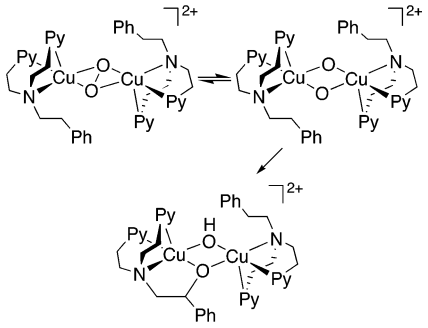

ligand that had been hydroxylated at a *i*Pr methine position. This type of substituent functionalization is similar to those observed for various Tp^{iPr2} (**16b**) complexes of metal ions other than Cu, such as Co or Mn.[236,237] In addition to decomposing via an N-dealkylation pathway, the bis(μ-oxo) complex supported by Me_3TMPA (**43c**) also yielded a ligand in which a methyl substituent had been oxidized to a carboxylate, with both O atoms derived from the bis(μ-oxo) core.[228] An autoxidation path involving an alcohol intermediate was ruled out by the observation of no carboxylate product upon treatment of the alcohol (Me_3TMPA with one Me replaced by CH_2OH) with Cu(II), Et_3N, and O_2. Similar derivatization of Me_3TMPA was observed upon decay of its bis(μ-oxo)-dinickel(III) complex.[238] Finally, it is likely that 2:1 Cu/O_2 adducts are involved in hydroxylations of $^{H}Py2^{Ind}$ (**13l**) and CalixNPy2 (**55**), but such species were not identified in these cases.[233,234] It is noteworthy that for the oxidation of $^{H}Py2^{Ind}$ (**13l**) (a) a large KIE (11 at 298 K) supports rate-determining benzylic C−H bond cleavage, and (b) hydroxylation is regio- and stereoselective, with deuterium labeling studies showing retention of configuration.[233]

Intramolecular hydroxylation of unactivated aliphatic C−H bonds of ligand substituents in copper complexes has been reported,[239−241] and in one instance the nature of the oxidizing Cu/O_2 intermediate was identified.[242] Oxygenation of the Cu(I) complex of *i*-Bu_3CY (**57**) yielded a bis(μ-oxo)dicopper species, identified by UV−vis and Raman spectroscopy, which upon warming decomposed to yield a bis(alkoxo)-dicopper complex resulting from hydroxylation at the substituent carbon β to the secondary amine donor atom (Scheme 18). An intramolecular hydrogen atom abstraction mechanism similar to those proposed for N-dealkylations (see above) was implicated by the first-order kinetics and the activation parameters (Table 5).

5.3. Other Intramolecular Ligand Oxidations

Inspired by the structure and function of galactose oxidase (GAO), which catalyzes the two-electron redox reaction in eq 4 via cycling between Cu(I)/phenol(ate) and Cu(II)/phenoxyl radical states (Figure 1a),[13−15] several research groups have examined the aerobic oxidation of alcohols to aldehydes or ketones using Cu(II)/phenolate and/or -phenoxyl radical precursors.[243,244] Of particular relevance to the current discussion are studies in which evidence is presented for involvement of a Cu/O_2 intermediate

Scheme 18

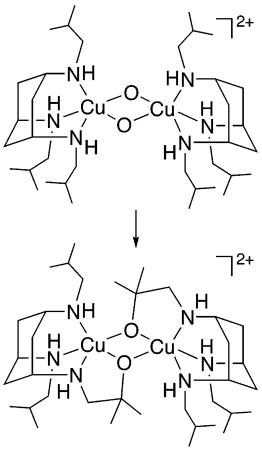

in the intramolecular generation of Cu/phenoxyl radical species (the reactant responsible for alcohol oxidation) concomitant with the ejection of H_2O_2. Copper(I) intermediates have been implicated in several aerobic alcohol oxidation systems,[122,245] but in only one instance with supporting ligand ^{1}L (**17**) has a Cu/O_2 species been identified, [(^{1}LH_3)Cu(O_2)-NEt_3].[122] This complex was formulated as a (η^1-superoxo)copper(II) species on the basis of UV−vis and FTIR spectroscopy. Interestingly, it equilibrates with H_2O_2 and an isolable Cu(II)-phenoxyl radical compound that is capable of oxidizing benzyl and ethyl alcohol. This process apparently involves H atom or proton coupled proton transfers to the CuO_2 unit that may be intramolecular, but the details have yet to be elucidated.

$$RCH_2OH + O_2 \rightleftharpoons RCHO + H_2O_2 \qquad (4)$$

Copper-dioxygen species have been implicated in studies of intramolecular oxidative C−C bond cleavage reactions of Cu-flavonolate (fla, **58**) complexes that model the monocopper active site of the enzyme quercetin 2,3-dioxygenase.[7−9] Several Cu(I and II)-flavonolate compounds have been shown to react with O_2, typically at elevated temperatures, to yield carbon monoxide and a depside (phenolic carboxylic acid ester, **H**, Scheme 19).[246−257] Shown in Scheme 19 are two related pathways for the reaction of a Cu(II)-flavonolate, which were suggested on the basis of the results of mechanistic studies for several systems, most notably [Cu(fla)$_2$],[253] [Cu(PPh_3)$_2$(fla)],[252] and [Cu(L)(fla)$_2$] (L = Me_4eda (**39e**), phen (**59**), bpy (**60**)).[257] Both mechanisms involve a prior rapid preequilibrium (with a small K_{eq}) between the Cu(II)-flavonolate and a redox isomer, a Cu(I)-flavonoxyl radical, in a process like that which is well established for simple catecholate/semiquinone complexes of metal ions.[258−261] Rate-determining binding of O_2 to the Cu(I) center is then postulated to occur, consistent with the observation of overall second-order kinetics (first order in complex and in O_2), negative entropies of activation, and negative Hammett ρ values when the substituent R is varied (Table 6). In subsequent fast steps, intramolecular coupling of the bound superoxide and the flavonoxyl radical is proposed to yield a trioxometallocycle (**E**), which then rearranges to form an endoperoxide (**F**) or an oxetane (**G**). Both intermediates would break down

Table 6. Selected Kinetic Parameters for the Oxygenolysis of Cu-Flavonolate Complexes[a]

complex	k[b]	activation parameters (k)	ρ[c]	ref
[Cu(fla)$_2$]	(1.57 ± 0.08) × 10^{-2} [d]	$\Delta H^{\ddagger} = 53 \pm 6$ $\Delta S^{\ddagger} = -138 \pm 11$	−0.63	253
[Cu(PPh_3)$_2$(fla)]	(4.16 ± 0.48) × 10^{-3} [e]	$\Delta H^{\ddagger} = 102 \pm 7$ $\Delta S^{\ddagger} = -13 \pm 21$	−1.32	252
[Cu(phen)(fla)$_2$]	(9.50 ± 0.60) × 10^{-2}	$\Delta H^{\ddagger} = 79 \pm 16$ $\Delta S^{\ddagger} = -40 \pm 44$	−1.03	257
[Cu(bpy)(fla)$_2$]	(2.40 ± 0.10) × 10^{-2}			257
[Cu(Me_4eda)-(fla)$_2$]	(2.00 ± 0.10) × 10^{-2}			257

[a] All data from kinetics measurements in DMF solvent. The rate and equilibrium constants are for the processes denoted in Scheme 19. Structures of the abbreviated ligands are shown in Chart 1, where fla = **58**, phen = **59**, bpy = **60**, and Me_4eda = **39e**. [b] Second-order rate constants (units are $M^{-1}s^{-1}$) measured at 353 K unless noted otherwise. [c] Hammett ρ value determined from the rate constants k for flavonolate derivatives with R = OCH_3, CH_3, H, and Cl. [d] Measured at 373 K. [e] Measured at 363 K.

Scheme 19

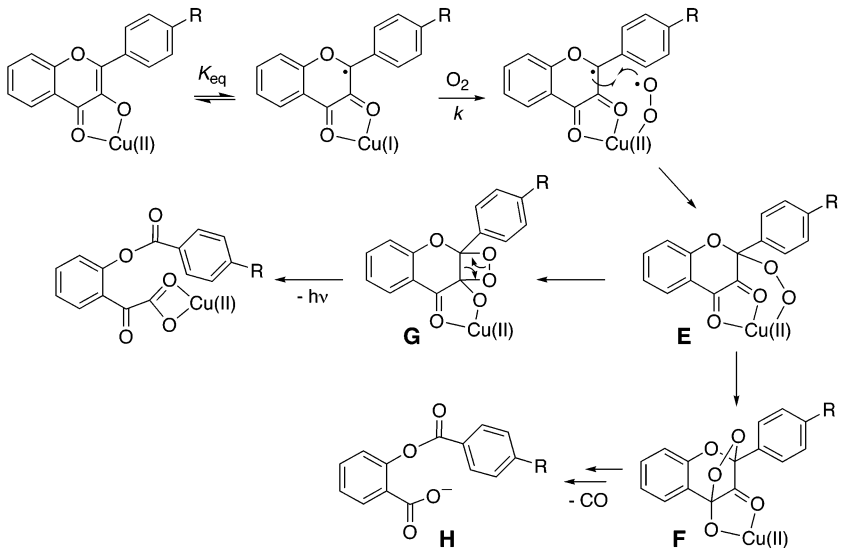

to yield a C−C bond cleaved product, the former by a pathway analogous to the Criegee-type rearrangements of peroxides that have been cited for other metal-dioxgenase reaction mechanisms (cf. nonheme iron)[262] and the latter in a route established for organic oxetanes that yields 2-benzoatophenylglyoxylic acid and is accompanied by chemiluminescence.[263] Indeed, the two routes are distinguished by the presence or absence of light emission during the reaction; chemiluminescence was observed for the faster reacting [Cu(phen)(fla)$_2$], implicating **G**, but not for the more sluggish complexes [Cu(fla)$_2$] or [Cu(PPh$_3$)$_2$(fla)], which were thus suggested to react via **F**. These mechanistic differences obviously are related to the nature of the supporting ligand, but it is not yet clear how, and none of the intermediates in the overall mechanism have been observed.

6. Intermolecular Reactions of Copper–Dioxygen Complexes

While intramolecular ligand oxidations by Cu/O$_2$ complexes have provided important insights into fundamental reactivity issues, the reactions of such complexes with exogenous substrates are particularly relevant to enzyme catalysis. Comparative studies of structurally varied Cu/O$_2$ compounds have revealed notable differences in reactivity with added substrates and have led to detailed understanding of oxidation mechanisms, both in synthetic and biological systems.

In a landmark study,[264] the reactivity with exogeneous reagents of three different 2:1 Cu/O$_2$ adducts that share similar pyridyl-amine N-donor ligation was compared: (a) [(TMPA)$_2$Cu$_2$(O$_2$)]$^{2+}$, comprising a trans-μ-η^1:η^1-peroxide with ligand **1**, (b) [(XYLO$^-$)Cu$_2$(O$_2$)]$^+$, with an asymmetrically bound end-on peroxide and ligand **24g** (Scheme 6), and (c) [(N$_4$Py2)Cu$_2$(O$_2$)]$^{2+}$, with ligand **14b** and a "bent" μ-η^2:η^2-peroxo ligand (Scheme 7, **B**). It was concluded that the end-on η^1-peroxides in the TMPA (**1**) and XYLO$^-$ (**24g**) complexes are nucleophilic in character. Thus, for example, addition of 1 equiv of HBF$_4$, HPF$_6$ or an acylating agent (*m*-ClC$_6$H$_4$C(O)Cl) to [(XYLO$^-$)Cu$_2$(O$_2$)]$^+$ yielded μ-1,1-hydroperoxo or acylperoxo derivatives, respectively, as noted above (section 4).[191,192] Hydrogen peroxide was evolved upon treatment of [(XYLO$^-$)Cu$_2$(O$_2$)]$^+$ and [(TMPA)$_2$Cu$_2$(O$_2$)]$^{2+}$ with excess protic acid. Both complexes also reacted readily with CO$_2$ at low temperature to yield putative peroxycarbonate (CO$_4^{2-}$) species that decayed to isolable carbonate complexes. Triphenylphosphine was not oxidized and instead displaced the peroxide ligand to yield Cu(I)−PPh$_3$ complexes. Phenols behaved as a source of H$^+$ ions resulting in the generation of H$_2$O$_2$ and phenoxodicopper(II) systems.

In contrast, the "bent" μ-η^2:η^2-peroxide in [(N$_4$Py2)Cu$_2$(O$_2$)]$^{2+}$ acts as an electrophile. No reaction was observed with acyl chlorides and only low yields (<15%) of H$_2$O$_2$ were obtained upon treatment of the complex with excess HPF$_6$. No reaction occurred with CO$_2$, but PPh$_3$ was converted to OPPh$_3$ upon warming of the complex. Rather than donating a proton, 2,4-di-*tert*-butylphenol was oxidized to its dihydroxybiphenyl radical coupling product. These and other results clearly demonstrate a disparity in reactivity between the end-on (nucleophilic) and side-on (electrophilic) peroxides in the dicopper complexes. Several rationales for this disparity have been offered. A steric argument has been suggested,[62] which is based on the hypothesis that because substrate attack on the peroxide moiety occurs along the O−O bond axis it would be inhibited when approach along the O−O bond vector is blocked by the bulk of the supporting ligand; such blocking would be decreased in a μ-η^2:η^2-peroxide compound. In an alternative argument based on simple valence bond considerations, μ-η^2:η^2-peroxo coordination requires three bonds to each O atom, and therefore may, in part, be responsible for partial positive charge being associated with these atoms (i.e., electrophilic character).[264] More quantitative insights were obtained from a detailed theoretical study of the relationship between the electronic structure of peroxo adducts and their observed reactivity toward substrates.[3,201,265] A key finding was that electron donation from the peroxide π^* orbital into a Cu(II) d orbital (π^*_σ interaction) is greater in the side-on bonded case, which corresponds to decreased electron density (greater electrophilic character) at the peroxide ligand. A further observation is that the side-on adduct exhibits an additional bonding interaction where the σ^* orbital of the peroxide acts as a π-acceptor, thus leading to an overall weakening of the O−O bond.

Further subtleties become evident upon comparing the reactivity of μ-η^2:η^2-peroxides with different N-donor ligands, such as N$_4$Py2 (**14b**) and Tp^{Me2} (**16c**), the cores of which adopt "bent butterfly" and planar geometries, respectively.[264,266] Unlike [(N$_4$Py2)Cu$_2$(O$_2$)]$^{2+}$, PPh$_3$ is not oxidized but displaces the bound O$_2$ in [(Tp^{Me2})$_2$Cu$_2$(O$_2$)] to form the Cu(I)-PPh$_3$ adduct. Similar reactivity is exhibited by the Tp^{iPr3} (**16b**) analogue.[180] It is only possible to oxidize cyclohexene under aerobic conditions with the Tp^{Me2} (**16c**) system and the O atoms in the product are derived from exogenous O$_2$, not the peroxo moiety. Phenols and catechols are oxidatively coupled under anaerobic conditions, as observed for the N$_4$Py2 (**14b**) system. The different geometries of the two side-on peroxo adducts may well explain their varying reactivity toward substrates, although other differences such as overall charge (2+ vs neutral) and ligand-based steric bulk may be contributing factors; more detailed study is required before drawing any strong conclusions. It is noteworthy that the presumably planar μ-η^2:η^2-peroxo complex supported by the secondary diamine *t*Bu$_2$H$_2$eda (**39d**) converts PPh$_3$ to OPPh$_3$ stoichiometrically and, in unprecedented fashion, oxidizes benzyl alcohol to benzaldehyde and benzylamine to benzonitrile.[177]

The reactions of (μ-η^2:η^2-peroxo)dicopper complexes with phenols, phenolates, and catechols have attracted particular attention because of direct relevance to the catalytic transformations of tyrosinase and catechol oxidase (Figure 1b),[3,5,196,197,267] for which strong spectroscopic evidence has been provided for the intermediacy of this 2:1 Cu/O$_2$ structural motif.[3,268] Phenol or catechol oxidations have been shown to be performed by a variety of copper complexes in

the presence of O_2, although specific data that would shed light on the nature of Cu/O_2 intermediates in the reactions are generally lacking.[269−278] In reactions in which an exogenous phenol is hydroxylated in the *ortho* position (as in tyrosinase), a μ-η^2:η^2-peroxo species has been observed and shown to be directly involved in a few instances.[150,177,279,280] Addition of sodium 4-carbomethoxyphenolate to the μ-η^2:η^2-peroxo complexes formed upon low-temperature oxygenation of the dicopper(I) complex of **30a**[150] and the monocopper(I) complex of L-6Ph (**61**) yielded the corresponding *ortho*-catecholate. In the latter case,[280] no quinone or dimers arising from C−C or C−O coupling reactions were identified. On the basis of kinetic results, a mechanism involving rapid hydroxylation after reversible generation of the spectroscopically observed μ-η^2:η^2-peroxo complex was proposed, and an alternative path involving phenolate coordination to the Cu(I) complex prior to hydroxylation was ruled out. In separate experiments with [(**30a**)Cu_2]$^{2+}$, prior phenolate coordination was shown to yield hydroxylated product upon oxygenation,[276] so it is less clear with the system supported by **30a** that the peroxo species reacts directly with added phenolate. It has also been suggested that in this system quinone rather than catechol is the direct reaction product.[269] This view is controversial,[281] and has been both supported[196] and refuted[50] in studies of tyrosinase.

In another example in which phenolate hydroxylation occurs, the μ-η^2:η^2-peroxo complex supported by the secondary diamine tBu$_2$H$_2$eda (**39d**) reacts with 2,4-di-*tert*-butylphenolate at 193 K to generate 3,5-di-*tert*-butylcatechol and 3,5-di-*tert*-butyl-1,2-benzoquinone in a 1:1 ratio.[177] The overall yield was ∼80%, assuming that quinone formation from the phenolate requires 2 equiv of the peroxo complex (with no formation of Cu(I)).

Extensive mechanistic information on phenolate hydroxylation by a discrete Cu/O_2 species is available for the conversion of the series of phenolates *p*-X-C_6H_4OLi to the corresponding catechols upon reaction with the μ-η^2:η^2-peroxo complex supported by ^{H}Py2^{Bz-d2} (**13j-*d*$_2$**, deuterated at the benzylic position to inhibit competing intramolecular benzylic oxidation) at low temperature (178 K).[86,279] In this case, only catechols were observed; no quinone or C−C/C−O coupling products were identified. The loss of the μ-η^2:η^2-peroxo spectroscopic features in the presence of excess phenolate followed pseudo-first-order kinetics, and plots of the k_{obs} values as a function of [*p*-X-C_6H_4-OLi] revealed saturation behavior indicative of reversible coordination of the phenolate to the μ-η^2:η^2-peroxo complex prior to ring hydroxylation (Scheme 20). Comparison of association constants (K_f) and hydroxylation rate constants (k_{ox}) determined from double reciprocal plots as a function of the nature of the *para* substituent X showed little effect on K_f, but revealed a clear influence on k_{ox}, such that greater electron donation increased the hydroxylation rate constant. No H/D isotope effect on k_{ox} was discerned. Overall, these data support an electrophilic aromatic substitution pathway for the k_{ox} step (Scheme 20).

Scheme 20

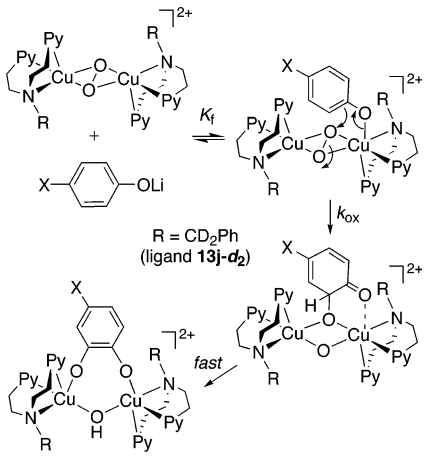

Scheme 21

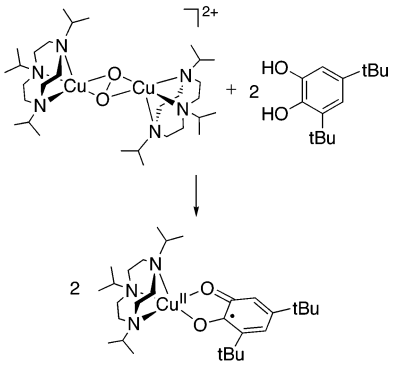

Direct treatment of well-defined Cu/O_2 adducts with catechols have revealed radical-based reaction pathways. As noted above, μ-η^2:η^2-peroxo complexes of N_4Py2 (**14b**) and Tp^{Me2} (**16c**) oxidatively couple catechols via radical processes; under excess O_2 the latter complex also generates the corresponding quinone.[266] In a related transformation, addition of 3,5-di-*tert*-butylcatechol to the μ-η^2:η^2-peroxo complex capped by L^{iPr3} (**7b**) afforded a mononuclear Cu(II)-semiquinonato complex (Scheme 21).[282] Because of the demonstrated propensity of this μ-η^2:η^2-peroxo complex to isomerize to its bis(μ-oxo) isomer, it is not clear which species reacts with catechol. In support of the possible involvement of the bis(μ-oxo) form in this reaction are (a) the known ability of bis(μ-oxo) complexes to abstract hydrogen atoms from phenols (see below) and (b) the finding that the bis(μ-oxo) compound supported by L^{Bn3} (**7c**), a ligand that does not appear to yield a μ-η^2:η^2-peroxo isomer, reacts analogously with catechols to form Cu(II)-semiquinonato products.[282] In contrast, the bis(μ-oxo) complex supported by the bidentate ligand Me$_4$pda (**23a**) quantitatively yields the corresponding quinone upon reaction with 3,5-di-*tert*-butylcatechol.[283]

Bis(μ-oxo) complexes are generally proficient at what appear to be hydrogen atom abstraction reactions, as illustrated by their reactions with phenols, which yield phenoxyl radicals or products derived therefrom. Hydrogen atom abstraction from substrates such as 1,4-cyclohexadiene or 9,10-dihydroanthracene that have weak C−H bonds has also been observed in several instances, although the nature of the oxidant in these studies is unclear. In one case

Scheme 22

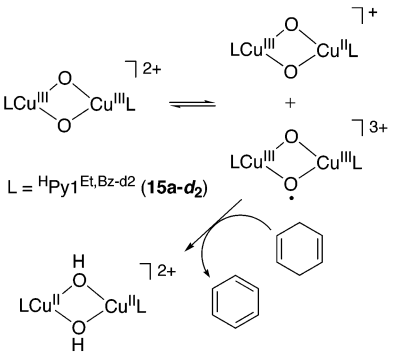

(with ^{H}Py2^{Me}, **13b**), equilibration between bis(μ-oxo) and μ-η^2:η^2-peroxo cores obfuscates matters,[119,171] while in another (with ^{H}Py1$^{Et,Bz-d2}$, **15a-*d*$_2$**, deuterated at the benzylic positions) a second-order dependence of the rate of oxidation of 10-methyl-9,10-dihydroacridine on the concentration of a bis(μ-oxo) species was observed.[284] A provocative hypothesis invoking generation of a more oxidizing (μ-oxo)(μ-oxyl radical)dicopper(III) intermediate via disproportionation of the bis(μ-oxo) complex was put forth in order to rationalize the kinetics data (Scheme 22). Interestingly, even though the bis(μ-oxo) complex of Me$_4$pda (**23a**) abstracts hydrogen atoms readily from phenols, it does not appreciably oxidize 1,4-cylohexadiene or 9,10-dihydroanthracene.[283]

In a recent detailed analysis of the one-electron oxidation of phenols by Cu/O$_2$ species, the kinetics of the reactions of the μ-η^2:η^2-peroxo complex of ^{H}Py2^{Bz-d2} (**13j-*d*$_2$**) and the bis(μ-oxo) complex of ^{H}Py1$^{Et,Bz-d2}$ (**15a-*d*$_2$**) with phenols of varying redox potentials were compared.[285] Marcus plots of the second-order rate constants (Figure 3) were linear with slopes (−0.7) more negative than the value of −0.5 predicted for rate-limiting ET (under the assumption that the driving force is significantly smaller than the reorganization energy). These data were interpreted to support a proton coupled electron transfer (PCET) pathway. Further support for this

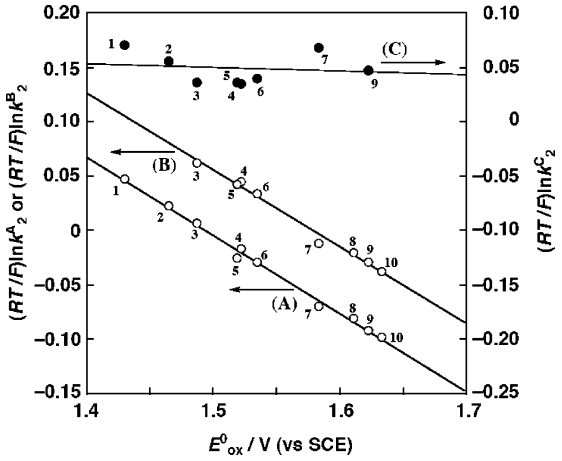

Figure 3. Marcus plots for the oxidation rates (k_2) of phenols (numbered 1−10) of variable redox potentials (E°_{ox}) by (A) the μ-η^2:η^2-peroxo complex of ^{H}Py2^{Bz-d2} (**13j-*d*$_2$**), (B) the bis(μ-oxo) complex of ^{H}Py1$^{Et,Bz-d2}$ (**15a-*d*$_2$**), and (C) cumylperoxyl radical. Figure reprinted with permission from ref 285. Copyright 2003 American Chemical Society.

Scheme 23

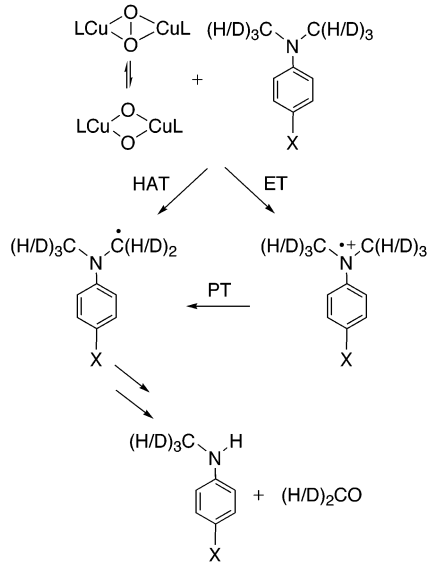

notion comes from (a) the lack of a dependence of the rate of phenol oxidation by cumylperoxyl radicals (which react via hydrogen atom transfer, HAT) on the substrate redox potential (Figure 3), (b) observation of modest KIE values (ArOH/D) between 1.2 and 1.6 that are similar to those previously reported for other PCET processes,[286] and (c) independent DFT calculations that indicate a preference for PCET over HAT in phenol oxidations.[287]

Intriguing ligand electronic effects on the reactivity of Cu/O$_2$ species with a variety of exogeneous substrates were revealed in studies of the mixture of μ-η^2:η^2-peroxo and bis(μ-oxo) complexes that result upon oxygenation of the Cu(I) complexes of ^{R}Py2^{Me} (R = H (**13b**), OMe (**41a**), Me$_2$N (**41b**)).[178] A wide range of oxidation reactions were reported, including ones not seen previously for any other characterized Cu/O$_2$ complex, such as the conversions of THF to 2-hydroxytetrahydrofuran, methanol to formaldehyde, and *N*,*N*′-dimethylaniline to methylaniline and formaldehyde. Yields and reaction rates generally increased when the most electron-donating supporting ligand was used (R = Me$_2$N, **41b**). An increased bis(μ-oxo):μ-η^2:η^2-peroxo isomer ratio also correlates with greater electron donation by the ligand (section 3), but this ratio difference probably is not the sole basis for the reactivity trend due to likely rapid equilibration of the isomers under the reaction conditions. Greater mechanistic insight into the oxidative dealkylation of *N*,*N*′-dimethylaniline was recently provided[288] by a comparison of intra- and intermolecular KIEs for reactions of the series of complexes of ^{R}Py2^{Me} (R = H (**13b**), OMe (**41a**), Me$_2$N (**41b**)) with *N*-trideuteriomethyl-*N*′-methylaniline (KIE$_{intra}$) or mixtures of *N*,*N*′-dimethylaniline and *N*,*N*′-hexadeuteriodimethylaniline (KIE$_{inter}$) with various *para*-substituents.[289] On the basis of the results, a dichotomy between hydrogen atom transfer (HAT) and electron transfer/proton transfer (ET/PT) pathways was proposed (Scheme 23), wherein the parent system reacted by ET/PT but the systems ligated by ^{R}Py2^{Me} (R = OMe (**41a**) or Me$_2$N (**41b**)) followed both pathways depending on the *para*-substituent of the

Scheme 24

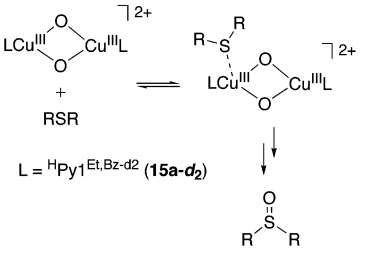

substrate. For electron-donating substituents MeO and Me, the reaction was suggested to involve rate-limiting ET, but HAT was proposed to become rate determining as the substituents become more electron withdrawing (H and CN).

A number of studies suggest that binding of substrates to available coordination positions of Cu/O_2 complexes (as in the phenolate oxidations by the peroxo complex supported by $^{H}Py2^{Bz-d2}$ (**13j-*d*$_2$**) described above) may be a generally important mechanistic feature in oxidation reactions. Thus, $[(Me_4pda)_2Cu_2(\mu\text{-}O)_2]^{2+}$ oxidizes alcohols to aldehydes or ketones and benzylamine to benzonitrile in reactions that are postulated to involve coordination to copper followed by deprotonation and then oxidation.[283] Support for the capability for substrate to coordinate to a Cu(III) center was provided by (a) EXAFS data that implicate ClO_4^- binding to this complex and (b) an X-ray crystal structure of a related bis(μ-oxo) compound $[(Me_2L^{Me2})(Me_4pda)Cu_2(\mu\text{-}O)_2]O_3SCF_3$ (Me_2L^{Me2} = **18b**) that shows $CF_3SO_3^-$ coordination to the Cu ligated by Me_4pda (**23a**).[125] Direct kinetic evidence for substrate coordination was provided in studies of the oxidation of thioethers to sulfoxides by the bis(μ-oxo) complex supported by $^{H}Py1^{Et,Bz-d2}$ (**15a-*d*$_2$**).[290] The kinetic data support rapid binding of thioether followed by slower oxidation (Scheme 24), which is suggested to involve direct oxygen atom transfer instead of electron transfer on the basis of a relatively small dependence of the rate constant on the substrate oxidation potential for a range of thioethers (value of -0.94 for the slope of log k_2 vs E^0_{ox}).[291]

The significance of substrate coordination has been stressed in a comparative study of the reactivity of isomeric bis(μ-oxo) and μ-η^2:η^2-peroxo dicopper complexes of tBu$_2$Me$_2$eda (**39a**) that equilibrate unusually slowly, $[(t\text{Bu}_2\text{Me}_2\text{eda})_2\text{Cu}_2(\mu\text{-O})_2]^{2+}$ and $[(t\text{Bu}_2\text{Me}_2\text{eda})_2\text{Cu}_2(\text{O}_2)]^{2+}$.[174] The μ-η^2:η^2-peroxo isomer reacts more readily than the bis(μ-oxo) with PPh_3 to yield $OPPh_3$, but the bis(μ-oxo) is more efficient at oxidatively coupling 3,5-di-*tert*-butylphenol. These results implicate reactivity differences intrinsic to the isomeric structure of the dicopper core, although other results suggest that accessibility of substrate to a copper center is just as critical. Thus, while the bis(μ-oxo) complex supported by iPr$_2$Me$_2$eda (**39b**, uncontaminated by measurable amounts of its peroxo isomer) is incapable of oxidizing PPh_3, that supported by the much less hindered Me_4pda (**23a**) produces $OPPh_3$ in high yield.

Substrate coordination to a Cu center has also been implicated by the results of kinetic data obtained for the reaction of 2,4-di-*tert*-butylphenol with the bis(μ_3-oxo)tricopper(II,II,III) complex supported by $^{H}Py1^{Me,Me}$ (**15b**).[161] The tricopper compound acts as a two-electron oxidant to yield the coupled bis-phenol dimer, a bis(μ-hydroxo)dicopper(II,II) species, and $[(^{H}Py1^{Me,Me})Cu]^+$ (Scheme 25). Two intermediates were identified by UV−vis spectroscopy (**I** and **J**). The rate of decay of the tricopper starting material displays a first-order dependence on its concentration and on that of the phenol ($k_1 = 0.46 \pm 0.02$ M^{-1} s^{-1} at 183 K, Scheme 25). Since the more hindered substrate 2,4,6-tri-*tert*-butylphenol did not react, phenol coordination is implicated in the generation of intermediate **I**. The slower conversion to intermediate **J** displayed substrate saturation kinetics ($K = 44.6 \pm 2.2$ M^{-1} and $k_2 = 9.5 \pm 0.5 \times 10^{-3}$ s^{-1} at 203 K), supporting substrate coordination in this step as well, and leading to the overall mechanistic postulate outlined in Scheme 25. Further work is required to delineate the structures of **I** and **J**.

Scheme 25

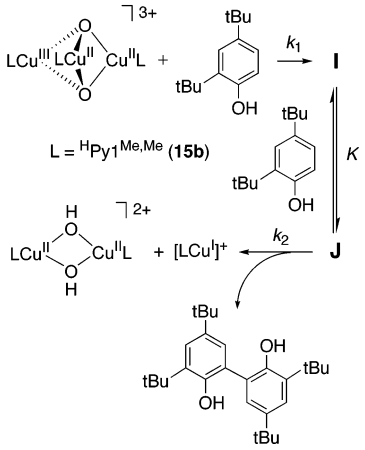

Protonation or acylation of peroxo copper species appears to enhance their O-atom transfer reactivity. This has been demonstrated by observation of facile, stoichiometric conversion of PPh_3 to $OPPh_3$ and/or R_2S to R_2SO by hydro- and acylperoxo complexes supported by Tp^{iPr2} (**16b**),[181,182] XYL-O$^-$ (**24g**),[191,192] UN−O$^-$ (**26b**),[143] TMPA (**1**),[187] 1,2-dimethylimidazole,[187] and $^{H}Py2^{BzO}$ (**13k**).[187] In most cases, copper(II) complexes with hydroxo- or carboxylate ligands, respectively, were isolated from the reactions. Detailed mechanistic information on these reactions are not available, although an analysis of O−O and Cu−O bond scission pathways in reactions of Tp^{iPr2}-CuOOH(R) complexes using spectroscopic and theoretical methods has been presented.[183] A key conclusion is that O−O homolysis or heterolysis in these complexes is energetically disfavored because of thermodynamic instability of the resulting Cu(III/IV)-oxo species. Further studies of supporting ligand effects on these energetics are needed.

Coupling of inter- and intramolecular reactivity has been reported for the reaction of the 2:1 Cu/O_2 adduct supported by the ligand PD (**27a**) with dimethylformamide (DMF, Scheme 26).[82,145] The product contains a hydroxylated arene linker and formate derived from hydrolysis of DMF, with both atoms from O_2 incorporated (one in the arene and the other in formate) as shown by a ^{18}O-isotope labeling experi-

Scheme 26

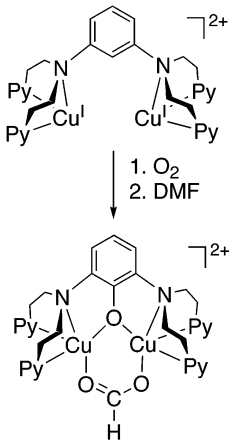

ment. Initial nucleophilic attack of the 2:1 Cu/O_2 adduct at the DMF carbon was suggested as one possible reaction pathway, but mechanistic data are lacking.

7. Perspective and Conclusion

Enormous research efforts over the past several decades have borne fruit, insofar as our understanding has deepened of the detailed mechanisms by which copper complexes bind and activate dioxygen. Through cryogenic stopped-flow studies of the oxygenation of Cu(I) compounds, critically important kinetic and thermodynamic information has been obtained. A notable general finding concerns the typical thermodynamic instability of Cu/O_2 adducts, which may be traced to a negative reaction entropy that offsets the favorable enthalpy for O_2 binding. One strategy for enhancing adduct stability is to manipulate the unfavorable entropy term by controlling the conformational flexibity of dinucleating ligands. Putting this notion into practice is not without pitfalls, however, such as enthalpic destabilization that can accompany imposition of conformational control,[99,100] and other approaches such as protecting supporting ligands from intramolecular oxidative attack may also be required.[194,195] To date, Cu/O_2 adducts that exhibit room-temperature stability are rare,[146,152,193−195] but others are sure to be discovered.

Processes by which Cu/O_2 adducts interconvert and O−O bonds are broken and formed are especially important to understand if enzymatic mechanisms of dioxygen activation are to be deconvoluted. The peroxo/bis(μ-oxo) equilibration in dicopper compounds is an illustrative example, and examination of the factors that control the relative stability of the two isomeric cores continues to be informative, as do efforts to dissect their relative reactivities toward exogenous substrates in order to develop new and useful oxidation reagents and to understand the nature of the oxidants involved in biological catalysis. Whether or not the peroxo/bis(μ-oxo) interconversion is important in specific copper proteins, such as in tyrosinase, is a matter of active debate, and we note that the bis(μ-oxo) form has not been observed in any protein system.[170,197] Irrespective of the ultimate conclusions drawn for its involvement in particular biological processes, work on the peroxo/bis(μ-oxo) equilibrium should continue to influence interpretations of studies of O_2 activation by a variety of synthetic compounds and/or proteins, including those that incorporate metal ions other than Cu, such as Fe,[292] Mn,[293] Co,[294,295] and Ni.[238,294,296] Finally, it is important to emphasize that the peroxo/bis(μ-oxo) equilibrium is just one of many possible dynamic transformations that may occur as O_2 is manipulated by metal sites for attack at organic substrates (cf. Schemes 7 and 16), and further elucidation of such processes is eagerly awaited.

Detailed insights into the mechanisms of intra- and intermolecular oxidations by well-characterized Cu/O_2 compounds have been obtained in several instances. Notable in this regard are the investigations of *m*-xylyl hydroxylations and N-dealkylations by peroxo and bis(μ-oxo)dicopper species, respectively, described in sections 5.1 and 5.2. Mechanistic understanding is less well-developed for intermolecular reactions of Cu/O_2 species, which display variable reactivity that depends on Cu/O_2 adduct and supporting ligand properties in ways that in many respects are difficult to fathom. An illustrative unresolved issue concerns the bases for one- vs two-electron redox chemistry by dicopper species (e.g., radical abstractions vs O-atom transfers) and for PCET vs HAT pathways. Addressing the nature of elementary reaction steps in oxidations by discrete Cu/O_2 complexes is thus a fertile area for future study, with success most likely to depend on the synergistic application of experimental and theoretical approaches.

A survey of the field also reveals the preponderance of systems comprising two copper ions, reflecting a particular thermodynamic preference with the ligands used to date that has arguably played a role in leading researchers to focus their efforts on such species. Particular interest on dicopper compounds also has been motivated by their relevance to the well-characterized proteins hemocyanin, tyrosinase, and catechol oxidase. Fewer mono-, tri-, or tetranuclear Cu/O_2 compounds have been studied, and it would appear that ingenious synthetic approaches will be required to access a diverse array of such species for comparative studies and to inhibit the formation of the generally more favored dicopper cores. Particular impetus for future research aimed at these types of molecules is provided by the established significance in oxygenase and oxidase enzymes of active sites with one or three (or more) copper ions. Unresolved questions centered on how O_2 is activated by these enzymes should inspire synthetic efforts for years to come.

8. Acknowledgments

We thank the coauthors cited in the references from our laboratory for their extensive efforts, and the NIH (GM47365) for financial support.

9. References

(1) Solomon, E. I.; Chen, P.; Metz, M.; Lee, S.-K.; Palmer, A. E. *Angew. Chem., Int. Ed.* **2001**, *40*, 4570.

(2) Klinman, J. P. *Chem. Rev.* **1996**, *96*, 2541.
(3) Solomon, E. I.; Sundaram, U. M.; Machonkin, T. E. *Chem. Rev.* **1996**, *96*, 2563.
(4) Magnus, K. A.; Ton-That, H.; Carpenter, J. E. *Chem. Rev.* **1994**, *94*, 727.
(5) Sánchez-Ferrer, A.; Rodríguez-López, J. N.; García-Cánovas, F.; García-Carmona, F. *Biochim. Biophys. Acta* **1995**, *1247*, 1.
(6) Gerdemann, C.; Eicken, C.; Krebs, B. *Acc. Chem. Res.* **2002**, *35*, 183.
(7) Fusetti, F.; Schröter, K. H.; Steiner, R. A.; van Noort, P. I.; Pijning, T.; Rozeboom, H. J.; Kalk, K. H.; Egmond, M. R.; Dijkstra, B. W. *Structure* **2002**, *10*, 259.
(8) Steiner, R. A.; Kooter, I. M.; Dijkstra, B. W. *Biochemistry* **2002**, *41*, 7955.
(9) Kooter, I. M.; Steiner, R. A.; Dijkstra, B. W.; van Noort, P. I.; Egmund, M. R.; Huber, M. *Eur. J. Biochem.* **2002**, *269*, 2971.
(10) Stewart, L. C.; Klinman, J. P. *Annu. Rev. Biochem.* **1988**, *57*, 551.
(11) Prigge, S. T.; Mains, R. E.; Eipper, B. A.; Amzel, L. M. *Cell. Mol. Life Sci.* **2000**, *57*, 1236.
(12) Blackburn, N. J.; Rhames, F. C.; Ralle, M.; Jaron, S. *J. Biol. Inorg. Chem.* **2000**, *5*, 341.
(13) Whittaker, J. W. *Chem. Rev.* **2003**, *103*, 2347.
(14) Whittaker, J. W.; Whittaker, M. M. *Pure Appl. Chem.* **1998**, *70*, 903.
(15) Knowles, P. F.; Ito, N. In *Perspectives in Bio-inorganic Chemistry*; Jai Press LTD: London, 1994; Vol. 2, p 207.
(16) Halcrow, M.; Phillips, S.; Knowles, P. In *Subcellular Biochemistry, Vol. 35: Enzyme-Catalyzed Electron and Radical Transfer*; Holzenburg, A., Scrutton, N. S., Eds.; Plenum: New York, 2000; pp 183−231.
(17) Whittaker, M. M.; Kersten, P. J.; Nakamura, N.; Sanders-Loehr, J.; Schweizer, E. S.; Whittaker, J. W. *J. Biol. Chem.* **1996**, *271*, 681.
(18) Whittaker, M. M.; Kersten, P. J.; Cullen, D.; Whittaker, J. W. *J. Biol. Chem.* **1999**, *274*, 36226.
(19) Kosman, D. J.; Hassett, R.; Yuan, D. S.; McCracken, J. *J. Am. Chem. Soc.* **1998**, *120*, 4037.
(20) Blackburn, N. J.; Ralle, M.; Hassett, R.; Kosman, D. J. *Biochemistry* **2000**, *39*, 2316.
(21) Palmer, A. E.; Quintanar, L.; Severancee, S.; Wang, T.-P.; Kosman, D. J.; Solomon, E. I. *Biochemistry* **2002**, *41*, 6438.
(22) Nguyen, H.-H. T.; Nakagawa, K. H.; Hedman, B.; Eliot, S. J.; Lidstrom, M. E.; Hodgson, K. O.; Chan, S. I. *J. Am. Chem. Soc.* **1996**, *118*, 12766.
(23) Elliott, S. J.; Randall, D. W.; Britt, R. D.; Chan, S. I. *J. Am. Chem. Soc.* **1998**, *120*, 3247.
(24) Nguyen, H.-H. T.; Elliot, S. J.; Yip, J. H.-K.; Chan, S. I. *J. Biol. Chem.* **1998**, *273*, 7957.
(25) Lieberman, R. L.; Shrestha, D. B.; Doan, P. E.; Hoffman, B. M.; Stemmler, T. L.; Rosenzweig, A. C. *Proc. Natl. Acad. Sci. U.S.A.* **2003**, *100*, 3820.
(26) Knowles, P. F.; Dooley, D. M. In *Metal Ions in Biological Systems*; Sigel, H., Sigel, A., Eds.; Marcel Dekker: Basel, Switzerland, 1994; Vol. 30, pp 361−403.
(27) Mure, M.; Mills, S. A.; Klinman, J. P. *Biochemistry* **2002**, *41*, 9269.
(28) Kishishita, S.; Okajima, T.; Kim, M.; Yamaguchi, H.; Hirota, S.; Suzuki, S.; Kuroda, S.; Tanizawa, K.; Mure, M. *J. Am. Chem. Soc.* **2003**, *125*, 1041.
(29) Arp, D. J.; Sayavedra-Soto, L. A.; Hommes, N. G. *Arch. Microbiol.* **2002**, *178*, 250.
(30) Bothe, H.; Jost, G.; Schloter, M.; Ward, B. B.; Witzel, K.-P. *FEMS Microbiol. Rev.* **2000**, *24*, 673.
(31) *Multi-Copper Oxidases*; Messerschmidt, A., Ed.; World Scientific: Singapore, 1997.
(32) Hakulinen, N.; Kiiskinen, L.-L.; Kruus, K.; Saloheimo, M.; Paananen, A.; Koivula, A.; Rouvinen, J. *Nat. Struct. Biol.* **2002**, *9*, 601.
(33) Bertrand, T.; Jolivalt, C.; Briozzo, P.; Caminade, E.; Joly, N.; Madzak, C.; Mougin, C. *Biochemistry* **2002**, *41*, 7325.
(34) Lee, S.-K.; George, S. D.; Antholine, W. E.; Hedman, B.; Hodgson, K. O.; Solomon, E. I. *J. Am. Chem. Soc.* **2002**, *124*, 6180.
(35) Messerschmidt, A.; Luecke, H.; Huber, R. *J. Mol. Biol.* **1993**, *230*, 997.
(36) Zaitseva, I.; Zaitsev, V.; Card, G.; Moshkov, K.; Bax, B.; Ralph, A.; Lindley, P. *J. Biol. Inorg. Chem.* **1996**, *1*, 15.
(37) Palmer, A. E.; Quintanar, L.; Severancee, S.; Wang, T.-P.; Kosman, D. J.; Solomon, E. I. *Biochemistry* **2002**, *41*, 6438.
(38) Wang, T.-P.; Quintanar, L.; Severance, S.; Solomon, E. I.; Kosman, D. J. *J. Biol. Inorg. Chem.* **2003**, *8*, 611.
(39) Barry, C. E., III; Nayar, P. G.; Begley, T. P. *J. Am. Chem. Soc.* **1988**, *110*, 3333−3334.
(40) Barry, C. E., III; Nayar, P. G.; Begley, T. P. *Biochemistry* **1989**, *28*, 6323−6333.
(41) Ferguson-Miller, S.; Babcock, G. T. *Chem. Rev.* **1996**, *96*, 2889.
(42) Michel, H.; Behr, J.; Harrenga, A.; Kannt, A. *Annu. Rev. Biophys. Biomol. Struct.* **1998**, *27*, 329.
(43) Dooley, D. M. *J. Biol. Inorg. Chem.* **1999**, *4*, 1−11.
(44) Whittaker, M. M.; Ballou, D. P.; Whittaker, J. W. *Biochemistry* **1998**, *37*, 8426.
(45) Francisco, W. A.; Knapp, M. J.; Blackburn, N. J.; Klinman, J. P. *J. Am. Chem. Soc.* **2002**, *124*, 8194.
(46) Francisco, W. A.; Blackburn, N. J.; Klinman, J. P. *Biochemistry* **2003**, *42*, 1813.
(47) Evans, J. P.; Ahn, K.; Klinman, J. P. *J. Biol. Chem.* **2003**, *278*, 49691.
(48) Blackburn, N. J.; Rhames, F. C.; Ralle, M.; Jaron, S. *J. Biol. Inorg. Chem.* **2000**, *5*, 341.
(49) Eicken, C.; Zippel, F.; Karentzopoulos, K. B.; Krebs, B. *FEBS Lett.* **1998**, *436*, 293.
(50) Yamazaki, S.; Itoh, S. *J. Am. Chem. Soc.* **2003**, *125*, 13034.
(51) Siegbahn, P. E. M. *J. Biol. Inorg. Chem.* **2003**, *8*, 567.
(52) Shin, W.; Sundaram, U. M.; Cole, J. L.; Zhang, H. H.; Hedman, B.; Hodgson, K. O.; Solomon, E. I. *J. Am. Chem. Soc.* **1996**, *118*, 3202.
(53) Palmer, A. E.; Lee, S. K.; Solomon, E. I. *J. Am. Chem. Soc.* **2001**, *123*, 6591.
(54) A different structure for the so-called "peroxo intermediate" has been proposed on the basis of X-ray crystallographic evidence: Messerschmidt, A.; Luecke, H.; Huber, R. *J. Mol. Biol.* **1993**, *230*, 997.
(55) Karlin, K. D. *Science* **1993**, *261*, 701.
(56) Parshall, G. W.; Ittel, S. D. *Homogeneous Catalysis*, 2nd ed.; John Wiley & Sons: New York, 1992; pp 172−177.
(57) Markó, I. E.; Giles, P. R.; Tsukazaki, M.; Brown, S. M.; Urch, C. J. *Science* **1996**, *274*, 2044.
(58) Palomino, G. T.; Fisicaro, P.; Bordiga, S.; Zecchina, A. *J. Phys. Chem. B* **2000**, *104*, 4064 and references therein.
(59) Reitz, J. B.; Solomon, E. I. *J. Am. Chem. Soc.* **1998**, *120*, 11467.
(60) *Molecular Mechanisms of Oxygen Activation*; Hayaishi, O., Ed.; Academic Press: New York and London, 1974.
(61) Karlin, K. D.; Gultneh, Y. *Prog. Inorg. Chem.* **1987**, *35*, 219.
(62) Sorrell, T. N. *Tetrahedron* **1989**, *45*, 3.
(63) Tyeklár, Z.; Karlin, K. D. *Acc. Chem. Res.* **1989**, *22*, 241.
(64) Spodine, E.; Manzur, J. *Coord. Chem. Rev.* **1992**, *119*, 171.
(65) Kitajima, N. *Adv. Inorg. Chem.* **1992**, *39*, 1.
(66) Kitajima, N.; Moro-oka, Y. *J. Chem. Soc., Dalton Trans.* **1993**, 2665.
(67) *Bioinorganic Chemistry of Copper*; Karlin, K. D., Tykelár, Z., Eds.; Chapman and Hall: New York, 1993.
(68) Kitajima, N.; Moro-oka, Y. *Chem. Rev.* **1994**, *94*, 737.
(69) Solomon, E. I.; Tuczek, F.; Root, D. E.; Brown, C. A. *Chem. Rev.* **1994**, *94*, 827.
(70) Tolman, W. B. *Acc. Chem. Res.* **1997**, *30*, 227.
(71) Akita, M.; Moro-oka, Y. *Catal. Today* **1998**, *44*, 183.
(72) Moro-oka, Y. *Catal. Today* **1998**, *45*, 3.
(73) Akita, M.; Fujisawa, K.; Hikichi, S.; Moro-oka, Y. *Res. Chem. Intermed.* **1998**, *24*, 291.
(74) Holland, P. L.; Tolman, W. B. *Coord. Chem. Rev.* **1999**, *190−192*, 855.
(75) Than, R.; Feldmann, A. A.; Krebs, B. *Coord. Chem. Rev.* **1999**, *182*, 211.
(76) Eicken, C.; Krebs, B.; Sacchettini, J. C. *Curr. Opin. Chem. Biol.* **1999**, *9*, 677.
(77) Moro-oka, Y.; Akita, M. *Catal. Today* **1999**, *41*, 327.
(78) Liang, H.-C.; Dahan, M.; Karlin, K. D. *Curr. Opin. Chem. Biol.* **1999**, *3*, 168.
(79) Blackman, A. G.; Tolman, W. B. *Struct. Bonding (Berlin)*; Meunier, B., Ed.; Springer-Verlag: 2000; Vol. 97, p 179.
(80) Mahadevan, M.; Klein Gebbink, R. J. M.; Stack, T. D. P. *Curr. Opin. Chem. Biol.* **2000**, *4*, 228.
(81) Kopf, M.-A.; Karlin, K. D. in *Biomimetic Oxidations Catalysed by Transition Metal Complexes*; Meunier, B., Ed.; Imperial College Press: 2000; p 309.
(82) Murthy, N. N.; Karlin, K. D. In *Mechanistic Bioinorganic Chemistry*; Thorp, H. H., Pecoraro, V. L., Eds.; American Chemical Society: Washington, DC, 1995; Adv. Chem. Ser. Vol. 246, p 165.
(83) Feiters, M. C. In *Metal Ions in Biological Systems*; Sigel, H., Sigel, A., Eds.; Marcel Dekker: New York, 2001; Vol. 38, pp 461−655.
(84) Solomon, E. I.; Chen, P.; Metz, M.; Lee, S.-K.; Palmer, A. *Angew. Chem., Int. Ed.* **2001**, *40*, 4570.
(85) Que, L., Jr.; Tolman, W. B. *Angew. Chem., Int. Ed.* **2002**, *41*, 1114.
(86) Itoh, S.; Fukuzumi, S. *Bull. Chem. Soc. Jpn.* **2002**, *75*, 2081.
(87) Halcrow, M. In *Comprehensive Coordination Chemistry II: From Biology to Nanotechnology*; McCleverty, J., Meyer, T. J., Eds.; Elsevier: Oxford, UK, 2003; Vol. 8, pp 395−436.
(88) Itoh, S. In *Comprehensive Coordination Chemistry II: From Biology to Nanotechnology*; McCleverty, J., Meyer, T. J., Eds.; Elsevier: Oxford, UK, 2003; Vol. 8, pp 369−393.
(89) Stack, T. D. P. *Dalton Trans.* **2003**, 1881.
(90) Stack, T. D. P. *Chem. Rev.* **2004**, *2*, 1013.
(91) Zuberbühler, A. D. *Helv. Chim. Acta* **1976**, *59*, 1448.
(92) Güntensperger, M.; Zuberbühler, A. D. *Helv. Chim. Acta* **1977**, *60*, 2584.

(93) Tolman, W. B.; Spencer, D. J. E. *Curr. Opin. Chem. Biol.* **2001**, *5*, 188.
(94) Elsevier, C. J.; Reedijk, J.; Walton, P. H.; Ward, M. D. *Dalton Trans.* **2003**, 1869.
(95) Schindler, S.; Hubbard, C. D.; van Eldik, R. *Chem. Soc. Rev.* **1998**, *27*, 387.
(96) Schindler, S. *Eur. J. Inorg. Chem.* **2000**, 2311.
(97) Weitzer, M.; Schatz, M.; Hampel, F.; Heinemann, F.; Schindler, S. *J. Chem. Soc., Dalton Trans.* **2002**, 686.
(98) SPECFIT/32, Spectrum Software Associates, 2000−2003.
(99) Karlin, K. D.; Kaderli, S.; Zuberbühler, A. D. *Acc. Chem. Res.* **1997**, *30*, 139.
(100) Karlin, K. D.; Tolman, W. B.; Kaderli, S.; Zuberbühler, A. D. *J. Mol. Catal. A* **1997**, *117*, 215.
(101) Niederhoffer, E. C.; Timmons, J. H.; Martell, A. E. *Chem. Rev.* **1984**, *84*, 137.
(102) Jacobsen, R. R.; Tyeklár, Z.; Farooq, A.; Karlin, K. D.; Lui, S.; Zubieta, J. *J. Am. Chem. Soc.* **1988**, *110*, 3690.
(103) Karlin, K. D.; Wei, N.; Jung, B.; Kaderli, S.; Zuberbühler, A. D. *J. Am. Chem. Soc.* **1991**, *113*, 5868.
(104) Karlin, K. D.; Wei, N.; Jung, B.; Kaderli, S.; Niklaus, P.; Zuberbühler, A. D. *J. Am. Chem. Soc.* **1993**, *115*, 9506.
(105) Zhang, C. X.; Kaderli, S.; Costas, M.; Kim, E.; Neuhold, Y.-M.; Karlin, K. D.; Zuberbühler, A. D. *Inorg. Chem.* **2003**, *42*, 1807.
(106) Fry, H. C.; Scaltrito, D. V.; Karlin, K. D.; Meyer, G. J. *J. Am. Chem. Soc.* **2003**, *125*, 11866.
(107) Lee, D.-H.; Wei, N.; Murthy, N. N.; Tyeklár, Z.; Karlin, K. D.; Kaderli, S.; Jung, B.; Zuberbühler, A. D. *J. Am. Chem. Soc.* **1995**, *117*, 12498.
(108) Becker, M.; Heinemann, F.; Schindler, S. *Chem. Eur. J.* **1999**, *5*, 3124.
(109) Weitzer, M.; Schindler, S.; Brehm, G.; Schneider, S.; Hörmann, E.; Jung, B.; Kaderli, S.; Zuberbühler, A. D. *Inorg. Chem.* **2003**, *42*, 1800.
(110) Wei, N.; Murthy, N. N.; Chen, Q.; Zubieta, J.; Karlin, K. D. *Inorg. Chem.* **1994**, *33*, 1953.
(111) Wei, N.; Lee, D.-H.; Murthy, N. N.; Tyeklár, Z.; Karlin, K. D.; Kaderli, S.; Jung, B.; Zuberbühler, A. D. *Inorg. Chem.* **1994**, *33*, 4625.
(112) Jung, B.; Karlin, K. D.; Zuberbühler, A. D. *J. Am. Chem. Soc.* **1996**, *118*, 3763.
(113) Itoh, S.; Nakao, H.; Berreau, L. M.; Kondo, T.; Komatsu, M.; Fukuzumi, S. J. *J. Am. Chem. Soc.* **1998**, *120*, 2890.
(114) Liang, H.-C.; Zhang, C. X.; Henson, M. J.; Sommer, R. D.; Hatwell, K. R.; Kaderli, S.; Zuberbühler, A. D.; Rheingold, A. L.; Solomon, E. I.; Karlin, K. D. *J. Am. Chem. Soc.* **2002**, *124*, 4170.
(115) Mahapatra, S.; Kaderli, S.; Llobet, A.; Neuhold, Y.-M.; Palanché, T.; Halfen, J. A.; Young, V. G., Jr.; Kaden, T. A.; Que, L., Jr.; Zuberbühler, A. D.; Tolman, W. B. *Inorg. Chem.* **1997**, *36*, 6343.
(116) Halfen, J. A.; Mahapatra, S.; Wilkinson, E. C.; Kaderli, S.; Young, V. G., Jr.; Que, L., Jr.; Zuberbühler, A. D.; Tolman, W. B. *Science* **1996**, *271*, 1397.
(117) Mahapatra, S.; Young, V. G., Jr.; Tolman, W. B. *Angew. Chem., Int. Ed. Engl.* **1997**, *36*, 130.
(118) Jazdzewski, B. A.; Reynolds, A. M.; Holland, P. L.; Young, V. G., Jr.; Kaderli, S.; Zuberbühler, A. D.; Tolman, W. B. *J. Biol. Inorg. Chem.* **2003**, *8*, 381.
(119) Obias, H. V.; Lin, Y.; Murthy, N. N.; Pidcock, E.; Solomon, E. I.; Ralle, M.; Blackburn, N. J.; Neubold, Y. M.; Zuberbühler, A. D.; Karlin, K. D. *J. Am. Chem. Soc.* **1998**, *120*, 12960.
(120) Itoh, S.; Taki, M.; Nakao, H.; Holland, P. L.; Tolman, W. B.; Que, L., Jr.; Fukuzumi, S. *Angew. Chem., Int. Ed.* **2000**, *39*, 398.
(121) Fujisawa, K.; Tanaka, M.; Moro-oka, Y.; Kitajima, N. *J. Am. Chem. Soc.* **1994**, *116*, 12079.
(122) Chen, P.; Root, D. E.; Campochiaro, C.; Fujisawa, K.; Solomon, E. I. *J. Am. Chem. Soc.* **2003**, *125*, 466.
(123) Chaudhuri, P.; Hess, M.; Weyhermüller, T.; Wieghardt, K. *Angew. Chem., Int. Ed.* **1999**, *38*, 1095.
(124) Spencer, D. J. E.; Aboelella, N. W.; Reynolds, A. M.; Holland, P. L.; Tolman, W. B. *J. Am. Chem. Soc.* **2002**, *124*, 2108.
(125) Aboelella, N. W.; Lewis, E. A.; Reynolds, A. M.; Brennessel, W. W.; Cramer, C. J.; Tolman, W. B. *J. Am. Chem. Soc.* **2002**, *124*, 10660.
(126) Harata, M.; Jitsukawa, K.; Masuda, H.; Einaga, H. *J. Am. Chem. Soc.* **1994**, *116*, 10817.
(127) Berreau, L. M.; Mahapatra, S.; Halfen, J. A.; Young, V. G., Jr.; Tolman, W. B. *Inorg. Chem.* **1996**, *35*, 6339.
(128) Harata, M.; Jitsukawa, K.; Masuda, H.; Einaga, H. *Bull. Chem. Soc. Jpn.* **1998**, *71*, 637.
(129) Harata, M.; Jitsukawa, K.; Masuda, H.; Einaga, H. *Chem. Lett.* **1996**, 813.
(130) Momenteau, M.; Reed, C. A. *Chem. Rev.* **1994**, *94*, 659.
(131) Suzuki, M.; Furutachi, H.; Okawa, H. *Coord. Chem. Rev.* **2000**, *200−202*, 105.
(132) Carrier, S. M.; Ruggiero, C. E.; Houser, R. P.; Tolman, W. B. *Inorg. Chem.* **1993**, *32*, 4889.
(133) Kiani, S.; Long, J. R.; Stavropoulos, P. *Inorg. Chim. Acta* **1997**, *263*, 357.
(134) Reim, J.; Krebs, B. *Angew. Chem., Int. Ed.* **1994**, *33*, 1969.
(135) Reim, J.; Werner, R.; Haase, W.; Krebs, B. *Chem. Eur. J.* **1998**, *4*, 289.
(136) Schatz, M.; Becker, M.; Thaler, F.; Hampel, F.; Schindler, S.; Jacobson, R. R.; Tyeklár, Z.; Murthy, N. N.; Ghosh, P.; Chen, Q.; Zubieta, J.; Karlin, K. D. *Inorg. Chem.* **2001**, *40*, 2312.
(137) Enomoto, M.; Aida, T. *J. Am. Chem. Soc.* **1999**, *121*, 874.
(138) Hilton, E.; Reynolds, A. R.; Tolman, W. B., unpublished results.
(139) Cruse, R. W.; Kaderli, S.; Karlin, K. D.; Zuberbühler, A. D *J. Am. Chem. Soc.* **1988**, *110*, 6882.
(140) Karlin, K. D.; Nasir, M. S.; Cohen, B. I.; Cruse, R. W.; Kaderli, S.; Zuberbühler, A. D *J. Am. Chem. Soc.* **1994**, *116*, 1324.
(141) Karlin, K. D.; Cruse, R. W.; Gultneh, Y.; Farooq, A.; Hayes, J. C.; Zubieta, J. *J. Am. Chem. Soc.* **1987**, *109*, 2668.
(142) Zhang, C. X.; Liang, H.-C.; Kim, E.-i.; Gan, Q.-F.; Tyeklár, Z.; Lam, K.-C.; Rheingold, A. L.; Kaderli, S.; Zuberbühler, A. D.; Karlin, K. D. *Chem. Commun.* **2001**, 631.
(143) Mahroof-Tahir, M.; Murthy, N. N.; Karlin, K. D.; Blackburn, N. J.; Shaikh, S. N.; Zubieta, J. *Inorg. Chem.* **1992**, *31*, 3001.
(144) Mahroof-Tahir, M.; Karlin, K. D. *J. Am. Chem. Soc.* **1992**, *114*, 7599.
(145) Murthy, N. N.; Mahroof-Tahir, M.; Karlin, K. D. *J. Am. Chem. Soc.* **1993**, *115*, 10404.
(146) Bol, J. E.; Driessen, W. L.; Ho, R. Y. N.; Maase, B.; Que, L., Jr.; Reedijk, J. *Angew. Chem., Int. Ed.* **1997**, *36*, 998.
(147) Gebbink, R. J. M. K.; Bosman, A. W.; Feiters, M. C.; Meijer, E. W.; Nolte, R. J. M. *Chem. Eur. J.* **1999**, *5*, 65.
(148) While competition between intramolecular and intermolecular paths has not been noted for these cases, whether one or the other is followed is not always possible to discern from the available data (cf. the case of ligand D in ref 142).
(149) Becker, M.; Schindler, S.; Karlin, K. D.; Kaden, T. A.; Kaderli, S.; Palanché, T.; Zuberbühler, A. D. *Inorg. Chem.* **1999**, *38*, 1989.
(150) Santagostini, L.; Gullotti, M.; Monzani, E.; Casella, L.; Dillinger, R.; Tuczek, F. *Chem. Eur. J.* **2000**, *6*, 519.
(151) Börzel, H.; Comba, P.; Katsichtis, C.; Kiefer, W.; Lienke, A.; Nagel, V.; Pritzkow, H. *Chem. Eur. J.* **1999**, *5*, 1716.
(152) Kodera, M.; Katayama, K.; Tachi, Y.; Kano, K.; Hirota, S.; Fujinami, S.; Suzuki, M. *J. Am. Chem. Soc.* **1999**, *121*, 11006.
(153) Klein Gebbink, R. J. M.; Martens, C. F.; Kenis, P. J. A.; Jansen, R. J.; Nolting, H.-F.; Solé, V. A.; Feiters, M. C.; Karlin, K. D.; Nolte, R. J. M. *Inorg. Chem.* **1999**, *38*, 5755.
(154) Spiccia, L.; Graham, B.; Hearn, M. T. W.; Lazarev, G.; Moubaraki, B.; Murray, K. S.; Tiekink, E. R. T. *J. Chem. Soc., Dalton Trans.* **1998**, 4089.
(155) Molenveld, P.; Stikvoort, W. M. G.; Kooijman, H.; Spek, A. L.; Engbersen, J. F. J.; Reinhoudt, D. N. *J. Org. Chem.* **1999**, *64*, 3896.
(156) Spencer, D. J. E.; Johnson, B. J.; Johnson, B. J.; Tolman, W. B. *Org. Lett.* **2002**, *4*, 1391.
(157) Suh, M. P.; Han, M. Y.; Lee, J. H.; Min, K. S.; Hyeon, C. *J. Am. Chem. Soc.* **1998**, *120*, 3819.
(158) In one study of a tricopper(I) complex of a trinucleating ligand, isolation of a product featuring a hydroxylated *m*-xylyl linker implicated generation of a peroxodicopper intermediate: Karlin, K. D.; Gan, Q.-F.; Farooq, A.; Liu, S.; Zubieta, J. *Inorg. Chem.* **1990**, *29*, 2549.
(159) Cole, A. P.; Root, D. E.; Mukherjee, P.; Solomon, E. I.; Stack, T. D. P. *Science* **1996**, *273*, 1848.
(160) Root, D. E.; Henson, M. J.; Machonkin, T.; Mukherjee, P.; Stack, T. D. P.; Solomon, E. I. *J. Am. Chem. Soc.* **1998**, *120*, 4982.
(161) Itoh, S.; Kondo, T.; Komatsu, M.; Ohshiro, Y.; Li, C.; Kanehisa, N.; Kai, Y.; Fukuzumi, S. *J. Am. Chem. Soc.* **1995**, *117*, 4714.
(162) Groothaert, M. H.; van Bokhoven, J. A.; Battiston, A. A.; Weckhuysen, B. M.; Schoonheydt, R. A. *J. Am. Chem. Soc.* **2003**, *125*, 7629.
(163) Yachandra, V. K.; Sauer, K.; Klein, M. P. *Chem. Rev.* **1996**, *96*, 2927.
(164) Cramer, C. J.; Smith, B. A.; Tolman, W. B. *J. Am. Chem. Soc.* **1996**, *118*, 11283.
(165) Liu, X.-Y.; Palacios, A. A.; Novoa, J. J.; Alvarez, S. *Inorg. Chem.* **1998**, *37*, 1202−1212.
(166) Hensen, M. J.; Mukherjee, P.; Root, D. E.; Stack, T. D. P.; Solomon, E. I. *J. Am. Chem. Soc.* **1999**, *121*, 10332.
(167) Flock, M.; Pierloot, K. *J. Phys. Chem. A* **1999**, *103*, 95.
(168) Lam, B. M. T.; Halfen, J. A.; Young, V. G., Jr.; Hagadorn, J. R.; Holland, P. L.; Lledós, A.; Cucurull-Sánchez, L.; Novoa, J. J.; Alvarez, S.; Tolman, W. B. *Inorg. Chem.* **2000**, *39*, 4059.
(169) Siegbahn, P. E. M.; Wirstam, M. *J. Am. Chem. Soc.* **2001**, *123*, 11819.
(170) Siegbahn, P. E. M. *J. Biol. Inorg. Chem.* **2003**, *8*, 577.
(171) Pidcock, E.; DeBeer, S.; Obias, H. V.; Hedman, B.; Hodgson, K. O.; Karlin, K. D.; Solomon, E. I. *J. Am. Chem. Soc.* **1999**, *121*, 1870.
(172) Cahoy, J.; Holland, P. L.; Tolman, W. B. *Inorg. Chem.* **1999**, *38*, 2161.
(173) Mahadevan, V.; Hou, Z.; Cole, A. P.; Root, D. E.; Lal, T. K.; Solomon, E. I.; Stack, T. D. P. *J. Am. Chem. Soc.* **1997**, *119*, 11996.

(174) Mahadevan, V.; Henson, M. J.; Solomon, E. I.; Stack, T. D. P. *J. Am. Chem. Soc.* **2000**, *122*, 10249.
(175) Mahapatra, S.; Halfen, J. A.; Wilkinson, E. C.; Pan, G.; Wang, X.; Young, V. G., Jr.; Cramer, C. J.; Que, L., Jr.; Tolman, W. B. *J. Am. Chem. Soc.* **1996**, *118*, 11555.
(176) Taki, M.; Teramae, S.; Nagatomo, S.; Tachi, Y.; Kitagawa, T.; Itoh, S.; Fukuzumi, S. *J. Am. Chem. Soc.* **2002**, *124*, 6367.
(177) Mirica, L. M.; Vance, M.; Rudd, D. J.; Hedman, B.; Hodgson, K. O.; Solomon, E. I.; Stack, T. D. P. *J. Am. Chem. Soc.* **2002**, *124*, 9332.
(178) Henson, M. J.; Vance, M. A.; Zhang, C. X.; Liang, H.-C.; Karlin, K. D.; Solomon, E. I. *J. Am. Chem. Soc.* **2003**, *125*, 5186.
(179) Groves, J. T.; Han, Y.-Z. In *Cytochrome P450: Structure, Mechanism, and Biochemistry*, 2nd ed.; Ortiz de Montellano, P. R., Ed.; Plenum Press: New York, 1995; pp 3−48.
(180) Kitajima, N.; Fujisawa, K.; Fujimoto, C.; Moro-oka, Y.; Hashimoto, S.; Kitagawa, T.; Toriumi, K.; Tatsumi, K.; Nakamura, A. *J. Am. Chem. Soc.* **1992**, *114*, 1277.
(181) Kitajima, N.; Fujusawa, K.; Moro-oka, Y. *Inorg. Chem.* **1990**, *29*, 357.
(182) Kitajima, N.; Katayama, T.; Fujisawa, K.; Iwata, Y.; Moro-oka, Y. *J. Am. Chem. Soc.* **1993**, *115*, 7872.
(183) Chen, P.; Fujisawa, K.; Solomon, E. I. *J. Am. Chem. Soc.* **2000**, *122*, 10177.
(184) Fujii, T.; Naito, A.; Yamaguchi, S.; Wada, A.; Funahashi, Y.; Jitsukawa, K.; Nagatomo, S.; Kitagawa, T.; Masuda, H. *Chem. Commun.* **2003**, 2700.
(185) Yamaguchi, S.; Nagatomo, S.; Kitagawa, T.; Funahashi, Y.; Ozawa, T.; Jitsukawa, K.; Masuda, H. *Inorg. Chem.* **2003**, *42*, 6968.
(186) Wada, A.; Harata, M.; Hasegawa, K.; Jitsukawa, K.; Masuda, H.; Mukai, M.; Kitagawa, T.; Einaga, H. *Angew. Chem., Int. Ed.* **1998**, *37*, 798.
(187) Sanyal, I.; Ghosh, P.; Karlin, K. D. *Inorg. Chem.* **1995**, *34*, 3050.
(188) Ohtsu, H.; Itoh, S.; Nagatomo, S.; Kitagawa, T.; Ogo, S.; Watanabe, Y.; Fukuzumi, S. *Inorg. Chem.* **2001**, *40*, 3200.
(189) Kodera, M.; Kita, T.; Miura, I.; Nakayama, N.; Kawata, T.; Kano, K.; Hirota, S. *J. Am. Chem. Soc.* **2001**, *123*, 7715.
(190) Osako, T.; Nagatomo, S.; Tachi, Y.; Kitagawa, T.; Itoh, S. *Angew Chem. Int. Ed.* **2002**, *41*, 4325.
(191) Karlin, K. D.; Ghosh, P.; Cruse, R. W.; Farooq, A.; Gultneh, Y.; Jacobson, R. R.; Blackburn, N. J.; Strange, R. W.; Zubieta, J. *J. Am. Chem. Soc.* **1988**, *110*, 6769.
(192) Ghosh, P.; Tyeklár, Z.; Karlin, K. D.; Jacobson, R. R.; Zubieta, J. *J. Am. Chem. Soc.* **1987**, *109*, 6889.
(193) Cvetkovic, M.; Batten, S. R.; Moubaraki, B.; Murray, K. S.; Spiccia, L. *Inorg. Chim. Acta* **2001**, *324*, 131.
(194) Hu, Z.; Williams, R. D.; Tran, D.; Spiro, T. G.; Gorun, S. M. *J. Am. Chem. Soc.* **2000**, *122*, 3556.
(195) Hu, Z.; George, G. N.; Gorun, S. M. *Inorg. Chem.* **2001**, *40*, 4812.
(196) Land, E. J.; Ramsden, C. A.; Riley, P. A. *Acc. Chem. Res.* **2003**, *36*, 300.
(197) Siegbahn, P. E. M. *J. Biol. Inorg. Chem.* **2003**, *8*, 567.
(198) Karlin, K. D.; Hayes, J. C.; Gultneh, Y.; Cruse, R. W.; McKown, J. W.; Hutchinson, J. P.; Zubieta, J. *J. Am. Chem. Soc.* **1984**, *106*, 2121.
(199) Pidcock, E.; Obias, H. V.; Zhang, C. X.; Karlin, K. D.; Solomon, E. I. *J. Am. Chem. Soc.* **1998**, *120*, 7841.
(200) Rys, P.; Skrabal, P.; Zollinger, H. *Angew Chem. Int. Ed. Engl.* **1972**, *11*, 874.
(201) Chen, P.; Solomon, E. I. *J. Inorg. Biochem.* **2002**, *88*, 368.
(202) Karlin, K. D.; Cohen, B. I.; Jacobson, R. R.; Zubieta, J. *J. Am. Chem. Soc.* **1987**, *109*, 6194.
(203) Nasir, M. S.; Cohen, B. I.; Karlin, K. D. *J. Am. Chem. Soc.* **1992**, *114*, 2482.
(204) Cruse, R. W.; Kaderli, S.; Meyer, C. J.; Zuberbühler, A. D.; Karlin, K. D. *J. Am. Chem. Soc.* **1988**, *110*, 5020.
(205) Battaini, G.; Monzani, E.; Perotti, A.; Para, C.; Casella, L.; Santagostini, L.; Gulloti, M.; Dillinger, R.; Näther, C.; Tuczek, F. *J. Am. Chem. Soc.* **2003**, *125*, 4185.
(206) Sorrell, T. N.; Vankai, V. A.; Garrity, M. L. *Inorg. Chem.* **1991**, *30*, 207.
(207) Sorrell, T. N.; Garrity, M. L. *Inorg. Chem.* **1991**, *30*, 210.
(208) Gelling, O. J.; van Bolhuis, F.; Meetsma, A.; Feringa, B. L. *J. Chem. Soc., Chem. Commun.* **1988**, 552.
(209) Gelling, O. J.; Feringa, B. L. *J. Am. Chem. Soc.* **1990**, *112*, 7599.
(210) Casella, L.; Gullotti, M.; Pallanza, G.; Rigoni, L. *J. Am. Chem. Soc.* **1988**, *110*, 4221.
(211) Alzuet, G.; Casella, L.; Villa, M. L.; Carugo, O.; Gullotti, M. *J. Chem. Soc., Dalton Trans.* **1997**, 4789.
(212) Menif, R.; Martell, A. E. *J. Chem. Soc., Chem. Commun.* **1989**, 1521.
(213) Menif, R.; Martell, A. E.; Squattrito, P. J.; Clearfield, A. *Inorg. Chem.* **1990**, *29*, 4723.
(214) Becker, M.; Schindler, S.; van Eldik, R. *Inorg. Chem.* **1994**, *33*, 5370.
(215) Utz, D.; Heinemann, F. W.; Hampel, F.; Richens, D. T.; Schindler, S. *Inorg. Chem.* **2003**, *42*, 1430.
(216) Ngwenya, M. P.; Chen, D.; Martell, A. E.; Reibenspies, J. *Inorg. Chem.* **1991**, *30*, 2732.
(217) Nasir, M. S.; Karlin, K. D.; McGowty, D.; Zubieta, J. *J. Am. Chem. Soc.* **1991**, *113*, 698.
(218) Murthy, N. N.; Mahroof-Tahir, M.; Karlin, K. D. *Inorg. Chem.* **2001**, *40*, 628.
(219) Fusi, V.; Llobet, A.; Mahía, J.; Micheloni, M.; Paoli, P.; Ribas, X.; Rossi, P. *Eur. J. Inorg. Chem.* **2002**, 987.
(220) Casella, L.; Carugo, O.; Gullotti, M.; Garofani, S.; Zanello, P. *Inorg. Chem.* **1993**, *32*, 2056.
(221) Réglier, M.; Amadeï, E.; Tadayoni, R.; Waegell, B. *J. Chem. Soc., Chem. Commun.* **1989**, 447.
(222) Gagne, R. R.; Gall, R. S.; Lisensky, G. C.; Marsh, R. E.; Speltz, L. M. *Inorg. Chem.* **1979**, *18*, 771.
(223) Holland, P. L.; Rodgers, K. R.; Tolman, W. B. *Angew. Chem., Int. Ed.* **1999**, *38*, 1139.
(224) Ortiz de Montellano, P. R., Ed. *Cytochrome P450: Structure, Mechanism, and Biochemistry*, 2nd ed.; Plenum Press: New York, 1995.
(225) Karki, S. B.; Dinnocenzo, J. P.; Jones, J. P.; Korzekwa, K. R. *J. Am. Chem. Soc.* **1995**, *117*, 3657.
(226) Mahapatra, S.; Halfen, J. A.; Tolman, W. B. *J. Am. Chem. Soc.* **1996**, *118*, 11575.
(227) Haysashi, H.; Fujinami, S.; Nagatomo, S.; Ogo, S.; Suzuki, M.; Uehara, A.; Watanabe, Y.; Kitagawa, T. *J. Am. Chem. Soc.* **2000**, *122*, 2124.
(228) Hayashi, H.; Uozumi, K.; Fujinami, S.; Nagatomo, S.; Shiren, K.; Furutachi, H.; Suzuki, M.; Uehara, A.; Kitagawa, T. *Chem. Lett.* **2002**, 416.
(229) This value differs from that originally published in ref 226 (−0.8), which is in error due to an incorrect Hammett plot.
(230) Russell, G. A. In *Free Radicals*; Kochi, J. K., Ed.; John Wiley & Sons: New York, 1973; Vol. I, pp 275−331.
(231) Cramer, C. J.; Pak, Y. *Theor. Chem. Acc.* **2001**, *105*, 477.
(232) Halfen, J. A.; Young, V. G., Jr.; Tolman, W. B. *J. Am. Chem. Soc.* **1996**, *118*, 10920.
(233) Blain, I.; Bruno, P.; Giorgi, M.; Lojou, E.; Lexa, D.; Réglier, M. *Eur. J. Inorg. Chem.* **1998**, 1297.
(234) Xie, D.; Gutsche, C. D. *J. Org. Chem.* **1998**, *63*, 9270.
(235) Allen, W. E.; Sorrell, T. N. *Inorg. Chem.* **1997**, *36*, 1732.
(236) Reinaud, O. M.; Theopold, K. H. *J. Am. Chem. Soc.* **1994**, *116*, 6979.
(237) Kitajima, N.; Osawa, M.; Tanaka, M.; Moro-oka, Y. *J. Am. Chem. Soc.* **1991**, *113*, 8952.
(238) Shiren, K.; Ogo, S.; Fujinami, S.; Hayashi, H.; Suzuki, M.; Uehara, A.; Watanabe, Y.; Moro-oka, Y. *J. Am. Chem. Soc.* **2000**, *122*, 254.
(239) Thompson, J. S. *J. Am. Chem. Soc.* **1984**, *106*, 8308.
(240) Blain, I.; Giorgi, M.; Riggi, I. D.; Réglier, M. *Eur. J. Inorg. Chem.* **2000**, 393.
(241) Halfen, J. A.; Young, V. G., Jr.; Tolman, W. B. *Inorg. Chem.* **1998**, *37*, 2102.
(242) Arii, H.; Saito, Y.; Nagatomo, S.; Kitagawa, T.; Funahashi, Y.; Jitsukawa, K.; Masuda, H. *Chem. Lett.* **2003**, *32*, 156.
(243) Jazdzewski, B. A.; Tolman, W. B. *Coord. Chem. Rev.* **2000**, *200−202*, 633.
(244) Fontecave, M.; Pierre, J. L. *Coord. Chem. Rev.* **1998**, *170*, 125.
(245) Wang, Y.; DuBois, J. L.; Hedman, B.; Hodgson, K. O.; Stack, T. D. P. *Science* **1998**, *279*, 537.
(246) Utaka, M.; Hojo, M.; Fujii, Y.; Takeda, A. *Chem. Lett.* **1984**, 635.
(247) Utaka, M.; Takeda, A. *J. Chem. Soc., Chem. Commun.* **1985**, 1824.
(248) Balogh-Hergovich, E.; Speier, G.; Argay, G. *J. Chem. Soc., Chem. Commun.* **1991**, 551.
(249) Lippai, I.; Speier, G.; Huttner, G.; Zsolnai, L. *Chem. Commun.* **1997**, 741.
(250) Balogh-Hergovich, E.; Kaizer, J.; Speier, G. *Inorg. Chim. Acta* **1997**, *256*, 9.
(251) Lippai, I.; Speier, G. *J. Mol. Catal.* **1998**, *130*, 139.
(252) Balogh-Hergovich, E.; Kaizer, J.; Speier, G.; Fülöp, V.; Párkányi, L. *Inorg. Chem.* **1999**, *38*, 3787.
(253) Balogh-Hergovich, E.; Kaizer, J.; Speier, G.; Argay, G.; Parkanyi, L. *J. Chem. Soc., Dalton Trans.* **1999**, 3847.
(254) Balogh-Hergovich, E.; Kaizer, J.; Speier, G. *J. Mol. Catal. A: Chem.* **2000**, *159*, 215.
(255) Balogh-Hergovich, E.; Kaizer, J.; Speier, G.; Huttner, G.; Jacobi, A. *Inorg. Chem.* **2000**, *39*, 4224.
(256) Balogh-Hergovich, E.; Kaizer, J.; Speier, G.; Huttner, G.; Zsolnai, L. *Inorg. Chim. Acta* **2000**, *304*, 72.
(257) Balogh-Hergovich, E.; Kaizer, J.; Pap, J.; Speier, G.; Huttner, G.; Zsolnai, L. *Eur. J. Inorg. Chem.* **2002**, 2287.
(258) Speier, G. *New J. Chem.* **1994**, *18*, 143.
(259) Pierpont, C. G.; Lange, C. W. *Prog. Inorg. Chem.* **1994**, *41*, 331.
(260) Pierpont, C. G. *Coord. Chem. Rev.* **2001**, *216−217*, 99.
(261) Kaim, W. *Dalton Trans.* **2003**, 761.
(262) Que, L., Jr.; Ho, R. Y. N. *Chem. Rev.* **1996**, *96*, 2607.
(263) Hiatt, R. In *Organic Peroxides*; Swern, D., Ed.; Wiley-Interscience: New York, 1971; Vol. III, p 70.

(264) Paul, P. P.; Tyeklár, Z.; Jacobson, R. R.; Karlin, K. D. *J. Am. Chem. Soc.* **1991**, *113*, 5322.
(265) Ross, P. K.; Solomon, E. I. *J. Am. Chem. Soc.* **1991**, *113*, 3246.
(266) Kitajima, N.; Koda, T.; Iwata, Y.; Moro-oka, Y. *J. Am. Chem. Soc.* **1990**, *112*, 8833.
(267) Hemocyanin has also been shown to exhibit phenoloxidase reativity: Decker, H.; Rimke, T. *J. Biol. Chem.* **1998**, *273*, 25889.
(268) Eiken, C.; Zippel, F.; Büldt-Karentzpoulos, K.; Krebs, B. *FEBS Lett.* **1998**, *436*, 293.
(269) Sayre, L. M.; Nadkarni, D. V. *J. Am. Chem. Soc.* **1994**, *116*, 3157.
(270) Maumy, M.; Capdevielle, P. *J. Mol. Catal. A: Chem.* **1996**, *113*, 159.
(271) Gupta, R.; Mukherjee, R. *Tetrahedron Lett.* **2000**, *41*, 7763.
(272) Speier, G. *J. Mol. Catal.* **1986**, *37*, 259.
(273) Balia, J.; Kiss, T.; Jameson, R. F. *Inorg. Chem.* **1992**, *31*, 58.
(274) Speier, G. *New J. Chem.* **1994**, *18*, 143.
(275) Monzani, E.; Battaini, G.; Perotti, A.; Casella, L.; Gullotti, M.; Santagostini, L.; Nardin, G.; Randaccio, L.; Geremia, S.; Zanello, P.; Opromolla, G. *Inorg. Chem.* **1999**, *38*, 5359 and references therein.
(276) Casella, L.; Monzani, E.; Gullotti, M.; Cavagnino, D.; Cerina, G.; Santagostini, L.; Ugo, R. *Inorg. Chem.* **1996**, *35*, 7516 and references therein.
(277) Gentschev, P.; Möller, N.; Krebs, B. *Inorg. Chim. Acta* **2000**, 442.
(278) Börzel, H.; Comba, P.; Pritzkow, H. *Chem. Commun.* **2001**, 97.
(279) Itoh, S.; Kumei, H.; Taki, M.; Nagatomo, S.; Kitagawa, T.; Fukuzumi, S. *J. Am. Chem. Soc.* **2001**, *123*, 6708.
(280) Battaini, G.; Carolis, M. D.; Monzani, E.; Tuczek, F.; Casella, L. *Chem. Commun.* **2003**, 726.
(281) Maumy, M.; Capdevielle, P. *J. Mol. Catal. A: Chem.* **1996**, *113*, 159.
(282) Berreau, L. M.; Mahapatra, S.; Halfen, J. A.; Houser, R. P.; Young, V. G., Jr.; Tolman, W. B. *Angew. Chem., Int. Ed.* **1998**, *38*, 207.
(283) Mahadevan, V.; DuBois, J. L.; Hedman, B.; Hodgson, K. O.; Stack, T. D. P. *J. Am. Chem. Soc.* **1999**, *121*, 5583.
(284) Taki, M.; Itoh, S.; Fukuzumi, S. *J. Am. Chem. Soc.* **2001**, *123*, 6203.
(285) Osako, T.; Ohkubo, K.; Taki, M.; Tachi, Y.; Fukuzumi, S.; Itoh, S. *J. Am. Chem. Soc.* **2003**, *125*, 11027.
(286) Weatherly, S. C.; Yang, I. V.; Thorp, H. H. *J. Am. Chem. Soc.* **2001**, *123*, 1236.
(287) Mayer, J. M.; Hrovat, D. A.; Thomas, J. L.; Borden, W. T. *J. Am. Chem. Soc.* **2002**, *124*, 11142.
(288) Shearer, J.; Zhang, C. X.; Hatcher, L. Q.; Karlin, K. D. *J. Am. Chem. Soc.* **2003**, *125*, 12670.
(289) Baciocchi, E.; Lanzalunga, O.; Lapi, A.; Manduchi, L. *J. Am. Chem. Soc.* **1998**, *120*, 5783.
(290) Taki, M.; Itoh, S.; Fukuzumi, S. *J. Am. Chem. Soc.* **2002**, *124*, 998.
(291) Goto, Y.; Matsui, T.; Ozaki, S.; Watanabe, Y.; Fukuzumi, S. *J. Am. Chem. Soc.* **1991**, *113*, 9497.
(292) Friesner, R. A.; Baik, M.-H.; Gherman, B. F.; Guallar, V.; Wirstam, M.; Murphy, R. B.; Lippard, S. J. *Coord. Chem. Rev.* **2003**, *238*−*239*, 267.
(293) Yachandra, V. K.; Sauer, K.; Klein, M. P. *Chem. Rev.* **1996**, *96*, 2927.
(294) Hikichi, S.; Yoshizawa, M.; Sasakura, Y.; Akita, M.; Moro-oka, Y. *J. Am. Chem. Soc.* **1998**, *120*, 10567.
(295) Reinaud, O. M.; Yap, G. P. A.; Rheingold, A. L.; Theopold, K. H. *Angew. Chem., Int. Ed. Engl.* **1995**, *34*, 2051.
(296) Mandimutsira, B. S.; Yamarik, J. L.; Brunold, T. C.; Gu, W.; Cramer, S. P.; Riordan, C. G. *J. Am. Chem. Soc.* **2001**, *123*, 9194.

CR020633R